3 Survey of Wave Types and Characteristics

3.1 Longitudinal Waves

3.1.1 Pure Longitudinal Waves

In solids, as in liquids and gases, there exists pure longitudinal waves that is, waves in which the direction of the particle displacements coincides with the direction of wave propagation. One may readily visualize such waves by studying the motion of two planes, which in the undisturbed medium are parallel to each other and perpendicular to the direction of propagation. In pure longitudinal wave motion, these planes experience absolute displacements from their positions of equilibrium and the distance between them also changes in general. For example, a plane which initially is at x is displaced a distance ξ, see Fig. 3.1; a second plane, which initially is at a distance dx from the first, is displaced a distance $\xi + \partial\xi/\partial x\, dx$. The material whose initial length was dx thus experiences an extensional strain ε_x in the x-direction, given by

$$\varepsilon_x = \frac{\partial \xi}{\partial x}. \tag{3.1}$$

Such a strain is associated with a stress or, more precisely, with a deviation of stress from the equilibrium condition. Unlike fluids, solids can sup-

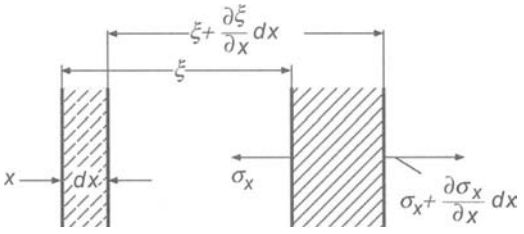

Fig. 3.1. Displacements, deformations, and stresses in longitudinal wave motion

port tensile stresses in absence of static pre-compression. Tensile stresses are usually taken as the positive normal stresses where "normal" indicates that the stress acts perpendicular to the surface. For the small deformations of interest in relation to structure-borne sound, Hooke's law holds and the tensile stress σ_x is proportional to the extensional strain ε_x (and the compressive stress $-\sigma_x$ is proportional to the compressive strain $-\varepsilon_x$). One thus may write

$$\sigma_x = D\varepsilon_x = D\frac{\partial \xi}{\partial x}. \tag{3.2}$$

The constant D has the same dimensions as σ_x, namely force/area, and represents the longitudinal stiffness of the material. The relation between D and the usually used constants of elasticity is discussed later in this chapter.

Also the stress depends on location (x-coordinate) and a net unbalanced stress causes the element to accelerate; if ρ represents the material density, the corresponding equation of motion may be written

$$\left(\sigma_x + \frac{\partial \sigma_x}{\partial x} dx\right) - \sigma_x = \rho \quad dx \frac{\partial^2 \xi}{\partial t^2},$$

or

$$\frac{\partial \sigma_x}{\partial x} = \rho \frac{\partial^2 \xi}{\partial t^2}. \tag{3.3}$$

The stress and the displacement thus are found to be related by two differential equations, Eqs. (3.2) and (3.3). In this derivation, the stress σ_x was treated not in terms of the location at which it occurs, which would be $(x + \xi)$, but in terms of the plane of the medium on which it acts - the plane that is indicated by its equilibrium position x. In structure-borne sound, the displacements ξ are very small compared to the distances over which there occur significant changes in the vibration field, which distances are fractions of the relevant wavelengths. Therefore, use of coordinates attached to the medium (as above) leads to the same results as use of coordinates attached to a reference frame fixed in space.

As has been shown in Chapter 2, it is convenient to describe the kinematics of a sound field in terms of the (particle) velocity

$$v_x = \frac{\partial \xi}{\partial t} \tag{3.4}$$

instead of the displacement ξ; this velocity appears directly in the expression for the kinetic energy per unit volume,

$$e_{kin} = \frac{1}{2}\rho v_x^2. \tag{3.5}$$

Every mechanical wave motion also has potential energy associated with it. Here, the potential energy per unit volume is given by

$$e_{pot} = \int_0^{\varepsilon_x} \sigma_x d\varepsilon_x = \frac{1}{2} D\varepsilon_x^2 = \frac{1}{2D}\sigma_x^2. \tag{3.6}$$

The total energy density (i.e., the total energy per unit volume) is given by the sum of these two parts,

$$e_{tot} = e_{kin} + e_{pot}, \tag{3.7}$$

and thus is completely specified only if both v_x and ε_x, or both v_x and σ_x, are given.

One now needs to consider whether one would prefer to use the strain or the stress in continuing the analysis. If one uses the strain, one obtains a certain mathematical symmetry, since the two field variables v_x and ε_x then are the derivatives of the displacement with respect to time and space, respectively. Also, one can usually measure only the strains (or deformations) directly, whereas one generally needs to deduce the stresses from the measured strains. In spite of these considerations, use of the stress as a variable in the analysis turns out to be preferable, not only because many physical boundary conditions involve the stresses directly, but also – and more significantly – because the product of stress and velocity give the power flow per unit area, i.e., the intensity of the sound field:

$$J_x = -\sigma_x v_x. \tag{3.8}$$

The negative algebraic sign here takes account of the fact that a positive (tensile) stress and a positive velocity result in energy transport in the negative x-direction.

By introducing the velocity, one may rewrite Eq. (3.3) as

$$\frac{\partial \sigma_x}{\partial x} = \rho \frac{\partial v_x}{\partial t}. \tag{3.9}$$

Similarly, one may rewrite Eq. (3.2), after differentiation with respect to time, as

$$D\frac{\partial v_x}{\partial x} = \frac{\partial \sigma_x}{\partial t}. \tag{3.10}$$

One observes that the relation between the two variables σ_x and v_x is such that the spatial derivative of one is proportional to the time derivative

of the other. This cyclic inter-relation for all is also obtained for the wave types discussed subsequently. Differentiation with respect to x or t and combination of Eqs. (3.9) and (3.10) results in the wave equation,

$$D\frac{\partial^2}{\partial x^2}(\sigma_x,\ v_x) = \rho\frac{\partial^2}{\partial t^2}(\sigma_x,\ v_x), \tag{3.11}$$

which applies for all of the field variables. One may easily verify that this equation is satisfied by all functions of the form

$$F\left(t \pm \sqrt{\frac{\rho}{D}}x\right). \tag{3.12}$$

Such functions describe waves that propagate without distortion in the positive or in the negative x-direction, depending on the algebraic sign of coefficient of x. If a certain variation with time occurs at $x = 0$, then exactly the same variation occurs also at any arbitrary location x, but delayed (or advanced) by an amount $x\sqrt{\rho / D}$. The parameter $\sqrt{D/\rho}$ thus represents the constant velocity c_L with which the disturbance propagates:

$$c_L = \sqrt{\frac{D}{\rho}}. \tag{3.13}$$

This velocity increases with increasing stiffness and decreases with increasing density. The subscript L indicates the longitudinal character of this type of wave.

The parameters D and ρ occur also in another important combination. If one considers, for example, a wave that propagates in the positive x-direction, and writes the corresponding displacement ξ as

$$\xi\left(t - \sqrt{\frac{\rho}{D}}x\right),$$

one then finds from Eq. (3.2) that the compressive stress associated with this wave is given by

$$-\sigma_x = \sqrt{D\rho}\,\xi'\left(t - \sqrt{\frac{\rho}{D}}x\right),$$

where the prime denotes differentiation with respect to space whereas the velocity obeys

$$v_x = \dot{\xi}\left(t - \sqrt{\frac{\rho}{D}}x\right).$$

The two field variables may be seen to depend on space and time in precisely the same way; their ratio represents a mechanical impedance per unit area and is called the "characteristic impedance" of the material:

$$Z_L'' = \frac{-\sigma_x}{v_x} = \sqrt{D\rho} = c_L \rho. \tag{3.14}$$

This proportionality of the two variables also implies that for such propagating waves, variations in the potential energy coincide in time and space with those in the kinetic energy. From the constant of proportionality one finds that these two energies are equal:

$$e_{pot} = \frac{1}{2D}\sigma_x^2 = e_{kin} = \frac{1}{2}\rho v_x^2 = \frac{1}{2}\rho\left[\dot{\xi}\left(t - \sqrt{\frac{\rho}{D}}x\right)\right]^2. \tag{3.15}$$

Finally, one also finds that the intensity

$$J = -\sigma_x v_x = Z_L''\left[\dot{\xi}\left(t - \sqrt{\frac{\rho}{D}}x\right)\right]^2$$

and the total energy density

$$e_{tot} = \rho\left[\dot{\xi}\left(t - \sqrt{\frac{\rho}{D}}x\right)\right]^2,$$

are related by the simple expression

$$J = e_{tot} c_L. \tag{3.16}$$

Equation (3.16) demonstrates that the energy density in a propagating wave advances with the velocity c_L.

Figure 3.2 summarizes the foregoing relations for the particularly simple case of a sinusoidal wave. Here, the time-function

$$\xi(t,\ 0) = \hat{\xi}\sin\omega t,$$

in terms of the radian frequency ω, leads to the space-time function

$$\xi\left(t - \frac{x}{c_L}\right) = \hat{\xi}\sin\left(\omega\left(t - \frac{x}{c_L}\right)\right) \tag{3.17}$$

The ratio ω/c_L is called the wavenumber and is generally represented by a separate symbol:

$$k_L = \frac{\omega}{c_L}. \tag{3.18}$$

The wavenumber k_L is the spatial analog of the radian frequency ω; ω is inversely proportional to the duration (period) T of a cycle,

$$\omega = \frac{2\pi}{T},$$

and the wavenumber k_L is inversely proportional to the spatial period, i.e., to the wavelength λ_L,

$$k_L = \frac{2\pi}{\lambda_L}. \tag{3.19}$$

The wavenumber indicates how many wavelengths correspond to 2π times the unit length.

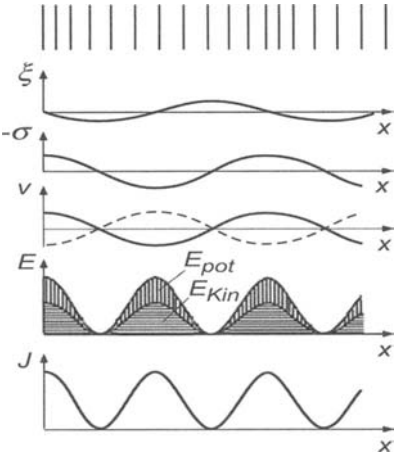

Fig. 3.2. Spatial variation of field variables and energy quantities in a sinusoidal longitudinal wave

Figure 3.2 is constructed for the instant at which the deformation is given by

$$\xi = -\hat{\xi} \sin k_L x. \tag{3.20a}$$

The top part of this figure shows this deformation in terms of the displacements of planes which are uniformly spaced at equilibrium. Below

this, the deformation is plotted as a function of x. The next lower graph shows the compressive stress distribution

$$-\sigma_x = \hat{\xi}\ Dk_L \cos k_L x = -\hat{\sigma}_x \cos k_L x, \tag{3.20b}$$

which is shifted by $\lambda_L/4$ with respect to the deformation function. Below the graph of $-\sigma(x)$ is given a plot of the velocity

$$v_x = \hat{\xi}\omega \cos k_L x = \hat{v}_x \cos k_L x, \tag{3.20c}$$

which is in phase with the compressive stress. Below these plots of the field variables are shown the energy contributions. The curve bounding the horizontally cross-hatched area represents the kinetic energy density

$$e_{kin} = \frac{1}{2}\rho \hat{v}_x^2 \cos^2 k_L x, \tag{3.20d}$$

and the distance between the aforementioned and the topmost curve (vertically cross-hatched area) represents the potential energy density

$$e_{pot} = \frac{1}{2}\rho \hat{v}_x^2 \cos^2 k_L x. \tag{3.20e}$$

The topmost curve thus corresponds to the total energy density

$$e_{tot} = \rho \hat{v}_x^2 \cos^2 k_L x. \tag{3.20f}$$

These energies are also seen to be periodic and in phase with each other, but their wavelength is half that of the field variables. The bottom-most plot shows the intensity

$$J = c_L \rho \hat{v}_x^2 \cos^2 k_L x, \tag{3.20g}$$

which is also in phase with the aforementioned energy densities.

3.1.2 Quasi-Longitudinal Waves on Beams and Plates

The previously discussed pure longitudinal waves can occur only in solids whose dimensions in all directions are much greater than a wavelength. Thus, some seismic waves are pure longitudinal waves, but one rarely encounters practical structures that are of sufficient extent in all directions to support pure longitudinal waves at the frequencies of interest here. The largest thickness of concern in building structures, for example, is likely to be that of a heavy brick or concrete wall; about 25 cm. For this thickness and for a longitudinal wavespeed of 2500 m/s (which value is representative for such a wall and corresponds to the lowest wavespeeds in typical

building structures), one finds that the wall thickness exceeds the wavelength only at frequencies above 10,000 Hz. For most cases of interest, at least one of the dimensions is small compared with a wavelength; for plate-like structures one cross-sectional dimension is smaller than a wavelength, for beam-like structures, two.

Although an unsteady axial force acting at one end of a beam may be expected to produce primarily wave motions parallel to the beam axis, it is well-known that even in a static tensile test there occurs a contraction of the cross-section in addition to the axial extension. This contraction per unit thickness (i.e., the strains $|\varepsilon_y|$ or $|\varepsilon_z|$ are proportional to the axial strain ε_x,

$$\varepsilon_y = \varepsilon_z = -\mu\varepsilon_x. \tag{3.21}$$

The constant of proportionality μ is a property of the material and is known as Poisson's ratio; Poisson was the first to derive a value, namely 0.25, for this constant on the basis of theoretical considerations. His value is of the same order as those actually observed, see Table 4.3. The greatest possible value that μ can take on is 0.5; this value is obtained for incompressible materials, for which the volume change associated with the cross-sectional contraction makes up for that due to the longitudinal extension. Obviously, the actual cross-sectional contractions must be less than those for an ideal incompressible material, but they are of the same order of magnitude.

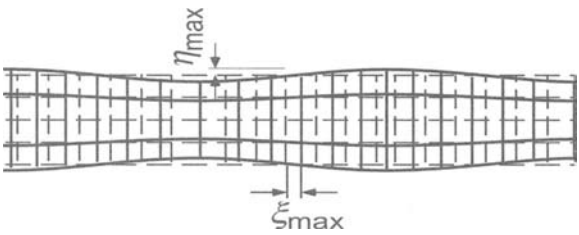

Fig. 3.3. Deformations associated with a quasi-longitudinal wave

Because of the cross-contraction phenomenon, there occur in a rod lateral displacements η and ζ in the y and z directions, in addition to the longitudinal displacements ξ of the material elements and, therefore, a wave travelling along the rod cannot be a pure longitudinal one. Rather, the wave motion appears in principle like that shown in Fig. 3.3 for a sinusoidal wave. The displacements shown in this figure are exaggerated, of

course, in order to display them more clearly; not only are the magnitudes of the displacements shown at least five orders of magnitude greater than in actuality, but also the ratio of the lateral displacement η to the amplitude of the longitudinal displacement ξ is shown as large as makes sense. For a circular or square rod of diameter or thickness d, and for a wavelength λ, the ratio of the transverse to the longitudinal displacement amplitude may be found from

$$\left|\hat{\varepsilon}_y\right| = \frac{2\hat{\eta}}{d} = \mu\left|\hat{\varepsilon}_x\right| = \mu\frac{2\pi}{\lambda}\hat{\xi},$$

to be given by

$$\frac{\hat{\eta}}{\hat{\xi}} = \frac{\pi\mu d}{\lambda}. \tag{3.22}$$

Since $\pi\mu$ is approximately equal to unity for most structural materials, one finds that the ratio of the greatest lateral displacement to the greatest longitudinal displacement is approximately equal to the ratio of the thickness of the wavelength; – and it has already been mentioned that this ratio usually is small for the audio-frequency range. The present discussion does not apply if the wavelength is of the same order as the thickness, because then the lateral displacements are no longer in phase over the cross-section and do not vary linearly with distance from the axis cf. 3.7.3. In quasi-longitudinal waves, the wave motions must be primarily longitudinal and, therefore, such waves are often also called longitudinal waves, although the "quasi-longitudinal waves" usage is to be preferred, because it indicates a deviation from the pure longitudinal waves.

Although the transverse motions may be very small, their presence has two important consequences. It is clear that only motions perpendicular to a surface can cause radiation of sound into an adjacent medium which cannot support shear stresses. Quasi-longitudinal waves can therefore radiate sound because of the cross-sectional contractions associated with them. Estimates of the magnitude of such radiation are given in Chapter 7, but it should be mentioned here that the associated radiation into air generally is insignificant unless inordinately large structure-borne sound energies are present. However, this type of radiation into water generally is not negligible, because of the considerably greater "acoustic hardness" of water. In fact, one may even make use of this radiation for measurement of the intensities of longitudinal waves propagating along a plate.

Transverse motions also cause the propagation velocities of quasi-longitudinal waves to be smaller than those of pure longitudinal waves. This difference comes about because the stiffness with which a rod resists

axial forces is smaller if the cross-section of the rod is not constrained. Because unconstrained cross-sections can easily be obtained in practice, the modulus of elasticity E was defined as the ratio of the stress to strain in the tension direction, as obtained in a simple tensile test:

$$E = \frac{\sigma_x}{\varepsilon_x} \quad ; \quad \left(\sigma_y = \sigma_z = 0\right). \tag{3.23}$$

If, on the other hand, the lateral contraction is constrained to zero, then there results a three-dimensional instead of a one-dimensional stress condition, because then there are produced the additional normal stresses σ_y and σ_z in the directions normal to the tension direction. These stresses reduce the displacement in the x-direction by an amount which, in view of the superposition principle, corresponds to the cross-contraction they would produce if they were present by themselves. For the general case, Eq. (3.23) must be replaced by three equations:

$$\begin{aligned} E\varepsilon_x &= \sigma_x - \mu\left(\sigma_y + \sigma_z\right) \\ E\varepsilon_y &= \sigma_y - \mu\left(\sigma_z + \sigma_x\right) \\ E\varepsilon_z &= \sigma_z - \mu\left(\sigma_x + \sigma_y\right) \ . \end{aligned} \tag{3.24}$$

For the case where no cross-sectional contraction is permitted, namely for

$$\varepsilon_y = \varepsilon_z = 0, \tag{3.25}$$

one finds by adding the last two of Eq. (3.24) that

$$\left(\sigma_y + \sigma_z\right) = \frac{2\mu}{1-\mu}\sigma_x,$$

which, after substitution into the first of these equations, leads to

$$E\varepsilon_x = \sigma_x\left(1 - \frac{2\mu^2}{1-\mu}\right).$$

Thus, the "longitudinal" stiffness D, which was introduced in Eq. (3.2) and which determines the propagation velocity of pure longitudinal waves, depends on the material parameters E and μ according to the relation

$$D = \frac{E}{1 - 2\mu^2/\left(1-\mu\right)} = \frac{E\left(1-\mu\right)}{\left(1+\mu\right)\left(1-2\mu\right)}. \tag{3.26}$$

Clearly, D is always greater than E. For the typical value of $\mu = 0.3$, $D/E \approx 1.35$.

Except for E taking the place of the longitudinal stiffness D, all the relations derived in Sect. 3.1.1 remain valid also for "quasi-longitudinal" waves on a rod. Instead of the tensile stress σ_x it is convenient here to introduce the longitudinal force F_x, which acts on the entire cross-sectional area S and to take this force as positive if it is compressive,

$$F_x = -S\sigma_x, \tag{3.27}$$

so that the power transported in the positive x-direction is given by the product

$$W = F_x v_x. \tag{3.28}$$

The coupled Eqs. (3.9) and (3.10) then become

$$-\frac{\partial F_x}{\partial x} = \rho S \frac{\partial v_x}{\partial t}, \tag{3.29}$$

$$-ES\frac{\partial v_x}{\partial x} = \frac{\partial F_x}{\partial t}. \tag{3.30}$$

In the development of the wave equation from these relations, the area and the algebraic sign-change drop out, and the only change that remains is replacement of D by E:

$$E\frac{\partial^2}{\partial x^2}\left(F_x,\ v_x\right) = \rho\frac{\partial^2}{\partial t^2}\left(F_x,\ v_x\right). \tag{3.31}$$

The propagation speed here is

$$c_{LII} = \sqrt{\frac{E}{\rho}}, \tag{3.32}$$

which is smaller than the speed of pure longitudinal waves. For $\mu = 0.3$, the difference between these two speeds amounts to 16 %, which is not entirely negligible. It thus is important to note which longitudinal wave speed is meant in any given situation.

In the rest of this book, Roman numeral subscripts indicating the number of directions along which the cross-sectional contraction is unconstrained will be used, in addition to the subscript L, to differentiate among the various longitudinal wavespeeds (at least where confusion may occur). Thus, the propagation speed of quasi-longitudinal waves on a rod is designated by c_{LII} in Eq. (3.32), in order to differentiate it from the speed c_L of pure longitudinal waves. Experimentally determined values of c_{LII} are given in Tables 4.3 and 4.5.

Quasi-longitudinal wave propagation on a plate constitutes a case, which lies between the two previously treated ones, because here cross-sectional contraction is unrestrained in only one direction, say, the *z*-direction. For this two-dimensional stress condition,

$$\varepsilon_y = 0;\ \sigma_z = 0. \tag{3.33}$$

The second of Eqs. (3.24) then yields

$$\sigma_y = \mu\sigma_x,$$

which, when substituted into the first of these equations, leads to

$$E\varepsilon_x = \sigma_x\left(1-\mu^2\right).$$

One finds that here the effective modulus of elasticity is

$$\frac{E}{1-\mu^2},$$

which lies between *E* and *D*, but nearer to *E*. The corresponding longitudinal wave speed

$$c_{LI} = \sqrt{\frac{E}{\rho\left(1-\mu^2\right)}} \tag{3.34}$$

differs so little from the value $c_{L\text{II}}$, which applies for rods (for $\mu = 0.3$, the difference amounts to 5 %) that the difference may often be neglected in practice.

For the purpose of rewriting Eqs. (3.9) and (3.10) for plates, it is convenient to use the compressive force per unit width

$$F_x' = -\sigma_x h, \tag{3.35}$$

where *h* represents the plate thickness, instead of the tensile stress σ_x. Then

$$W' = F_x' v_x \tag{3.36}$$

gives the power propagating per unit width. The coupled Eqs. (3.9) and (3.10) then become

$$-\frac{\partial F_x'}{\partial x} = \rho h \frac{\partial v_x}{\partial t}, \tag{3.37}$$

$$-\frac{Eh}{1-\mu^2}\frac{\partial v_x}{\partial x} = \frac{\partial F_x'}{\partial t}, \tag{3.38}$$

and the wave equation resulting from these may be written as

$$\frac{E}{1-\mu^2}\frac{\partial^2}{\partial x^2}\left(F_x',\ v_x\right) = \rho\frac{\partial^2}{\partial t^2}\left(F_x',\ v_x\right). \tag{3.39}$$

The case of the plate differs from that of a rod in that the cross-sectional contractions occur in only one direction, but it also follows from Eqs. (3.24) (appropriately modified for this case) that the cross-sectional contraction ε_z for a plate is larger than the two equal contractions for a rod; namely, for a plate,

$$\varepsilon_z = -\frac{\mu}{1-\mu}\varepsilon_x. \tag{3.40}$$

In effect, the material in this case "makes better use" of the one direction it can move to "get out of the way". For $\mu = 0.3$, this increase in the cross-sectional contraction amounts to 43 %, but does not change significantly the previous estimates of the kinematic relations. However, this difference should be considered in calculations of sound radiation, which, at any rate, always is greater for plate-like than for beam-like structures, because for beams the fluid motions on two opposite sides may cancel each other in the acoustic nearfield.

3.2 Transverse Waves

3.2.1 Transverse Plane Waves

Solids do not only resist changes in volume but also changes in shape. This resistance to changes in shape comes about because, unlike a liquid or gas, a solid can support tangential stresses on any cutting plane, even with the material at rest. Because these tangential stresses oppose "shearing" displacements parallel to the cutting plane, they are called shear stresses. It is the shear stresses, which make it possible for solids to exist in the shape of rods, plates, shells, etc. It is also because of shear stresses that transverse plane wave motions can occur in solid bodies, where the direction of propagation (here again taken as the x-direction) is perpendicular to the direction of the displacement η (here taken as the y-direction). Since the transverse displacements of two planes, a distance dx apart, differ by an amount $\partial\eta/\partial x\, dx$, an element, which originally was a rectangle with sides dx and dy, is distorted into a parallelogram. The acute angle of this parallelogram differs from a right angle (see Fig. 3.4) by the shear angle

$$\gamma_{xy} = \frac{\partial \eta}{\partial x}. \tag{3.41}$$

One may observe that here the deformation is not associated with a change in volume.

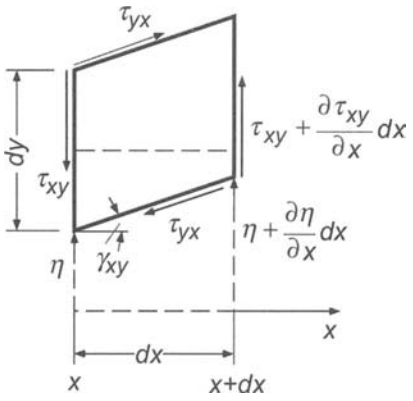

Fig. 3.4. Displacements, deformations, and stresses in transverse wave motion

On the other hand, there does occur a "rotation" of the element by the (of course, very small) angle $\gamma_{xy}/2$. Therefore, transverse waves are also known as "rotational" waves, see Sect. 3.5.

The previously discussed shear deformations always are associated with shear stresses τ_{xy} and τ_{yx}, where the first subscript indicates the axis normal to the plane on which the stress acts, and the second indicates the direction of the stress. Moment equilibrium of the element *dx dy* requires that the shear stresses on two perpendicular planes must be of equal magnitude. These stresses are proportional to the strain γ_{xy} they produce, so that one may write

$$\tau_{xy} = \tau_{yx} = G\gamma_{xy}, \tag{3.42}$$

or, with the aid of Eq. (3.41),

$$\tau_{xy} = G\frac{\partial \eta}{\partial x}. \tag{3.42a}$$

The constant of proportionality *G* again has the dimension of a stress and is known as the shear modulus.

If one replaces the displacement in the *y*-direction by the corresponding velocity

$$v_y = \frac{\partial \eta}{\partial t}, \tag{3.43}$$

then one may write the result of a differentiation of Eq. (3.42a) with respect to time as

$$G \frac{\partial v_y}{\partial x} = \frac{\partial \tau_{xy}}{\partial t}. \tag{3.44}$$

This differential equation replaces Eq. (3.10). Correspondingly, the version of Newton's law in Eq. (3.9) is replaced by the equation

$$\frac{\partial \tau_{xy}}{\partial x} = \rho \frac{\partial v_y}{\partial t}, \tag{3.45}$$

which one may obtain by noting that the difference between the shear stresses which act on two planes separated by a distance *dx* accelerate the element in the *y*-direction. Combination of the coupled Eqs. (3.44) and (3.45) again yields a wave equation

$$G \frac{\partial^2}{\partial x^2}\left(\tau_{xy},\ v_y\right) = \rho \frac{\partial^2}{\partial t^2}\left(\tau_{xy},\ v_y\right), \tag{3.46}$$

from which one finds that the propagation speed in this case is given by

$$c_T = \sqrt{\frac{G}{\rho}}, \tag{3.47}$$

where the constant *G* appears instead of *D* or *E*. The subscript *T* is used to indicate transverse waves and experimentally determined values of c_T are given in Table 4.3.

Although *G* at a first glance may appear to be a new material property, which is independent of those discussed previously, this is not the case. That *G* must be related to *E* may be deduced by noting that normal stresses are always associated with shear stresses, and vice versa. In longitudinal waves there occur also shear stresses, and in pure transverse waves there occur normal stresses. It is therefore incorrect to call pure transverse waves shear waves. Normal or shear stresses occur by themselves only on planes which are either parallel or perpendicular to the direction of propagation. In general, the stresses at a given point in a solid depend on the orientation of the hypothetical cutting plane through that point. Consider, for example,

the diagonal planes of a square whose edges are subject only to shear stresses, see Fig. 3.5a.

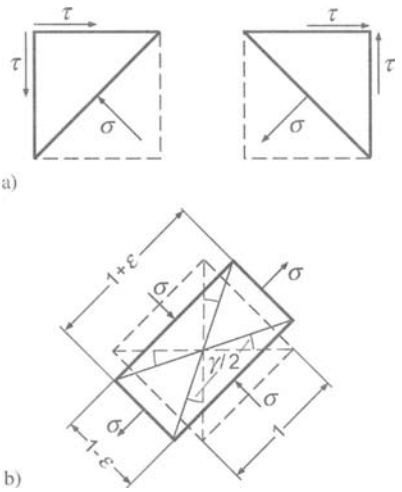

Fig. 3.5. Relations between a) normal and shear stresses; b) extensional strains and shear angles

Equilibrium of the forces demands that depending on which diagonal is being considered there act on the diagonal plane a compressive or a tensile stress, which is equal to the shear stresses acting on the edges:

$$2\tau \cos 45° = \frac{\sigma}{\cos 45°};\ \tau = \sigma .$$

The cos 45° term on the left-hand side results from the taking of force components, that on the right-hand side accounts for the greater surface area on the diagonal. Also the deformation of a differential rectangle depends on its orientation relative to the stresses. Under plane stress conditions, a square with edges parallel to the aforementioned diagonals experiences a normal (extension or contraction) strain, which may be found from Eq. (3.24) to be given by

$$\varepsilon = \frac{\sigma (1+\mu)}{E}.$$

These strains, however, are related to the angle γ, as evident from Fig. 3.5b, as

$$\frac{1-\varepsilon}{1+\varepsilon} = \tan\left(45° - \frac{\gamma}{2}\right) \approx \frac{1-\gamma/2}{1+\gamma/2},$$

which means that

$$\varepsilon = \frac{\gamma}{2}.$$

If one combines these equations with

$$\tau = G\gamma,$$

then one obtains the desired relation between G and E:

$$G = \frac{E}{2(1+\mu)}. \tag{3.48}$$

One may observe that the shear modulus is always considerably smaller than the modulus of elasticity E, and thus much smaller than the longitudinal stiffness D. The propagation speed c_T of transverse waves, therefore, also is smaller than that of quasi-longitudinal waves,

$$\frac{c_T}{c_{LII}} = \sqrt{\frac{G}{E}} = \sqrt{\frac{1}{2(1+\mu)}}, \tag{3.49a}$$

$$\frac{c_T}{c_{LI}} = \sqrt{\frac{G(1-\mu^2)}{E}} = \sqrt{\frac{1-\mu}{2}}, \tag{3.49b}$$

and much smaller than that of pure longitudinal waves,

$$\frac{c_T}{c_L} = \sqrt{\frac{G}{D}} = \sqrt{\frac{1-2\mu}{2(1-\mu)}}. \tag{3.50}$$

For $\mu = 0.3$, the foregoing ratios become

$$c_T/c_{LII} = 0.620, \quad c_T/c_{LI} = 0.592, \text{ and } c_T/c_L = 0.535.$$

From the similarity of the form of the equations one may determine without a detailed analysis that in a sinusoidal transverse wave the distribution of kinetic and potential energy is the same as in sinusoidal longitudinal waves as shown in Fig. 3.2.

Plane transverse waves also can occur only in bodies, which are large compared to the wavelength in all three dimensions. However, a free surface, which is parallel to the propagation and displacement directions (here, parallel to the x-y plane), has no effect on this type of wave. Plane transverse waves thus also can occur in flat plates of uniform thickness.

Since the motions at the surfaces of the plates in such cases are purely tangential, the motions can neither excite an ambient, non-viscous fluid nor can these motions be excited by the fluid.

3.2.2 Torsional Waves

Another type of transverse waves occurs when a narrow beam is excited by a torque or a torsional moment i.e., a moment, which varies with time and whose axis coincides with the axis of the beam. In such wave-motions, cross-sections rotate about the axis of the beam, so that all points on a cross-section experience circumferential displacements, which increase with the distance from the beam axis. If the beam axis coincides with the x-axis as in Fig. 3.6a, then the y- and z-components of these displacements may be written as

$$\eta = -\chi z, \tag{3.51a}$$

$$\zeta = \chi y, \tag{3.51b}$$

where χ represents the angular displacement, in radians, from the equilibrium position.

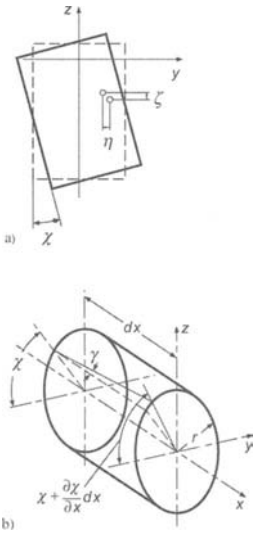

Fig. 3.6. Rotation of cross-section in torsion (a) and relation between change in rotation and shear angle (b)

For circular or annular cross-sections, it follows from rotational symmetry that none of the points in a cross-sectional plane are displaced out of that plane, so that

$$\xi = 0. \tag{3.52}$$

In this case, one may even obtain pure transverse waves. The infinite extent of the lateral displacement associated with the previously discussed plane transverse waves is here replaced by closure of these displacements around the circle. It will therefore be no surprise to find that the wave motion propagates with the speed given by Eq. (3.47).

In order to derive this result, it is convenient here – as for all configurations of finite lateral extent – to describe the system in terms of integrals of the field variables. The shear stresses, which act circumferentially everywhere on the cross-section and are proportional to the radius, may be found from Eq. (3.42) and from the relation between the angles,

$$\gamma = r\frac{d\chi}{dx}, \tag{3.53}$$

which is evident from Fig. 3.6b, to obey

$$\tau = Gr\frac{\partial\chi}{\partial x}. \tag{3.54}$$

Instead of this shear stress, one may use the torsional moment (acting about the x-axis)

$$M_x = 2\pi\int_{r_i}^{r_a}\tau r^2 dr = \frac{\pi}{2}G\left(r_a^4 - r_i^4\right)\frac{d\chi}{dx}, \tag{3.55}$$

where r_i and r_a represent the inner and outer radii of an annular cross-section.

One may note that

$$T = \frac{\pi}{2}G\left(r_a^4 - r_i^4\right) \tag{3.56}$$

represents the torsional stiffness of a rod with an annular (or circular) cross-section. Since the torque is proportional to the rate of change of the angular displacement for all cross-sectional shapes, that is,

$$M_x = T\frac{\partial\chi}{\partial x}, \tag{3.56a}$$

this proportionality serves to define a torsional stiffness for all cases. If one introduces the time-derivative of the angle of rotation χ, that is, the angular velocity about the x-axis,

$$w_x = \frac{\partial \chi}{\partial t}, \tag{3.57}$$

then one may differentiate Eq. (3.56a) with respect to time to obtain a relation between the space-wise variation of the angular velocity and the time-wise variation of the torque:

$$\frac{\partial M_x}{\partial t} = T \frac{\partial w_x}{\partial x}. \tag{3.58}$$

This partial differential equation must again be complemented by a relation between the spatial variation of the torque and the time-variation of the angular velocity. Such a relation may be obtained by equating the net moment acting on an elementary length of the rod about its axis to the angular inertia of that element. By this process one finds

$$\frac{\partial M_x}{\partial x} = \Theta' \frac{\partial w_x}{\partial t}, \tag{3.59}$$

where Θ' represents the mass moment of inertia per unit length of the rod. For a circularly symmetric cross-section with inside radius r_i and outside radius r_a this moment of inertia is given by

$$\Theta' = 2\pi\rho \int_{r_i}^{r_a} r^3 dr = \frac{\pi}{2} \rho \left(r_a^4 - r_i^4 \right). \tag{3.60}$$

By combining Eqs. (3.58) and (3.59) one obtains the wave equation

$$T \frac{\partial^2}{\partial x^2} \left(M_x,\ w_x \right) = \Theta' \frac{\partial^2}{\partial t^2} \left(M_x,\ w_x \right), \tag{3.61}$$

from which it follows that the propagation speed is given by the square-root of the ratio of the torsional stiffness to the moment of inertia. As evident from Eqs. (3.56) and (3.60), which follow from the same integrations, the geometric parameters cancel each other in this ratio, so that only the material constants G and ρ remain, and

$$c_T = \sqrt{\frac{G}{\rho}}. \tag{3.62}$$

The aforementioned identical dependence of T and Θ' on geometry holds only for rotationally symmetric cross-sections. If one considers a

narrow rectangle (keeping the total area constant), its torsional stiffness decreases while its moment of inertia increases. The increase in the moment of inertia is evident from the well-known expression

$$\Theta' = \frac{\rho\left(bh^3 + hb^3\right)}{12} = \frac{\rho S^2}{12}\left(\frac{h}{b} + \frac{b}{h}\right). \tag{3.63}$$

This expression, which is symmetric with respect to the height h and the width b, takes on its minimum value for $h = b$ i.e., for a square, but even this value is larger than that for a circle of the same area. For narrow rectangles, the second term in the parentheses is negligible in comparison with the first, and the foregoing relation simplifies to

$$\Theta' = \rho\frac{bh^3}{12}. \tag{3.63a}$$

On the other hand, one obtains the following values for the torsional stiffnesses of rectangles with various ratios of h/b:

Table 3.1. Torsional stiffnesses some rectangular cross-sections

$\frac{h}{b}$	1	1.5	2	3	6
$T/(GS^2b/h)$	0.141	0.196	0.229	0.263	0.298

As h/b approaches infinity, the torsional stiffness approaches the limiting value

$$T = \frac{Gb^3h}{3}. \tag{3.64}$$

If one introduces values of Θ' and T given by Eqs. (3.63) and (3.64) into Eq. (3.62), then one obtains the following values for the propagation velocities c_{TI} of torsional waves on bars with rectangular cross-sections:

Table 3.2. Torsional wave speed corrections for some rectangular cross-sections

$\frac{h}{b}$	1	1.5	2	3	6
$\frac{c_{TI}}{c_T}$	0.92	0.85	0.74	0.56	0.32

One notes that c_{TI} becomes smaller and smaller in comparison with the value given by Eq. (3.62), as the height-to width ratio becomes larger and

larger. For large values of *h/b*, one obtains from Eqs. (3.63a) and (3.64) the approximation

$$c_{TI} = \frac{2b}{h} c_T . \tag{3.65}$$

A comparison with the values given in Eq. (3.65) shows that this approximate relation is acceptably accurate for *h/b* greater than 6.

The phenomena, which here have been investigated quantitatively for a rectangular cross-section, are also valid in principle for all other cross-sections with no rotational symmetry. Their moments of inertia are always greater, and their torsional stiffness always smaller than those for a circular cross-section of the same area. From the values tabled as well as given by Eq. (3.65) for a special case, one may deduce the general result that the propagation speeds of torsional waves in rods with elongated cross-sections are considerably lower than those of transverse waves.

Torsional waves in rods whose cross-sections are not rotationally symmetric are not pure transverse waves, because motions in the direction of propagation accompany them, so that

$$\xi \neq 0. \tag{3.66}$$

Surfaces which initially are planes perpendicular to the axis of the rod become curved. One may observe such distortions by twisting an eraser with a rectangular cross-section. The longitudinal displacements, of course, are again very small compared with the transverse ones, so that one may again classify all torsional waves on bars with non-rotationally-symmetric cross-sections as “quasi-transverse”. (In order to differentiate the propagation speed of such waves from c_T, the notation c_{TI} was introduced, in analogy with the notation to differentiate c_L from c_{LI}; in both cases, the additional subscript *I* indicates that there occurs a secondary motion perpendicular to the primary motion.)

A completely rigorous analysis must also explore the validity of the assumption (which was taken from statics) that the axial displacements can propagate longitudinally without obstruction i.e., that there occur no longitudinal stresses σ_x. For the present purposes, however, it suffices to note that in every wave motion there occur opposite conditions (changes in algebraic sign) at all locations which are half a wavelength apart. Since these half-wavelengths here always are smaller than the corresponding longitudinal half-wavelengths, which determine the equalization of alternating longitudinal stresses, one may conclude that the assumption to unobstructed longitudinal stress propagation can lead to no significant discrepancies. One may also readily determine on the basis of simple estimates

that the inertia forces, which oppose the longitudinal motions, are negligibly small compared with the elastic forces.

Torsional waves on bars with non-rotationally-symmetric cross-sections also differ from those on bars with circular and annular cross-sections in another significant way. In the latter, the surface only moves tangential to itself and thus can produce no sound radiation, whereas for the former under torsion, there also occur components of motion normal to the surface. But because here regions of opposite motion perpendicular to the axis of a bar always lie close to each other, significant radiation associated with torsional waves can result only at high frequencies. (Of course, at high enough frequencies, the entire cross-section no longer vibrates in phase.)

All of the wave types discussed so far make only negligible direct contributions to the radiation of sound into air. However, they may be important as intermediate carriers of energy, which may eventually be radiated elsewhere into the surrounding medium.

3.3 Bending Waves

3.3.1 Pure Bending Waves

Of all the various wave types, bending waves, which also are called flexural waves are by far the most important for sound radiation. Because of the rather large transverse deflections associated with them, one might be inclined to include bending waves in the class of transverse waves. But such a classification would be wrong – not only because the stresses and strains that dominate the potential energy in bending waves act in the longitudinal direction, but also because the entire behaviour of such waves and the underlying differential equations differ so greatly from those of the previously discussed transverse waves that even use of a name like pseudo-transverse waves would be misleading. Flexural waves also differ no less basically from quasi-longitudinal waves. In short, flexural waves fall into a class by themselves.

Flexural waves, unlike the other wave types, must be represented by four field variables instead of two, and therefore also the boundary conditions are more complex. It is convenient to use the following four variables. The (transverse) velocity v_y of an element, the angular velocity w_z about the z-axis, which is perpendicular both to the axis of the beam and to the transverse displacement, the bending moment M_z, which acts on a cross-section (again about the z-axis), and the shear force F_y transmitted across the section. For a plate, the moments and forces are considered per unit width and are represented by M'_z and F'_y. One may select appropriate

algebraic signs by taking v_y positive in the positive y-direction, selecting w_z as positive for counter-clockwise rotation in Fig. 3.9, and choosing M_z and F_y so that the products

$$M_z \cdot w_z = W_M \tag{3.67a}$$

and

$$F_y \cdot v_y = W_F \tag{3.67b}$$

represent power flow in the x-direction. Even at this stage one observes that two different forms of power flow occur, a fact which will turn out to be of considerable importance.

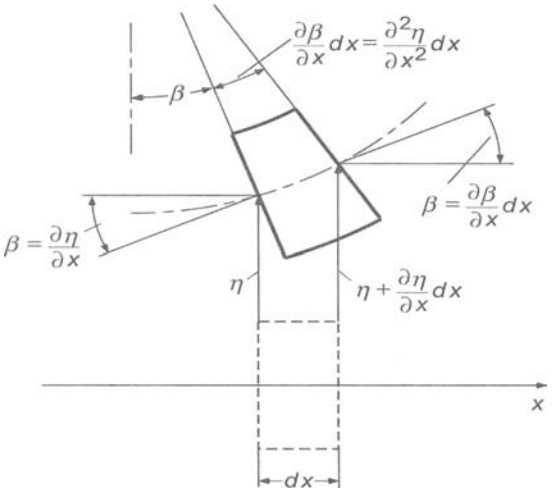

Fig. 3.7. Displacements and deformations in bending

The four field variables here are related by four differential equations, which again couple these variables cyclically. The lateral displacement η and the rotation of a cross-section through the small angle β (see Fig. 3.7) are related by the approximate expression

$$\beta = \frac{\partial\eta}{\partial x}. \tag{3.68}$$

Differentiation with respect to time then leads to the following relation between the angular and lateral velocities:

$$w_z = \frac{\partial v_y}{\partial x}. \tag{3.69}$$

The rate of change of the angular velocity with distance is equal to the time-wise rate of change of the curvature, because for small lateral displacements η, both can be represented in terms of $\partial^2\eta/\partial x^2$:

$$\frac{\partial w_z}{\partial x} = \frac{\partial^2 v_y}{\partial x^2} = \frac{\partial}{\partial t}\left(\frac{\partial^2 \eta}{\partial x^2}\right). \tag{3.70}$$

As is shown in elementary strength of materials, the curvature depends primarily on the local bending moment and is proportional to it i.e.,

$$\frac{\partial^2 \eta}{\partial x^2} = -\frac{M_z}{B}. \tag{3.71}$$

The negative algebraic sign results from taking M_z positive for power flow in the positive x-direction i.e., from taking M_z positive on the left (smaller x) surface of an element as shown in Fig. 3.9 if M_z acts in the same direction as w_z. This direction of M_z, however, is opposite to that which produces a positive curvature.

The constant of proportionality B is called the bending stiffness or flexural stiffness. This stiffness may be determined on the basis of the experimentally verified assumptions that plain sections remain plane and merely rotate by an angle $\partial\eta/\partial x$ (so that two neighbouring sections rotate with respect to each other by an amount $\partial^2\eta/\partial x^2\ dx$) and that this rotation affects only the extensions or compressions in the axial direction. The additional deformations that result from shear displacements produced by the shearing forces may be neglected, provided that the bending wavelength is large compared with the cross-sectional dimensions; this relative size of wavelength may be considered as a necessary condition “pure bending waves”.

The strains ε_x in the axial direction increase linearly with the distance y from a neutral fiber,

$$\varepsilon_x = -y\frac{\partial^2 \eta}{\partial x^2}. \tag{3.72}$$

For symmetric cross-sections, the neutral fibre is located at the midpoint of the section, see Fig. 3.8. The negative algebraic sign indicates the occurrence of compression at locations above the neutral fibre i.e., for positive y there occur compressive strains. The same sign applies also for the tensile and compressive stresses,

$$\sigma_x = E\varepsilon_x = -Ey\frac{\partial^2 \eta}{\partial x^2}. \tag{3.73}$$

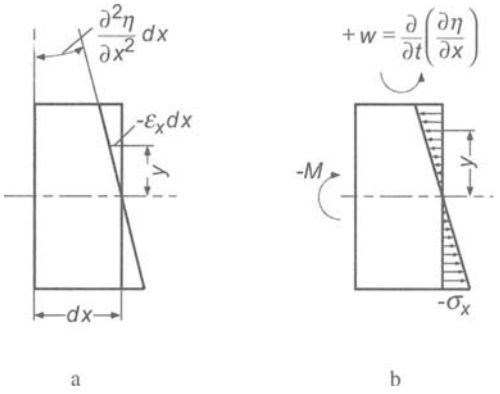

Fig. 3.8. Distribution of a) strain and b) stress over cross-section

For plane bending of plates, one must again replace E by $E/(1\text{-}\mu^2)$, in order to account for the fact that cross-sectional contraction is prevented in one direction. One may obtain the bending moments by multiplying the stresses σ_x by the lever y, see Fig. 3.8 and summing them over the area of the cross-section:

$$M_z = \int_S \sigma_x y \; dS = -E\frac{\partial^2\eta}{\partial x^2}\int_S y^2 dS = -EI\frac{\partial^2\eta}{\partial x^2}. \tag{3.74}$$

In this expression, I is the second moment of area about the z-axis. As is observed from a comparison of Eqs. (3.71) and (3.74), the bending stiffness of the system is given by the product of the material related Young's modulus and cross-sectional shape related second area moment I

$$B = EI = E\int_s y^2 dS \tag{3.75}$$

The second moment of area for a rectangular cross-section of height h and width b, a tube with inner radius r_i and outer r_o as well as a solid cylinder of radius r_o are given by:

$$\frac{bh^3}{12};\quad \frac{\pi}{4}\left(r_o^4 - r_i^4\right);\quad \frac{\pi}{4}r_o^4 \tag{3.76}$$

For complicated cross-sectional shapes, the second area moment can be taken from a handbook but also calculated analytically or numerically employing Eq. (3.75). It should be noted that the reference $y = 0$ for the integration must first be estimated from

$$\int_S E y dS = 0 \tag{3.76a}$$

This procedure is also applicable when multi-layered beams are considered, where Young's modulus E is a function of y.

Upon differentiating (3.71) with respect to time and introducing the rotational velocity from (3.70) one obtains

$$\frac{\partial M_z}{\partial t} = -B \frac{\partial w_z}{\partial x}. \tag{3.77}$$

The expression relating the shear force F_y to the bending moment M_z may also be obtained from static bending theory. This relation results from the moment equilibrium of an element of length dx, as shown in Fig. 3.9 together with the positive direction, and can be written as

$$M_z - \left(M_z + \frac{\partial M_z}{\partial x} dx \right) - F_y dx = 0 \tag{3.78}$$

yielding

$$F_y = -\frac{\partial M_z}{\partial x} \tag{3.78a}$$

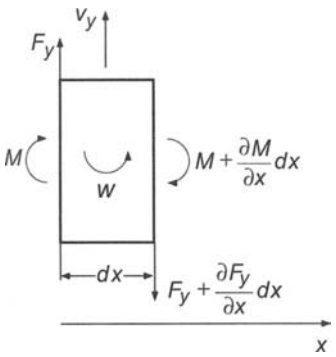

Fig. 3.9. Field variables for a beam element in bending indicating the positive directions

For the dynamics, also an inertia term have to be included on the right hand side of (3.78), which amounts to

$$I \rho dx \frac{\partial w_z}{\partial t}$$

but, as will be shown later, the kinetic energy associated with such rotational motion can be neglected in comparison with that associated with translational motion as long as the bending wavelength is large composed with the cross-sectional dimensions cf., Sect. 3.8.2.

Finally, is needed a relation between the shear force and the transverse velocity to complete the cycle of equations. This relation may be obtained from an application of Newton's second law to an element of the beam, see Fig. 3.9,

$$F_y - \left(F_y + \frac{\partial F_y}{\partial x} dx \right) = m' dx \frac{\partial v_y}{\partial t} \tag{3.79}$$

which reduces to

$$\frac{\partial F_y}{\partial x} = m' \frac{\partial v_y}{\partial t}. \tag{3.79a}$$

Here,

$$m' = \rho S \tag{3.80}$$

is the mass per unit length.

The combination of Eqs. (3.69), (3.77), (3.78a) and (3.79a) furnishes the one-dimensional form of the bending wave equation, which is valid for all field variables

$$-B \frac{\partial^4}{\partial x^4} \left(v_y, w_z, M_z, F_y \right) = m' \frac{\partial^2}{\partial t^2} \left(v_y, w_z, M_z, F_y \right) \tag{3.81}$$

This equation resembles the usual wave equations only in that the time derivative is of second order. In contrast to the other wave equations, the left-hand side of Eq. (3.81) involves the fourth derivative with respect to space and appears with a negative sign. This algebraic sign, which affects the basic character of the solutions, is not the result of arbitrary choices of signs for the field variables and cannot be changed by modified choices.

The fact that the spatial and temporal derivatives appear with different orders implies that the wave motion is dispersive. Furthermore, the dispersion, in general, cannot be given a simple functional description.

On the other hand, Fourier analysis is still applicable such that any time dependence can be decomposed in pure tonal components and the propagation of those temporally sinusoidal components investigated.

The spatial variation of temporally waves can readily be shown to allow also sinusoidal forms i.e., sinusoidal flexural waves are also possible. By substituting

$$v_y = \hat{v}_y \sin\left(\omega t - kx + \varphi_v\right) \tag{3.82}$$

in (3.81), it is seen that the velocity assumed satisfies the wave equation for arbitrary amplitudes and phase angles as long as the angular frequency and wave number characterizing the temporal and spatial periodicity respectively, obey

$$\frac{B}{m'} k^4 = \omega^2 \tag{3.83}$$

Also in this case, the ratio of angular frequency to wavenumber

$$\frac{\omega}{k} = c \tag{3.84}$$

represents the speed with which one has to move to remain at the same phase of the sinusoidal wave motion. This 'phase speed' of bending waves, designated by subindex *B* thus depends on frequency as seen from Eq. (3.83),

$$c_B = \sqrt[4]{\frac{B}{m'}} \sqrt[2]{\omega}. \tag{3.85}$$

Such a phase speed clearly represents speed of propagation only of one infinite sinusoidal wave. Waveforms that in a Fourier analysis sense are composed of various sinusoidal components always distort since high frequency components propagate with higher speed than those of low frequency.

In optics, the corresponding process, is called dispersion and this concept is carried over to all wave carrying systems with frequency dependent phase speed.

For a plate of thickness *h*, Eq. (3.85) can be simplified to

$$c_B \approx \sqrt{1.8 c_{LI} h f} = c_{LI} \sqrt{\frac{1.8h}{\lambda_{LI}}} \tag{3.85a}$$

In Fig. 3.10 are shown some bending wave speeds for plates of various materials as function of the product of thickness and frequency. The curves are approximately valid also for beams with rectangular cross-sections since Poisson's contraction only has a minute effect. In the figure, moreover, the frequency independent phase speeds of waves in air and water are included as is the limit of validity of the Kirchhoff bending theory cf., (3.196b).

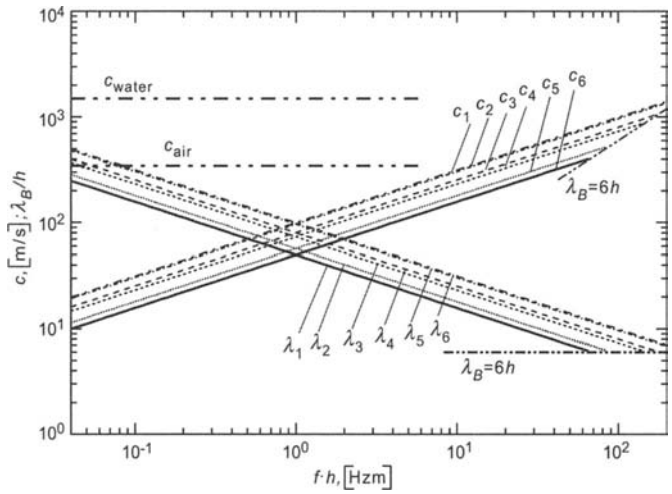

Fig. 3.10. Flexural wave speed (c_1 to c_6) and normalized wavelength (λ_1 to λ_6) for plates of various materials versus product of thickness and frequency. (1) Steel, aluminium, (2) glass, (3) brass, dense concrete, (4) brick stone, chipboard, (5) light-weight concrete, Gypsum board, perspex and (6) lead

Besides the theoretical case of an infinite sinusoidal wave, there is another special case, in which it is meaningful to consider a definite propagation speed. This is the case, in which a wave motion occurs composed of several components of slightly differing periodicity. Intuitively, one could jump to the conclusion that these phase speeds have a small variation around some mean which also could be used as a mean speed. Unfortunately, it is a bit more involved as can be gathered from the simplest case with two superimposed, equally strong components, of frequencies ω, and ω_2 and wavenumbers k_1 and k_2. Such a superposition results in a modulation

$$\begin{aligned}&\sin\left(\omega_1 t - k_1 x\right) + \sin\left(\omega_2 t - k_2 x\right)\\ &= 2\sin\left(\frac{\omega_1+\omega_2}{2}t - \frac{k_1+k_2}{2}k\right)\cos\left(\frac{\omega_1-\omega_2}{2}t - \frac{k_1-k_2}{2}x\right),\end{aligned} \tag{3.86}$$

which means that a sinusoidal carrier wave of the mean frequency $(\omega_1 + \omega_2)/2$ and of the mean wave number $(k_1 + k_2)/2$ is amplitude modulated by the substantially lower wavenumber $(k_1 - k_2)/2$. This envelope curve, however, is of primary interest since it determines the average energy transport. Although the carrier wave indeed propagates with the average phase speed

$$c = \frac{\omega_1 + \omega_2}{k_1 + k_2}, \tag{3.87}$$

the envelope curve, which encloses the group of the wave peaks, propagates at the 'group speed'

$$c_g = \frac{\omega_1 - \omega_2}{k_1 - k_2} = \frac{\Delta\omega}{\Delta k}. \tag{3.88}$$

This group velocity can be considerably larger as well as considerably smaller than the phase speed. In the limiting case, where the frequencies and wavenumbers are arbitrarily close to each other, c_g is given by the derivative

$$c_g = \frac{d\omega}{dk} \tag{3.88a}$$

The group speed as defined here does not apply only to the envelope function of a modulation given by Eq. (3.86) but in general is applicable to the envelope function of all processes composed of arbitrarily many adjacent wave trains of arbitrary amplitudes and phases. The group speed is also applicable to continuous spectra which have negligible components outside of the immediate vicinity of the carrier frequency. Such individual wave-groups are of significant interest since they represent the only type of excitation signals for which dispersive systems exhibit clearly defined transit times.

From Eq. (3.83), the group velocity of bending waves c_{gB} obeys

$$c_{gB} = 2\sqrt{\frac{B}{m'}}k = 2c_B, \tag{3.89}$$

which thus is twice the phase speed. In Fig. 3.11a, this relation is exemplified. The upper and lower curves represent two points in time respectively, which are displaced half a period of the carrier wave. Therefore, the carrier wave is shifted half a wavelength of the carrier wave rightwards whereas thereby, the envelope curve is shifted the double distance. The lower part of Fig. 3.11b shows a continuous wavenumber spectrum - in this case represented by a Gaussian error curve. The significant position of this curve encompasses only a small wavenumber range. There above is the dispersion relation ω (k) plotted and indicated is the difference between group and phase speeds via the associated angles.

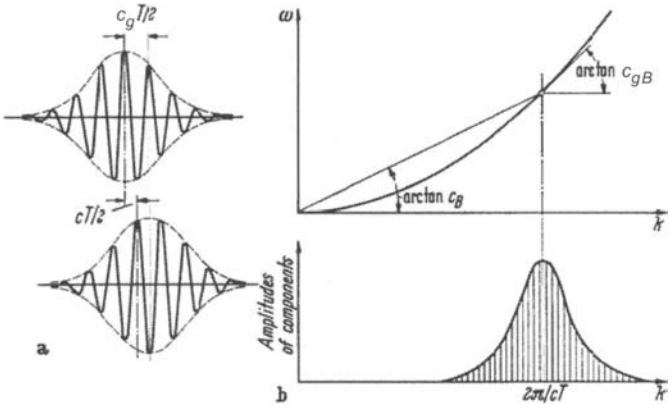

Fig. 3.11. Illustration of the difference between group and phase speeds

3.3.2 Energy Relations

The fact that the energy is propagated with the group speed can be demonstrated by means of the energy relations that holds for pure sinusoidal waves. These energy relations for bending waves differ markedly from those of the previously discussed wave types as is observed from a comparison of Fig. 3.12 pertaining to bending waves and Fig. 3.2 associated with a longitudinal wave. The sinusoidal displacement in the former case can be written as

$$\eta = \hat{\eta} \sin(\omega t - kx). \tag{3.90}$$

At the top of Fig. 3.12 is shown the corresponding deformation at time $t = 0$. Next follow the spatial distributions of the translational velocity, the rotational velocity, the bending moment and the cross-sectional force. Pairwise, F_y and v_y are in phase as are M_z and w_z but group-wise a quarter period out-of-phase. These phase relations lead to a remarkable property of the energy flow composed of

$$\begin{aligned} W_F &= F_y v_y = \hat{\eta}^2 B\omega k^3 \cos^2 kx = \hat{F}_y \hat{v}_y \cos^2 kx \\ W_M &= M_z w_z = \hat{\eta}^2 B\omega k^3 \sin^2 kx = \hat{M}_z \hat{w}_z \sin^2 kx \end{aligned} \tag{3.91}$$

Their sum, however, establishes a time-invariant power

$$W = W_F + W_M = \hat{\eta}^2 B\omega k^3 \tag{3.92}$$

For the sinusoidal flexural wave, the energy flow does not vary with the period λ/2 between zero and a maximum value but is spatially constant.

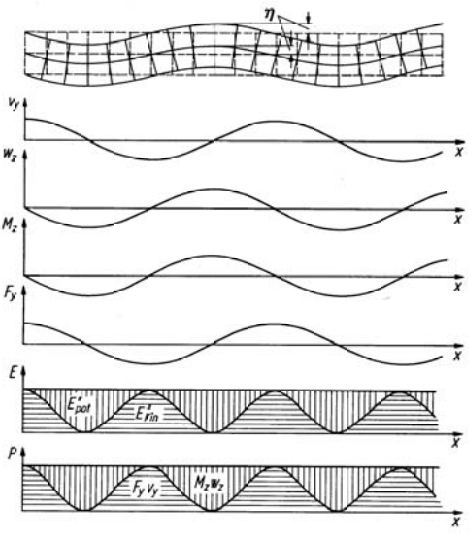

Fig. 3.12. Field variable and energy distribution of a sinusoidal flexural wave

Accordingly, the same must be true also for the sum of potential and kinetic energy. Per unit length, the latter amounts to

$$SE_{kin,T} = \frac{m'}{2} v_y^2 = \frac{m'}{2} (\omega\eta)^2 \cos^2 kx = \frac{\rho S}{2} \hat{v}_y^2 \cos kx \qquad (3.92a)$$

and is essentially governed by the translational energy. Upon comparing it with that associated with rotations

$$SE_{kin,R} = \frac{\rho I}{2} w_z^2 = \frac{\rho I}{2} k^2 \hat{v}_y^2 \sin^2 kx,$$

it is noted that the rotational energy maximum is a factor

$$\frac{\mathrm{Max}\left(\overline{E}_{kin,R}\right)}{\mathrm{Max}\left(E_{kin,T}\right)} = \left(\frac{2\pi\sqrt{I/S}}{\lambda}\right)^2$$

smaller. Owing to the fact that the rotational energy grows towards the boundaries, an average value is understood, which is denoted by an over bar. As has already been mentioned, in pure bending the cross-sectional

dimensions must be small compared with the wavelength. For this reason, Eqs. (3.85) and (3.89) are also only valid in the range where the calculated wave speeds are substantially below that of the longitudinal wave, c_L. The potential energy, on the other hand, is controlled by the axial stresses and strains,

$$S\overline{E}_{pot} = \frac{1}{2}\int_S \sigma_x \varepsilon_x dS = \frac{E}{2}\left(\frac{\partial^2 \eta}{\partial x^2}\right)^2 \int_S y^2 dS = \frac{B}{2} k^4 \hat{\eta}^2 kx. \tag{3.92b}$$

Both the energy components vary between zero and a maximum value with period of $\lambda/2$. This maximum value is, furthermore, in both cases the same, which can be seen by substituting expression (3.83) in the relation for the potential energy. The two energy components oscillations are quarter wavelength displaced, however, and where the beam, for example, has its maximum curvature and is about to change the direction of motion and thus momentarily at rest, the potential energy is a maximum. Thus, the sum of the two energy components is a constant,

$$\begin{aligned} S\overline{E}_{tot} &= \left(S\overline{E}_{pot} + S\overline{E}_{kin}\right) = \frac{\hat{\eta}^2}{2}\left(m'\omega^2 \cos^2 kx + Bk^4 \sin^2 kx\right) \\ &= \frac{B}{2} k^4 \hat{\eta}^2. \end{aligned} \tag{3.92c}$$

This is illustrated in Fig. 3.12 with horizontally and vertically hatched regions. The constant energy per unit length can be found to be related to the constant energy flow W as

$$W = 2\frac{\omega}{k} S\overline{E}_{tot} = 2c_B S\overline{E}_{tot} = c_{gB} S\overline{E}_{tot}, \tag{3.93}$$

and the power transmission is again determined by the group speed.

3.4 Wave Motions on Beams of Finite Length

Waves that propagate in one direction, which have been the subject of discussion until now, can occur only as long as they encounter no change in the wave carrying system. Every homogeneous wave guide, however, have ends and at those ends the wave motion always change direction, usually also its amplitude and phase, and often even its basic characters.

This section deals only with the one-dimensional case, and for the sake of further simplicity, only with waves in beams of the types treated in Sects. 3.1.2, 3.2.2, and 3.3.1, in the presence of ideal boundary conditions.

3.4.1 Longitudinal Natural Vibrations

It is convenient to begin by considering a quasi-longitudinal wave arriving at the end of a beam at $x = 0$, which end may be either free or clamped (i.e., built into a rigid body). At a rigidly constrained end, the velocity must vanish whereas at a free end, the force. For airborne sound in ducts, rigid ends can be approximated well in practice, but for sound in liquid – and even more so for sound in solids – free ends can be obtained much more easily. It is therefore preferable, particularly because experimental verifications will also be of interest, to study first a beam with a free, for which the boundary conditions are

$$F = 0 \quad ; \quad x = 0. \tag{3.94}$$

These conditions must be satisfied at all times. However, the arriving wave

$$F_+\left(t - \frac{x}{c}\right),$$

where the subscript + indicates that the waves propagates in the positive x-direction, cannot satisfy the boundary conditions by itself. An additional wave, which propagates in the negative x-direction,

$$F_-\left(t + \frac{x}{c}\right),$$

must be added. Then

$$F(x,\ t) = F_+\left(t - \frac{x}{c}\right) + F_-\left(t + \frac{x}{c}\right), \tag{3.95}$$

and satisfaction of the boundary condition of Eq. (3.94) requires that

$$F_-(t,\ 0) = -F_+(t,\ 0). \tag{3.96a}$$

Thus, as far as the force is concerned, the wave merely changes its sign becomes "ideally reflected".

One may now determine the behaviour of the velocity, by noting first that the velocity in the arriving wave has the same dependence as the force,

$$v_+ = \frac{1}{\rho S c_L} F_+\left(t - \frac{x}{c}\right),$$

as is evident from Eq. (3.14) for a pure longitudinal wave, and as may be easily derived from Eqs. (3.29) and (3.30). In the reflected wave, however, the ratio of v_- to F_- occurs with a changed algebraic sign,

$$v_{-} = \frac{-1}{\rho S c_L} F_{-}\left(t + \frac{x}{c}\right),$$

because in this wave energy is transported in the negative direction. At the boundary, therefore,

$$v_{-}(t,0) = v_{+}(t,0). \tag{3.96b}$$

Thus, while the force vanishes at the boundary, the velocity there is twice that of the arriving wave:

$$v(t,0) = 2v_{+}(t,0). \tag{3.97}$$

An assumption of zero motion at $x = 0$ would have led to a doubling of the force at this end.

The equations for torsional waves, which are discussed in Sect. 3.2.2, are analogous to those for quasi-longitudinal waves, and this analogy also holds for the boundary conditions at free and clamped ends where either the moment M or the angular velocity w vanishes. Without needing to analyse torsional waves in detail, one may therefore conclude that torsional waves also experience ideal reflection at free or rigid ends. Also, M changes sign at a free end, but w does not, and the reverse is true at clamped end. Similarly, the angular velocity is doubled at a free end, and the moment, at a clamped end.

A wave propagating on a beam which has the same type of boundary at both ends is reflected similarly at both ends. After two reflections, the wave again propagates in the same direction as originally, and both field variables again have the original algebraic sign. This implies that everywhere each field variable varies periodically in time. The period,

$$T = \frac{2l}{c}, \tag{3.98a}$$

corresponds to the time taken by the wave to propagate to one end, from there in the reverse direction to the other end, and from there again to its starting place, all with the same velocity c.

Because every periodic process with frequency

$$f_1 = \frac{1}{T} = \frac{c}{2l} \tag{3.98b}$$

can be analysed in terms of sinusoidal components with frequencies

$$f_n = n\frac{c}{2l}, \tag{3.98c}$$

one is led to consider the character of these component waves or, the character of the vibrations that result from these waves in the presence of the boundary conditions. Because these vibrations are characteristic of the particular beam under consideration, they are called characteristic vibrations. Since such vibrations can occur "naturally" in absence of external driving forces, they are also called natural vibrations.

In the simplest case, such as that of pendulum or an elastically supported mass, constrained to move in only one direction, the natural vibration obeys

$$u = \hat{u}\cos\left(\omega t + \varphi_u\right) \tag{3.99a}$$

for every field variable u (displacement, velocity, restoring force, etc.). The natural vibrations of systems with m independent degrees of freedom, m independent co-ordinates are required, all varying sinusoidally in time, generally with different amplitudes. In the absence of energy losses i.e., in undamped natural vibrations all co-ordinates of the same type transverse their extreme (and their zero) values simultaneously. Therefore, if one takes the time origin $t = 0$ at an instant when all co-ordinates pass through their extreme values, and if one admits positive and negative values for the amplitudes $\hat{u}$, then one may choose $\varphi_u = 0$ and write for any coordinate, say, the k^{th},

$$u_k = \hat{u}_k \cos\omega t. \tag{3.99b}$$

As one progresses toward a continuum, the number of degrees of freedom becomes infinite. Correspondingly, the discreet coordinate amplitudes become a continuous function of space:

$$u\left(x,\ t\right) = \hat{u}\left(x\right)\cos\omega t. \tag{3.99c}$$

This separation of the field behaviour into a function of space and one of time (a process named after D. Bernoulli) can provide even more insight into the concept of natural vibrations than can the decomposition of vibratory motions into propagating waves as in Eq. (3.95) (which goes back to D'Alembert).

From what has been proven so far namely, that the time variation of each field variable is periodic with the period $2l/c$ and may be analysed in terms of its Fourier components, one may conclude only that these Fourier components must be of the form

$$u\left(x,\ t\right) = \hat{u}\left(x\right)\cos\left(\omega t + \varphi_u\left(x\right)\right). \tag{3.99d}$$

This means that one cannot exclude possible phase differences. The more general expression in (3.99d) is of importance, not only because it de-

scribes the natural vibrations of interest here, but also because it can describe any oscillation, which involves sinusoidal vibrations with time, if x is replaced by a positive vector **r**.

The expression of Eq. (3.99d) is no longer separable into multiplicative terms, but may be written either as the sum of two such separable expressions (phase shifted in time with respect to each other),

$$u(x,\ t) = \left[\hat{u}(x)\cos\varphi_u(x)\right]\cos\omega t + \left[-\hat{u}(x)\sin\varphi_u(x)\right]\sin\omega t, \tag{3.99e}$$

or as the real part of a product of two quantities, each of which depends both on space and on time,

$$u(x,\ t) = \mathrm{Re}\left\{\left[\hat{u}(x)e^{j\varphi_u(x)}\right]e^{j\omega t}\right\} = \mathrm{Re}\left\{\underline{\hat{u}}(x)e^{j\omega t}\right\}. \tag{3.99f}$$

By extending the phasor notation introduced in Sect. 2.2, to include a location dependence, the one-dimensional wave Eqs. (3.11), (3.31), (3.46), and (3.61), reduce to the simple vibration equation

$$\frac{d^2\underline{\hat{u}}}{dx^2} + k^2\underline{\hat{u}} = 0. \tag{3.100}$$

By again considering the vibration in terms of two waves propagating in opposite directions, as in Eq. (3.95), one may write the solution of the "spatial" vibration for the special case of the longitudinal force in a beam as

$$\underline{\hat{F}}(x) = \underline{\hat{F}}_+ e^{-jkx} + \underline{\hat{F}}_- e^{+jkx}. \tag{3.101}$$

One may observe that for the first term, which represents a wave propagating in the positive x-direction, the phase must increase with increasing x, because a given phase arrives later at a location for which x is larger.

The first boundary condition, requiring that the axial force at $x = 0$ vanishes, implies that the two phasors $\underline{\hat{F}}_+$ and $\underline{\hat{F}}_-$ must have opposite algebraic signs, as in Eq. (3.96a).

Since one may also write

$$\underline{\hat{F}}_- = -\underline{\hat{F}}_+ \tag{3.102a}$$

as

$$\underline{\hat{F}}_- = \underline{\hat{F}}_+ e^{-j\pi}, \tag{3.102b}$$

one may consider the change of the sign of the force wave due to reflection as a "phase jump" of

$$\gamma = -\pi. \tag{3.102c}$$

From the first boundary condition, one may deduce that the spatial distribution of the axial force is a sinusoid, beginning at $x = 0$:

$$\underline{\hat{F}}(x) = \underline{\hat{F}}_{\max} \sin kx. \tag{3.103}$$

Because of the second boundary condition, which requires vanishing of the force at $x = l$, this sinusoid also must vanish there. This requirement determines k and, therefore, the wavelengths λ

$$k_n l = n\pi;\ l = \frac{n\lambda_n}{2}. \tag{3.104}$$

The frequencies that correspond to these values are the same as those given by Eq. (3.98c), as one would expect. These frequencies are called "natural frequencies", "eigen-frequencies" or "characteristic frequencies". The left-hand part of Fig. 3.13 shows the force distributions for $n = 1, 2, 3$ at the instant at which the greatest absolute values occur. The right-hand part similarly shows the corresponding velocity distributions, and thus also the displacement distributions given by

$$\underline{\hat{v}}_n(x) = \underline{\hat{v}}_{n\max} \cos k_n x\ ,\ \underline{\hat{\xi}}(x) = \underline{\hat{\xi}}_{n\max} \cos k_n x\ , \tag{3.105}$$

respectively the condition that the "round-trip" path length $2l$ is an integral multiple of the wavelength, which is indicated by Eq. (3.104), may also be deduced from a general, easily visualized *principle* which holds for all natural vibrations. This principle states that a natural vibration occurs if a propagating wave, after reflection at all boundaries along its path, returns to its starting point with the same amplitude and phase that is, if such a wave can form a *wave train that closes on itself.* In the present case, the reflections at the ends do not change the amplitudes. Therefore, formation of a closed wave-train requires only phase-matching of the wave as it closes on itself after being reflected at both ends. By applying this principle to a velocity wave, which is reflected without phase change, one obtains the relation (3.104) directly. A corresponding closed wave train for the case of $n = 2$ is illustrated in Fig. 3.14, where the rightward moving part is shown as a solid curve, the leftward moving part as a dotted curve.

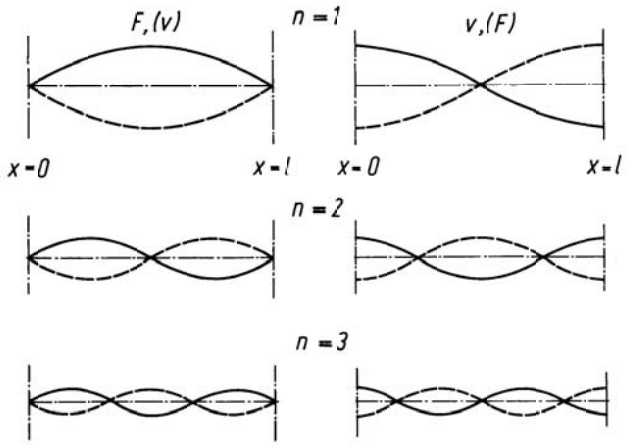

Fig. 3.13. Longitudinal natural vibrations of a rod. F, v without parentheses correspond to free end; F, v in parentheses correspond to clamped ends. (The solid and dashed curves represent conditions half a period apart.)

Application of the "wave train closure principle" to the force wave is a little more difficult, because there occur phase jumps γ_0 and γ_l at $x = 0$ and $x = l$. One must take these phase jumps into account in expressing the requirement that the wave train close on itself in phase. This leads to the general relation

$$2kl - \gamma_0 - \gamma_l = 2m\pi. \tag{3.106}$$

Because each phase jump in this case is equal to -π, Eq. (3.106) differs from Eq. (3.104) only in that it involves $n - 1$ instead of n. Since n can be any integer, the two equations amount to the same thing. One would not expect otherwise, because the natural frequencies obviously cannot depend on which variable one imposes the requirement of phase continuity.

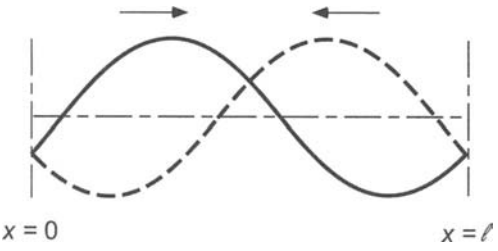

Fig. 3.14. Sketch to illustrate the principle of phase-continuous closure

From the foregoing result one may also deduce that a bar with both ends rigidly constrained has the same natural frequencies as one with free ends. One needs only to note that in an axially constrained bar, the force and velocity boundary conditions and, therefore, also the associated phase jumps, are interchanged with respect to those in a free bar.

From phase continuity at wave train closure, one also may readily determine the natural frequencies of a rod, which is clamped on one end and free on the other, irrespective of if the wave is longitudinal or torsional waves. For any field variable, one obtains a reflection with zero phase change at one end, and a phase jump of -π at the other end. One thus obtains

$$2k_n l = (2n-1)\pi;\ l = \frac{(2n-1)\lambda_n}{4};\ f_n = \frac{(2n-1)c}{4l} \tag{3.107}$$

Like the natural frequencies of a closed-ended organ pipe, the natural frequencies here are associated with the odd integers.

3.4.2 Natural Vibrations in Bending

It is instructive to turn now to flexural vibration of a beam of finite length and to determine the natural frequencies on the basis of the principle of phase continuity. For this purpose first, the phase jumps must be determined, which result from the various boundary conditions. In this case it is not sufficient to deal only with the ideal limiting cases of "clamped" or "free" ends, but also with boundaries where these descriptions apply only to the translational or to the rotational deflections.

A simple support, as represented in the upper let-hand part of Fig. 3.15, prevents a beam from deflecting vertically ($v = 0$) but permits it to rotate. Such a support therefore does not produce bending moments ($M = 0$). At a "built-in" or clamped end, as shown at the upper right of the figure, the translational and rotational displacements both vanish, and thus also the corresponding velocities ($v = 0$, $w = 0$). At a free end, on the other hand, the moment and the shear force vanish ($M = 0$, $F = 0$). Finally, at a "guided" end, as indicated schematically by guidepins in the lower right part of the figure, the beam is free to translate, but prevented from rotating. Thus, the shear force and angular velocity must vanish ($F = 0$, $w = 0$).

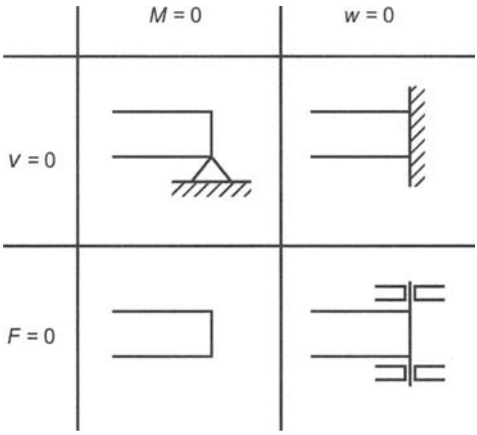

Fig. 3.15. Summary of ideal boundary conditions for bending vibrations of beams

In each of the four cases, two boundary conditions must be satisfied. Addition of a reflected wave to the incident one thus clearly is not enough. This insufficiency demonstrates how closely the doubling of the number of boundary conditions is related to the doubling of the order of the differential equation for the wave system. The differential equation also has other types of solutions than those which correspond to propagating waves.

For sinusoidal time-variation, the bending wave equation, Eq. (3.81), may be rewritten in terms of the phasors $\underline{\hat{v}}$, $\underline{\hat{w}}$, $\underline{\hat{M}}$, $\underline{\hat{F}}$. For example, for $\underline{\hat{v}}$ one obtains

$$\frac{d^4 \underline{\hat{v}}}{dx^4} - k^4 \underline{\hat{v}} = 0, \tag{3.108}$$

where k, which has been written in place of $\sqrt[4]{m'/B}\sqrt{\omega}$ in accordance with Eq. (3.83), represents the wavenumber of a propagating bending wave. Wave motion of the type that result from solutions of the ordinary second-order wave equation also satisfy the bending wave equation. One may arrive at this conclusion by factoring the operator that acts on the $\underline{\hat{v}}$ in Eq. (3.108) to obtain

$$\left(\frac{d^4}{dx^4} - k^4 \right) = \left(\frac{d^2}{dx^2} + k^2 \right) \left(\frac{d^2}{dx^2} - k^2 \right). \tag{3.108a}$$

The first of the factor operators corresponds to the "spatial" equation of vibrations, Eq. (3.100) i.e., it leads to propagating sinusoidal waves of the form given in Eq. (3.101) for the axial force phasor or to the following similar expression for the transverse velocity:

$$\underline{\hat{v}}_1 = \underline{\hat{v}}_+ e^{-jkx} + \underline{\hat{v}}_- e^{+jkx}.$$

Because one may obtain the second operator from the first by replacing $\pm k$ by $\pm jk$, there must also exist solutions of the form

$$\underline{\hat{v}}_2 = \underline{\hat{v}}_{-j} e^{-kx} + \underline{\hat{v}}_j e^{+kx}$$

corresponding to the second operator. Such solutions represent fields with constant phase, which decrease exponentially with the distance from a disturbance (or an end), and which are also called "near fields".

The general solution thus consists of four parts, corresponding to the fourth order of the differential equation

$$\underline{v} = \underline{\hat{v}}_+ e^{-jkx} + \underline{\hat{v}}_- e^{+jkx} + \underline{\hat{v}}_{-j} e^{-kx} + \underline{\hat{v}}_j e^{+kx}, \tag{3.109}$$

and this solution must satisfy two independent boundary conditions at each of the two ends.

If a wave $\underline{\hat{v}}_+ e^{-jkx}$ arrives from the left ($x < 0$) at an end located at $x = 0$, then there results at that location a reflected wave $\underline{\hat{v}}_- e^{+jkx}$ and a near-field $\underline{\hat{v}}_j e^{kx}$, which together make it possible to satisfy the two boundary conditions there.

In some special cases, the nearfield may vanish. This happens, for example, at a simply supported end. For such an end, the boundary conditions $\underline{v} = 0; \underline{M} = 0$, which are equivalent to

$$\underline{v} = 0; \ \frac{d^2 \underline{v}}{dx^2} = 0, \tag{3.110a}$$

leading to the two equations

$$\underline{\hat{v}}_- + \underline{\hat{v}}_j = -\underline{\hat{v}}_+ \quad , \quad -\underline{\hat{v}}_- + \underline{\hat{v}}_j = +\underline{\hat{v}}_+. \tag{3.110b}$$

In these equations, the known quantities appear on the right-hand side, those to be determined appear on the left-hand side. By adding these equations, one finds

$$\underline{\hat{v}}_j = 0 \quad , \quad -\underline{\hat{v}}_- = \underline{\hat{v}}_+, \tag{3.110c}$$

which means that the same -π phase jump is obtained as for the velocity of longitudinal waves in a rigidly constrained beam.

The distributions indicated in the left-hand part of Fig. 3.13 therefore also correspond to the velocity and displacement of a beam that is simply supported on both ends. However, because of the dispersive nature of bending waves, the frequencies are proportional to the square of the wavenumber, according to Eq. (3.83). Therefore, the natural frequencies here are proportional to the squares of the integers:

$$f_n = \frac{1}{2\pi}\sqrt{\frac{B}{m'}}k^2 = \frac{\pi}{2}\sqrt{\frac{B}{m'}}\frac{n^2}{l^2}. \tag{3.110d}$$

For a beam with "guided" ends (lower right-hand side of Fig. 3.15), one finds the same natural frequencies, because for this case the equations for the angular velocity *w* are identical to those for *v* for a simply supported beam.

Reflection of a wave from a free end, on the other hand, gives rise to a nearfield. Since the corresponding boundary conditions,

$$\underline{M} = 0,\ \underline{F} = 0, \tag{3.111a}$$

may also be written as

$$\underline{M} = 0,\ \frac{d\underline{M}}{dx} = 0, \tag{3.111b}$$

it is convenient to describe the field in terms of the phasors for the moments in the incident wave $\underline{\hat{M}}_+ e^{-jkx}$, the reflected wave $\underline{\hat{M}}_- e^{+jkx}$, and the nearfield $\underline{\hat{M}}_j e^{kx}$.

The boundary conditions lead to two equations

$$\begin{aligned} \underline{\hat{M}}_- + \underline{\hat{M}}_j &= -\underline{\hat{M}}_+ \\ j\underline{\hat{M}}_- + \underline{\hat{M}}_j &= j\underline{\hat{M}}_+, \end{aligned} \tag{3.111c}$$

from which one may obtain the reflected nearfield and propagating wave phasors

$$\underline{\hat{M}}_j = \left(-1 + j\right)\underline{\hat{M}}_+, \qquad \underline{\hat{M}}_- = -j\underline{\hat{M}}_+ \tag{3.111d}$$

The magnitude of this nearfield phasor at the beam's end is even greater than that for the incident wave. Although this greater magnitude extends the effective length of the nearfield, it does not change the fact that at some distance from the beam end there remains only the reflected wave, and that only the latter wave transports energy. Because the reflected energy must be equal to the incident energy, the amplitude of the reflected wave must be equal to that of the incident one. Indeed, the solution for $\underline{\hat{M}}_-$ correspond to a phase jump of $\gamma = -\pi/2$.

If one assumes that the nearfield which results at one end is negligible at the other end (an assumption which becomes increasingly valid for shorter wavelengths, that is, at higher frequencies), then wave-train closure is again obtained if the wave train closes on itself with equal phase. In this case one obtains the following approximate expression for the natural frequencies of free-free beams (i.e., beams with both ends free).

$$2k_n l \approx (2n-1)\pi \ , \ f_n = \frac{1}{2\pi}\sqrt{\frac{B}{m'}}k_n^2 \approx \frac{\pi}{8}\sqrt{\frac{B}{m'}}\frac{(2n-1)^2}{l^2}. \qquad (3.111e)$$

The above relation between the wavenumber and the length of the beam is the same as that which previously was obtained for longitudinal waves in a clamped-free beam. In the latter case, the phase change of -π was produced at one end, whereas in the present case a phase jump of -π/2 occurs at each of the two ends.

Figure 3.16 shows the velocity (or the displacement) distributions for three natural vibrations of a free-free beam. The thick curves include the nearfield contributions, whereas the thin curves correspond to only the pure propagating waves.

Although Eq. (3.111e) admits the case of $n = 1$, this case must be ruled out on physical grounds. It would imply either a rigid-body translation of the beam and thus an oscillating motion of its centre of gravity or a rigid-body rotational oscillation of the beam about its centre; the former is impossible because no external forces are present, the second, because there is no external moment.

The natural frequencies of free-free beams are approx. in the ratio 9:25:49:81… . The "overtones" thus are not related harmonically to the fundamental.

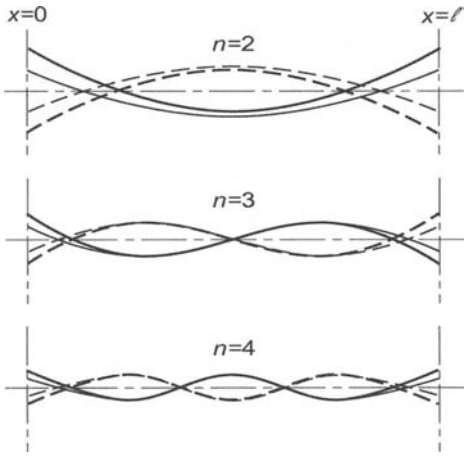

Fig. 3.16. Flexural natural vibrations of a free-free beam. Light curves: without nearfield; heavy curves: with nearfield. (Again, solid and dashed curves represent conditions half a period apart.)

For a clamped-clamped beam, the boundary conditions are

$$\underline{v} = 0, \quad \frac{d\underline{v}}{dx} = 0.$$

Therefore, if one uses v instead of M, one obtains the same results as before, and one finds that Eq. (3.111e) applies equally well also for clamped-clamped beams.

In most cases, the difference between the actual and the ideally rigid constraint at the support is likely to have a greater effect on the natural frequencies than does neglecting of the nearfield effects in the derivation Eq. (3.111e) and the exact values is generally smaller for $n > 2$ than the accuracy with which one can determine B, m', l, or with which can measure the frequency.

Corrections to Eq. (3.111e) are of practical interest only for the lowest natural frequencies of free-free beams. It is also instructive to investigate these corrections, in order to remove any impression that the wave-train closure is only an approximation. Indeed, this principle always yields exact results also for flexural wave problems, provided one takes into account that the nearfields generated at one end still have finite values at the other and there again give rise to additional waves and nearfields.

As shown by means of (3.111c) and (3.111d), a propagating wave of amplitude $\hat{M}_+$ results in

$$\begin{aligned} \underline{\hat{M}}_- &= j\underline{\hat{M}}_+ = \underline{\hat{M}}_+ e^{-j\pi/2}, \\ \underline{\hat{M}}_{-j} &= -(1-j)\underline{\hat{M}}_+ = -\sqrt{2}\,\underline{\hat{M}}_+ e^{-j\pi/4}, \end{aligned} \tag{3.111f}$$

as reflected propagating wave and nearfield respectively.
Upon applying this on a nearfield of amplitude $\hat{M}_{+j}$, the boundary conditions in (3.111b) require that $\underline{\hat{M}}_{+j} + \underline{\hat{M}}_{-j} + \underline{\hat{M}}_- = 0$ and $-\underline{\hat{M}}_{+j} + \underline{\hat{M}}_{-j} + j\hat{M}_- = 0$ respectively. It follows that subsequent to the reflection are formed

$$\begin{aligned} \underline{\hat{M}}_{-j} &= j\underline{\hat{M}}_{+j} = \underline{\hat{M}}_{+j} e^{j\pi/2}, \\ \underline{\hat{M}}_- &= -(1+j)\underline{\hat{M}}_{+j} = -\sqrt{2}\,\underline{\hat{M}}_{+j} e^{j\pi/4}, \end{aligned} \tag{3.111g}$$

as reflected nearfield and propagating waves respectively. The principle of phase continuity requires that after a roundtrip, comprising two reflections with the conversions from propagating wave to nearfield as well as from nearfield to propagating wave, the initial conditions are regained. Since a single passage leads to a phase shift of kl and hence a multiplication by e^{-jkl} for the propagating part and by e^{-kl} for the nearfield, the former component of amplitude $\hat{M}_+$ yields

$$\begin{aligned}&\underline{\hat{M}}_{+}\left\{e^{-2jkl}\left(-j\right)^{2}+e^{-jkl}e^{-kl}\left(1+j\right)\left(1-j\right)\right\}\\&-\underline{\hat{M}}_{+}\left\{e^{-2jkl}j\left(1-j\right)+e^{-jkl}e^{-kl}j\left(1-j\right)\right\}\end{aligned}\tag{3.111h}$$

subsequent on a complete roundtrip. If the abbreviations *P* and *N* are introduced for the propagating wave and nearfield respectively, the separate terms in the expression correspond to *PPP*, *PNP*, *PPN* and *PNN*. In these combinations, the first letter denotes the initial wave, the second its form after the first reflection whilst the last that resulting after completing the roundtrip.

Employed on an initial nearfield of amplitude $\hat{M}_{+j}$ follows the combinations *NPP*, *NNP*, *NPN* and *NNN*. This means that the roundtrip is described by

$$\begin{aligned}&\underline{\hat{M}}_{+j}\left\{e^{-jkl}e^{-kl}j\left(1+j\right)-e^{-2kl}j\left(1+j\right)\right\}\\&-\underline{\hat{M}}_{+j}\left\{e^{-jkl}e^{-kl}\left(1-j\right)\left(1+j\right)+e^{-2kl}j^{2}\right\}.\end{aligned}\tag{3.111i}$$

The wave-train-closure principle now requires that the sum of the propagating field components (the first brackets in the above two expressions) equal the initial amplitude $\hat{M}_{+}$. Similarly, the sum of the nearfield components (the second brackets) must equal the amplitude $\hat{M}_{+j}$. Accordingly,

$$\begin{aligned}&\underline{\hat{M}}_{+}\left[-e^{-2jkl}+2e^{-jkl-kl}-1\right]+\underline{\hat{M}}_{+j}\left[j\left(1+j\right)\left(e^{-jkl-kl}-e^{-2kl}\right)\right]=0,\\&\underline{\hat{M}}_{+}\left[j\left(1-j\right)\left(e^{-2jkl}-e^{-jkl-kl}\right)\right]+\underline{\hat{M}}_{+j}\left[2e^{-jkl-kl}-e^{-2kl}-1\right]=0,\end{aligned}$$

for which the solution is obtained from the vanishing determinant. This means that

$$1+e^{-2kl}+e^{-2jkl}+e^{-2kl-2jkl}-4e^{-kl-jkl}=0\,,\tag{3.111j}$$

which can readily be rewritten as [3.1]

$$\cosh kl\cos kl-1=0\,.\tag{3.111k}$$

One may observe that for large *kl* this exact result reduces to

$$\cos kl=0,$$

which was used as the basis for the previous approximate analysis. As has been noted, the difference between the exact and the approximate results is of practical interest only in relation to the first zero, for which the exact relation gives

$$k_1 l=3\pi/2+0.0176,$$

compared with the approximate value of $kl = 3\pi/2$. Thus, the exact wavenumber is about 0.37 % greater than that given by the approximation of Eq. (3.111e), and the exact natural frequency is about 0.7 % higher than the value obtained from the approximation. The exact fundamental natural frequency is given by

$$f_1 = 3.8\sqrt{\frac{B}{m'}}\frac{1}{l^2}. \tag{3.111l}$$

Finally, it is instructive to consider the case of a cantilever beam but without carrying out the corresponding analysis in full detail. In an analogous way, the characteristic equation for the cantilever beam is found to be given by

$$\cosh kl \cos kl + 1 = 0.$$

This means that the approximation

$$f_n \approx \frac{\pi}{8}\sqrt{\frac{B}{m'}}\frac{(2n-1)^2}{l^2} \tag{3.112}$$

also holds for these boundary conditions and high eigenfrequencies. The first eigenfrequency, which again is insufficiently determined from Eq. (3.112), is found to be given by

$$f_1 = 0.56\sqrt{\frac{B}{m}}\frac{1}{l^2} \tag{3.112a}$$

for $n = 1$ in this case since no rigid body motion is possible.

3.5 The General Field Equations

The previous analyses have been based on postulating particular types of deformations, and each has lead to new types of wave propagation. Thus, one is led to inquire whether there exist arbitrarily many wave types, or – conversely – whether one may analyse all possible waves in terms of a limited number of basic types.

In order to answer this question, one must first determine what wave processes can occur in an infinite solid medium, and then investigate what effect free surfaces have on these processes.

Figure 3.17 indicates the most general deformation that a surface element *dx dy* can have in the *xy* plane. For the sake of clarity, *dx* is shown equal in length to *dy*. First of all, this element is displaced by an amount ξ

in the x-direction and by an amount η in the y-direction. Because the displacements, as already discussed after Eq. (3.3), must always be small compared with the wavelength, their spatial derivatives $\partial\xi/\partial x$, $\partial\xi/\partial y$, $\partial\eta/\partial x, \partial\eta/\partial y$ always represent very small strains or angles. The deformations associated with these derivatives are shown in Fig. 3.17, exaggerated by several orders of magnitude for the sake of clarity. It is useful to investigate separately the three different types of deformations, as also shown at the bottom of Fig. 3.17.

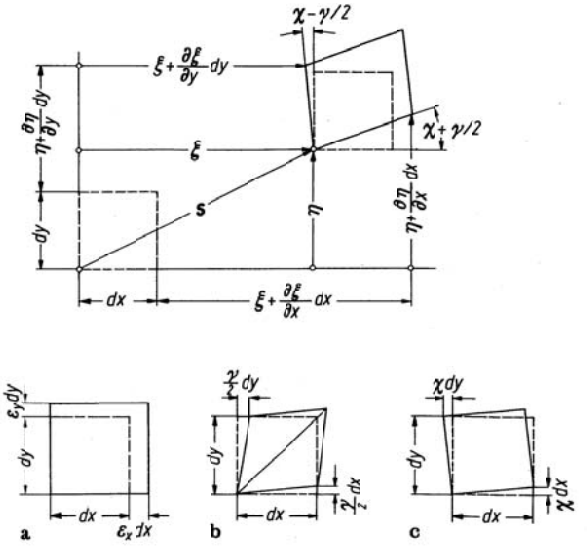

Fig. 3.17. Displacements and strains in two dimensions. a) pure extension in x- and y-directions; b) pure shear deformation; c) pure rotation about x-axis

a) Extensions $\varepsilon_x = \partial\xi/\partial x$, $\varepsilon_y = \partial\eta/\partial y$.
Their sum corresponds to the fractional increase in the element's area, if one neglects the product $\varepsilon_x\varepsilon_y$. These strains need not be of the same magnitude, and may even have opposite signs and therefore generally imply a change in the shape i.e., a change in the ratio of length to width of the element's area.

b) Shear, corresponding to the shear angle γ_{xy}.
This leads to an additional change in shape, namely to distortion of the original rectangle into a parallelogram. In Fig. 3.4, which dealt with a pure transverse wave, this change in shape resulted only from an η displacement, and the strain energy was due only to τ_{xy}. But because the shear stress τ_{yx} must play exactly the same role as τ_{xy} in causing

such a deformation, it is clear that one should define a pure shear deformation as one where the total shear angle γ_{xy} is equally divided over two planes which originally are perpendicular to each other, as shown in part *b* of Fig. 3.17. The distorted shape similarly should have been shown in part *a* as symmetric with respect to the original undistorted shape. There, however, the strains were so small compared with the displacements ξ and η that one could completely neglect the fact that the deformations shown in part *a* and *b* of Fig. 3.17 consist of a pure extension by $\varepsilon_x\, dx$ and $\varepsilon_y\, dy$ plus a translation by $\varepsilon_x dx/2$ and $\varepsilon_y dy/2$. But one must be careful concerning these components in analysing the changes in the angles associated with deformations like that shown in Fig. 3.4, where the deformation consist of a superposition of a pure shear deformation and a pure rotation.

c) Rotations χ_z.
As indicated in part *c* of Fig. 3.17, χ_z typically take on only very small values for elastic waves, such as pure transverse waves. One may therefore take the rotations angle χ_z (about the *z*-axis) as proportional to the components $\partial\xi/\partial y$ and $\partial\eta/\partial x$.

As may easily be seen from Fig. 3.17, these differentials obeys

$$\begin{aligned} \frac{\partial \xi}{\partial y} &= \frac{1}{2}\gamma_{xy} - \chi_z, \\ \frac{\partial \eta}{\partial x} &= \frac{1}{2}\gamma_{xy} + \chi_z. \end{aligned} \tag{3.113}$$

Their sum thus determines the shear angle,

$$\gamma_{xy} = \frac{\partial \xi}{\partial y} + \frac{\partial \eta}{\partial x}, \tag{3.114a}$$

and their difference, twice the rotational angle,

$$2\chi_z = \frac{\partial \eta}{\partial x} - \frac{\partial \xi}{\partial y}. \tag{3.115a}$$

One observes that with a deformation in all three coordinate directions there is associated also an additional displacement component ζ in the *z*-direction, as well as an additional shear angle in the *yz*-plane,

$$\gamma_{yz} = \frac{\partial \eta}{\partial z} + \frac{\partial \zeta}{\partial y}, \tag{3.114b}$$

and one in the *xy*-plane,

$$\gamma_{zx} = \frac{\partial \zeta}{\partial x} + \frac{\partial \xi}{\partial z}, \tag{3.114c}$$

and in general also rotations about the *x*-axis,

$$2\chi_x = \frac{\partial \zeta}{\partial y} - \frac{\partial \eta}{\partial z}, \tag{3.115b}$$

and about the *y*-axis,

$$2\chi_y = \frac{\partial \xi}{\partial z} - \frac{\partial \zeta}{\partial x}. \tag{3.115c}$$

If one writes the three displacement components in terms of a displacement vector

$$\mathbf{s} = \mathbf{i}\xi + \mathbf{j}\eta + \mathbf{k}\zeta, \tag{3.116}$$

then also, the three Eqs. (3.115) can be written as a single vector equation. $2\chi_x$, $2\chi_y$ and $2\chi_z$ are simply the components of the rotation of the displacement vector,

$$\mathbf{i}\chi_x + \mathbf{j}\chi_y + \mathbf{k}\chi_z = \frac{1}{2}\,\mathrm{rot}\ \mathbf{s}. \tag{3.117}$$

The additional extensional strain component $\varepsilon_z = \partial\zeta / \partial z$, together with ε_x and ε_y, determines the relative increase in volume of an element. This volume change is also known as the dilatation δ, and corresponds to a well-known differential operation on the vector *s*, namely its divergence,

$$\delta = \varepsilon_x + \varepsilon_y + \varepsilon_z = \mathrm{div}\ \mathbf{s}. \tag{3.118}$$

It is instructive now to determine the relations between the deformations and the stresses. The shear stresses depend on the corresponding shear angles through

$$\begin{aligned}
\tau_{xy} &= \tau_{yx} = G\left(\frac{\partial \xi}{\partial y} + \frac{\partial \eta}{\partial x}\right), \\
\tau_{yz} &= \tau_{zy} = G\left(\frac{\partial \eta}{\partial z} + \frac{\partial \zeta}{\partial y}\right), \\
\tau_{zx} &= \tau_{xz} = G\left(\frac{\partial \zeta}{\partial x} + \frac{\partial \xi}{\partial z}\right).
\end{aligned} \tag{3.119}$$

On the other hand, the normal stresses are coupled to each other, as a result of the Poisson effect, as has already been pointed out in Sect. 3.1.2. By

adding Eqs. (3.24) of that section and replacing E by G by means of Eq. (3.48), one obtains

$$2G(1+\mu)\delta = (1-2\mu)(\sigma_x + \sigma_y + \sigma_z).$$

If one uses this result to express the sum of the normal stresses in terms of the dilatation, then one finds from Eq. (3.24) that

$$\begin{aligned}
\sigma_x &= 2G\left[\frac{\partial \xi}{\partial x} + \frac{\mu}{1-2\mu}\,\mathrm{div}\ \mathbf{s}\right],\\
\sigma_y &= 2G\left[\frac{\partial \eta}{\partial y} + \frac{\mu}{1-2\mu}\,\mathrm{div}\ \mathbf{s}\right],\\
\sigma_z &= 2G\left[\frac{\partial \zeta}{\partial z} + \frac{\mu}{1-2\mu}\,\mathrm{div}\ \mathbf{s}\right].
\end{aligned} \tag{3.120}$$

To complete the description, the previously in Eqs. (3.29) and (3.45) applied dynamic relations are required. In the present three-dimensional case, are considered all normal and shear stresses acting on a volume element as well as the inertia forces per unit volume. This means

$$\begin{aligned}
\frac{\partial \sigma_x}{\partial x} + \frac{\partial \tau_{xy}}{\partial y} + \frac{\partial \tau_{xz}}{\partial z} &= \rho \frac{\partial^2 \xi}{\partial t^2}\\
\frac{\partial \sigma_y}{\partial y} + \frac{\partial \tau_{yx}}{\partial x} + \frac{\partial \tau_{yz}}{\partial z} &= \rho \frac{\partial^2 \eta}{\partial t^2}\\
\frac{\partial \sigma_z}{\partial z} + \frac{\partial \tau_{zx}}{\partial x} + \frac{\partial \tau_{zy}}{\partial y} &= \rho \frac{\partial^2 \zeta}{\partial t^2}
\end{aligned} \tag{3.121}$$

Upon substituting (3.119) and (3.120), making use of (3.116), results

$$G\left\{\nabla^2 \mathbf{s} + \frac{1}{1-2\mu}\,\mathrm{grad\ div}\ \mathbf{s}\right\} = \rho \frac{\partial^2 \mathbf{s}}{\partial t^2} \tag{3.122a}$$

or, in terms of the velocity vector,

$$G\left\{\nabla^2 \mathbf{v} + \frac{1}{1-2\mu}\,\mathrm{grad\ div}\ \mathbf{v}\right\} = \rho \frac{\partial^2 \mathbf{v}}{\partial t^2}, \tag{3.122b}$$

where ∇^2 is the Laplace operator. By using the velocity components $v_1 = \partial\xi/\partial t$, $v_2 = \partial\eta/\partial t$, $v_3 = \partial\zeta/\partial t$, the same expression becomes

$$\nabla^2 v_i + \frac{1}{1-2\mu}\frac{\partial}{\partial x_i}\left(\frac{\partial v_k}{\partial x_k}\right) = \frac{\rho}{G}\frac{\partial^2 v_i}{\partial t^2};\ i,k = 1,2,3 \tag{3.122c}$$

In the last version use is made of the summation convention i.e., to sum over equal indices. This general differential equation, which all elastic oscillatory motions in the interior of a solid must satisfy, resembles the wave equations discussed in Sections 3.1 and 3.2, only in that it is also of second order with respect to space and time. It differs from them in its spatial character, in that its argument (the displacement vector) contains three components, and in that the differentiations corresponding to the vector operators extend in all coordinate directions. The latter property is characteristic of all wave problems in three-dimensional space. The fact that two operators appear on the left-hand side is characteristic of solid bodies. This indicates that the equation encompasses two wave equations simultaneously.

According to a general theorem of vector analysis, one may separate any continuous vector field into an irrotational and a divergence-free (source-free) part. If these parts are represented by $\mathbf{s}_1$ and $\mathbf{s}_2$ respectively, then the first satisfies

$$\text{rot } \mathbf{s}_1 = 0, \tag{3.123a}$$

and the second

$$\text{div } \mathbf{s}_2 = 0. \tag{3.123b}$$

The irrotational component therefore contains the same dilatation as the entire field,

$$\text{div } \mathbf{s}_1 = \text{div } \mathbf{s} = \delta \tag{3.124a}$$

and the divergence-free part contains the same rotation as the entire field,

$$\text{rot } \mathbf{s}_2 = \text{rot } \mathbf{s}. \tag{3.124b}$$

In terms of the vector of the angular velocity, the latter expression becomes

$$\mathbf{w} = \frac{1}{2}\text{rot } \mathbf{v}_2 = \frac{1}{2}\text{rot } \mathbf{v}. \tag{3.124c}$$

If one applies the divergence operation to Eq. (3.122a) once more, taking into account that

$$\text{div}\nabla^2 = \nabla^2\text{div} \quad , \quad \text{div}\frac{\partial}{\partial t^2} = \frac{\partial}{\partial t^2}\text{div} \, ,$$

then one obtains the three-dimensional wave equation for the dilatation:

$$G\frac{2(1-\mu)}{(1-2\mu)}\nabla^2\delta = \rho\frac{\partial^2\delta}{\partial t^2}. \tag{3.125}$$

This equation includes the case where the same conditions exist on every plane perpendicular to the x-axis. Then ∇^2 reduces to $\partial^2 / \partial \xi^2$, and one obtains the one-dimensional wave equation, as has already been derived in Sect. 3.1.1, as Eq. (3.11). The propagation speed obtained there, according to Eq. (3.50), is the same at that obtained here, namely that of pure longitudinal waves,

$$c_L = \sqrt{\frac{2G(1-\mu)}{\rho(1-2\mu)}}\,. \tag{3.126}$$

Since a three-dimensionally infinite medium was also assumed in Sect. 3.1.1, the wave type discussed there must also be subject to the present general representation. One may recognize that this previously treated wave type corresponds to a plane dilatational wave. Therefore, "pure longitudinal waves" are often called "dilatational waves". It must remembered, however, that in finite media, other disturbances that include dilatations can also propagate at different speeds. But "pure longitudinal waves" are the only type that is "irrotational".

A three-dimensionally infinite medium was also postulated for the pure transverse wave discussed in Sect. 3.2.1. Therefore, such a transverse wave must also satisfy Eq. (3.122a). One finds further that the two above-mentioned types of waves are the only types of plane waves that can occur in an infinite medium. By applying to Eq. (3.122a) the rotation operator and making use of the relations

$$\mathrm{rot}\nabla^2 = \nabla^2 \mathrm{rot}, \quad \mathrm{rot}\frac{\partial^2}{\partial t^2} = \frac{\partial^2}{\partial t^2}\mathrm{rot}\,,$$

as well as the identity

$$\mathrm{rot\ grad} \equiv 0\,,$$

one obtains the three-dimensional wave equation for rot **s**,

$$G\nabla^2(\mathrm{rot}\,\mathbf{s}) = \rho\frac{\partial^2}{\partial t^2}(\mathrm{rot}\,\mathbf{s})\,, \tag{3.127a}$$

or

$$G\nabla^2\mathbf{w} = \rho\frac{\partial^2\mathbf{w}}{\partial t^2}, \tag{3.127b}$$

which describe the behaviour of the source-free (non-divergent and incompressible) part of the wave field. For planar distributions of the vari-

ables, this relation reduces to Eq. (3.46), and implies that all plane rotational processes with the transverse wave velocity

$$c_T = \sqrt{\frac{G}{\rho}}\,. \tag{3.128}$$

Therefore, c_T is also known as the rotational wave velocity. Again, in finite media there can occur other wave types with rotational components propagating with other speeds. The solutions to Eq. (3.127) represent the only possible "source-free (non-divergent) wave motions".

At this point it should be supplemented that in theoretical physic in particular, the strains and stresses can be elegantly written by means of 3*3 tensors. If u_i is the displacement component of the space co-ordinate x_i i.e., $u_1 = \xi$, $u_2 = \eta$, $u_3 = \zeta$ and $x_1 = x$, $x_2 = y$, $x_3 = z$ in the classical notation, then the strain tensor has the elements

$$\varepsilon_{ij} = \frac{1}{2}\left(\frac{\partial u_i}{\partial x_j} + \frac{\partial u_j}{\partial x_i}\right); i, j = 1, 2, 3. \tag{3.128a}$$

The stress-strain relations in Eqs. (3.119) and (3.120) for isotropic materials read

$$\sigma_{ij} = \frac{2G\mu}{1-2\mu}\left(\varepsilon_{11} + \varepsilon_{22} + \varepsilon_{33}\right)\delta_{ij} + 2G\varepsilon_{ij}. \tag{3.128b}$$

Herein, $\delta_{ij} = 0$ for $i \neq j$ and $\delta_{ii} = 1$ is the Kronecker delta. In tensor formalism, force equilibrium is written as

$$\frac{\partial \sigma_{ij}}{\partial x_j} = \rho \frac{\partial^2 u_i}{\partial t^2} \tag{3.128c}$$

Summation is here made for equal indices. A substitution of (3.128a, b) yields the wave Eq. (3.122c).

Although the tensor formalism is elegant and offers many advantages especially in the treatise of anisotropic and piezo-electric materials, the classical notation will be retained in this book owing to its common usage in the engineering science literature.

The question raised at the beginning of this section, concerning whether all waves may be treated in terms of a few basic types, has so far been answered only in part. It has been shown that in the interior of a solid body, only pure longitudinal and pure transverse waves can occur as plane waves. These two wave types are completely independent of each other, and therefore can be excited separately. In practice, however, one usually cannot avoid exciting both waves or, in more general terms, obtaining both

an irrotational and a source-free wave field. But because these propagate with different speeds, one can obtain separated "wave pulses" as the result of short-duration excitation, provided that the dimensions of the solid body are greater than the product of the speed difference ($c_L - c_T$) and the pulse duration. This requirement is satisfied, for example, for seismic waves in the earth, or in the testing of thick structural parts by means of ultrasound, in other words, whenever the "interior" of the solid body extends over many wavelengths in all directions.

The usually employed method to solve Eq. (3.122b) consists of introducing a scalar potential Φ and a vector potential $\boldsymbol{\psi}$ with the following properties

$$\mathbf{v_L} = \frac{d\mathbf{s}_1}{dt} = \text{grad}\Phi, \quad \mathbf{v_T} = \frac{d\mathbf{s}_2}{dt} = \text{rot}\,\boldsymbol{\psi}, \quad \mathbf{v} = \mathbf{v_L} + \mathbf{v_T} \tag{3.129}$$

These potentials satisfy the wave Eqs. (3.125) and (3.127) respectively, analogous to the quantities δ and $\mathbf{w}$. The problem hence, is returned to the solution of two wave equations for which exists a battery of procedures. It should be noted, however, that any boundary condition is given by the velocity and stress. This means that since these quantities are linear combinations of Φ and ψ, there results a coupling of the two fields at boundaries of solid structures. Such conversions from one wave type to another will be further treated in the following sections.

Within the scope of this book, only plane problems will be analysed in conjunction with elastic, isotropic continua. Therefore, the vectorial nature of the vector potential can be omitted since its direction always will be perpendicular to the plane of the field. This means that as in previously studied examples, the solution of the wave equations can be constructed from one or more plane waves i.e.,

$$v_i = \hat{v}_i\left(k_x, k_y, k_z\right) e^{-jk_x x} e^{-jk_y y} e^{-jk_z z}; \quad i = 1,2,3. \tag{3.130}$$

The phasor notation is hereby directly introduced which means that pure harmonic processes are understood at an angular frequency ω. The time base $e^{j\omega t}$ and the prefix Re […] are omitted as is usual. k_x, k_y and k_z are the wavenumber components. Together they reveal the wavelength and wave direction. The expression in (3.130), of course, is not a complete solution to the wave equation. (3.122). Rather it constitutes a fundamental solution with which all other solutions can be constructed by summation or integration as Fourier series or integrals respectively. With the fundamental solution in (3.130) inserted in (3.122c)

$$\begin{aligned}
&\left(k_T^2-k^2-\frac{1}{1-2\mu}k_x^2\right)\hat{v}_1-\frac{1}{1-2\mu}k_xk_y\hat{v}_2-\frac{1}{1-2\mu}k_xk_z\hat{v}_3=0\\
&\frac{-1}{1-2\mu}k_yk_x\hat{v}_1-\left(k_T^2-k^2-\frac{1}{1-2\mu}k_y^2\right)\hat{v}_2-\frac{1}{1-2\mu}k_yk_z\hat{v}_3=0\\
&\frac{-1}{1-2\mu}k_zk_x\hat{v}_1-\frac{1}{1-2\mu}k_zk_y\hat{v}_2-\left(k_T^2-k^2-\frac{1}{1-2\mu}k_z^2\right)\hat{v}_3=0
\end{aligned}\tag{3.131}$$

is obtained, where $k^2=k_x^2+k_y^2+k_z^2$ and $k_T^2=\omega^2/c_T^2$. This homogeneous set of linear equations has non-trivial solutions only when the determinant vanishes. With a few manipulations, the condition

$$\left(k_T^2-k^2\right)^2\left(k_T^2-\frac{2(1-\mu)}{1-2\mu}k^2\right)=0$$

is obtained, which means that the admissible wavenumbers are

$$k_I^2=k_x^2+k_y^2+k_z^2=k_T^2,\tag{3.132a}$$

and

$$k_{II}^2=k_x^2+k_y^2+k_z^2=k_T^2\frac{1-2\mu}{2-2\mu}=\frac{\omega^2}{c_L^2}=k_L^2.\tag{3.132b}$$

As can be seen, Eq. (3.132a) corresponds to a propagation of transversal waves whereas (3.132b) to that of longitudinal. Thus, the subdivision is again possible in the two wave types.

From (3.131) furthermore, it is found that certain relations exist between the phasors $\hat{v}_1,\hat{v}_2$ and $\hat{v}_3$. By letting $k^2=k_T^2$ in (3.131),

$$k_x\hat{v}_{1T}+k_y\hat{v}_{2T}+k_z\hat{v}_{3T}=0,\tag{3.132c}$$

and by inserting $k^2=k_L{}^2$

$$\hat{v}_{2L}=\frac{k_y}{k_x}\hat{v}_{1L},\quad \hat{v}_{3L}=\frac{k_z}{k_x}\hat{v}_{1L}.\tag{3.132d}$$

Thence, the complete, fundamental solution in Cartesian co-ordinates to (3.122b) reads

$$v_i=\left[\hat{v}_{1L}\left(k_x,k_{yL},k_z\right)e^{-jk_{yL}y}+\hat{v}_{1T}\left(k_x,k_{yT},k_z\right)e^{-jk_{yT}y}\right]e^{-jk_xx-jk_zz};\ i=1,2,3.\tag{3.133a}$$

The additional conditions given by (3.132a, b) are

$$k_{yT}^2=k_T^2-k_x^2-k_z^2,\quad k_{yL}^2=k_T^2\frac{1-2\mu}{2-2\mu}-k_x^2-k_z^2=k_L^2-k_x^2-k_z^2,\tag{3.133b}$$

which have to be taken into account. The fact that the index y here happens to be singled out lacks further meaning. The expressions could also have been written differently. Important is only that the wavenumber component of one direction is prescribed for (3.133a) to constitute a solution to the wave equation. The expression in (3.132c), moreover, does not reveal more than rot $\mathbf{v_L} = 0$ and, similarly, that in (3.132d) that div $\mathbf{v_T} = 0$. This can readily be demonstrated since the spatial differentiations simply are replaced by multiplications by jk_x, jk_y or jk_z respectively.

3.6 Wave Field at a Free Surface

3.6.1 Reflection of Plane Waves

As the first application of the fundamental continuum-equations, is considered the reflection of a plane wave at a free surface. Without sacrificing generality, it is assumed that the wave propagates in the x-y-plane such that all field variables are independent of the z co-ordinate. The co-ordinate system and the angles are indicated in Fig. 3.18. In this figure, are depicted wave strips for the sake of clarity although the wave fronts are considered infinite in the analysis.

The assumed two-dimensionality of the problem means that $k_z = 0$ in Eq. (3.133). Therefore, a reasonable form of the longitudinal waves – in the following termed L-waves – is

$$\begin{aligned} v_1 &= \hat{v}_{1L} e^{-jk_x x} e^{-jk_{yL} y} \\ v_2 &= \frac{k_{yL}}{k_x} \hat{v}_{1L} e^{-jk_x x} e^{-jk_{yL} y} \\ v_3 &= 0 \end{aligned} \tag{3.134}$$

in which $k_{yL} = \sqrt{k_L^2 - k_x^2}$. Herein is $k_L = \omega/c_L$ the wavenumber of L-waves (see Eq. (3.132b)), which is a material property for a given frequency. The relation in (3.132b) is already accounted for in (3.134).

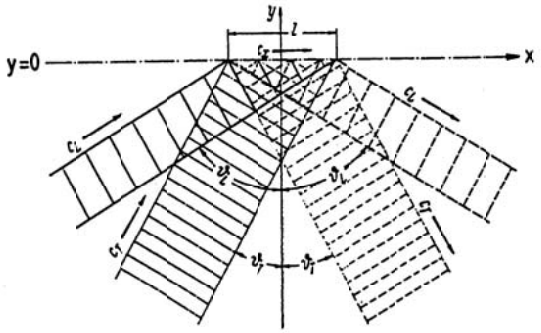

Fig. 3.18. Reflection of longitudinal and transversal waves at a free surface

In Eq. (3.134) is assumed a wave with angle of incidence ϑ_L. This is so since the wave fronts are given by the exponents i.e.,

$$k_x x + k_{yL} y = k_L \left[\frac{k_x}{k_L} x + \sqrt{1 - \left(k_x / k_L\right)^2}\, y \right] \\ = k_L \left[x \sin\vartheta_L + y \cos\vartheta_L \right] = \text{const.} + 2m\pi . \tag{3.135}$$

These wave fronts are planes which are perpendicular to the direction of propagation. The wave fronts are also perpendicular to the particle motion (velocity vector), which is seen from a substitution of $k_x = k_L \sin \vartheta_L$ and $k_{yL} = k_L \cos \vartheta_L$ in Eq. (3.134).

3.6.1.1 Trace speed and angular relations

In the following, is required the trace wavelength λ_x. This length is the distance between two wave fronts at y = const. and thus establishes the period in the x-direction. Alternatively, the wavelength is the projection of the trace wavelength on the direction of propagation. Equation (3.135) yields

$$k_L \lambda_x \sin\vartheta_L = 2\pi ; \quad \lambda_x = \frac{2\pi}{k_L \sin\vartheta_L} = \frac{\lambda_L}{\sin\vartheta_L} . \tag{3.135a}$$

Herein is $\lambda_L = c_L/f$ the physical wavelength of the L-wave i.e., in the direction of propagation.

The used transformation in (3.135), $k_x = k_L \sin \vartheta_L$, means that $k_x \le k_L$ since otherwise k_{yL} would be imaginary. That would correspond to an exponentially decaying near-field and not a propagating incident wave, which is of primary interest here. Instead of $k_x \le k_L$, the relation $\lambda_x \ge \lambda_L$ can

be used or, if the concept of trace speed is introduced, $c_x = \lambda_x f \geq c_L$. The contradiction of either of the conditions above implies that the motion is only possible as exponentially decaying near-field, which, however, realizes a solution to the wave Eq. (3.122).

At the incidence of the L-wave on the free surface, a reflection is anticipated that fulfils the boundary conditions together with the incident wave. If it is assumed that the free surface coincides with $y = 0$ and that this surface is free of external stress or other constraints, then the boundary conditions can be expressed as

$$\sigma_y = 0, \quad \tau_{yx} = 0, \quad \tau_{yz} = 0; \quad y = 0 \text{ and } \forall x,$$

cf., Fig. 3.18. In view of Eq. (3.134), a comparatively simple solution for the total field comprising incident and reflected waves can be written on the form

$$\begin{aligned} v_1 &= \hat{v}_{1L}\left[e^{-jk_x x}e^{-jk_{yL}y} + r_{LL}e^{-j\tilde{k}_x x}e^{-j\tilde{k}_{yL}y} + r_{LT}e^{-j\bar{\bar{k}}_x x} + e^{+j\bar{\bar{k}}_{yL}y}\right], \\ v_2 &= \hat{v}_{1L}\left[\frac{k_{yL}}{k_x}e^{-jk_x x}e^{-jk_{yL}y} - \frac{k_{yL}}{k_x}r_{LL}e^{-j\tilde{k}_x x}e^{-j\tilde{k}_{yL}y} + \frac{k_x}{k_{yT}}r_{LT}e^{-j\bar{\bar{k}}_x x} + e^{+j\bar{\bar{k}}_{yL}y}\right], \\ v_3 &= 0. \end{aligned} \tag{3.136}$$

It is thus assumed that beside the incident L-wave, exist a reflected L-wave and, additionally, an inwards propagating transversal T-wave which emanates at the free surface. The wavenumbers $\tilde{k}_x$ and $\bar{\bar{k}}_x$ of these new waves are still considered unknown. The remaining wavenumber components must satisfy $\tilde{k}_{yL}^2 = k_L^2 - \tilde{k}_x^2$ and $\bar{\bar{k}}_{yT}^2 = k_T^2 - \bar{\bar{k}}_x^2$ respectively since each of the terms in (3.136) alone must be a solution to the wave equation. r_{LL} and r_{LT} can be seen as reflection factors because the amplitudes of the inwards propagating waves are given as fractions of that of the incident wave. In the calculation of v_2 is used the relation (3.132c) for the T-wave and (3.132d) for the L-wave.

To proceed with the analysis, the stresses are required. They are obtained from (3.119) and (3.120) and can be written as

$$\begin{aligned}
\frac{\partial \sigma_y}{\partial t} &= 2G\left[\frac{\partial v_2}{\partial y} + \frac{\mu}{1-2\mu}\left(\frac{\partial v_1}{\partial x} + \frac{\partial v_2}{\partial y} + \frac{\partial v_3}{\partial z}\right)\right] \\
\frac{\partial \tau_{xy}}{\partial t} &= G\left[\frac{\partial v_2}{\partial x} + \frac{\partial v_1}{\partial y}\right] \\
\frac{\partial \tau_{yz}}{\partial t} &= G\left[\frac{\partial v_2}{\partial z} + \frac{\partial v_3}{\partial y}\right],
\end{aligned} \tag{3.137}$$

after conversion from displacement to velocity. Upon substituting Eq. (3.136) expressions are obtained in the form

$$\sigma_y = A_1 e^{-jk_x x} e^{-jk_{yL} y} + A_2 e^{-j\tilde{k}_x x} e^{j\tilde{k}_{yL} y} + A_3 e^{-j\bar{\bar{k}}_x x} e^{j\bar{\bar{k}}_{yT} y},$$

since the exponents remain unaltered in the differentiations as is the spatial dependence. Moreover, A_1, A_2 and A_3 are independent of x and y. From the boundary conditions in this case, all the stresses must vanish at $y = 0$. This is possible if and only if $k_x = \tilde{k}_x = \bar{\bar{k}}_x$ such that

$$\tilde{k}_{yL} = \sqrt{k_L^2 - k_x^2} = k_{yL}, \quad \bar{\bar{k}}_{yT} = \sqrt{k_T^2 - k_x^2} = k_{yT}. \tag{3.138a}$$

Accordingly, the fact that the boundary conditions apply for all of the free surface, automatically implies equality of the wavenumber components in the x-direction. This is equivalent to equality of trace wavelengths and trace speeds in view of (3.135a). The equality of trace speeds and hence also of k_x could have been derived directly from the boundary conditions. This is so since two or more waves can only satisfy a uniform, prescribed boundary condition at a plane when they propagate with equal speed along that plane.

Through (3.135), the angles of propagation can be found for the wave field components. The spatial dependence of the incident wave leads to

$$e^{-jk_x x} e^{-jk_{yL} y} = e^{-jk_L (x \sin \vartheta_L + y \cos \vartheta_L)},$$

and for the reflected L-wave follows from (3.138a) that

$$e^{-jk_x x} e^{jk_{yL} y} = e^{-jk_L (x \sin \vartheta_L - y \cos \vartheta_L)}.$$

For the, at the free surface, emanating T-wave

$$e^{-jk_x x} e^{jk_{yT} y} = e^{-jk_T (x \sin \vartheta_T - y \cos \vartheta_T)},$$

whereby $k_T \sin \vartheta_T = k_x$ and $k_T \cos \vartheta_T = k_{yT}$. The expressions reveal that the angle of reflection equals that of incidence for the L-waves but that they travel in opposite direction and that the T-wave propagates under an angle of

$$\vartheta_T = \arcsin\left(\frac{k_x}{k_T}\right) = \arcsin\left(\frac{k_L}{k_T}\frac{k_x}{k_L}\right) = \arcsin\left(\frac{k_L}{k_T}\sin\vartheta_L\right).$$

The relations above can also be written in the form

$$\sin\vartheta_T = n\sin\vartheta_L, \tag{3.138b}$$

in analogy with Snell's law wherein

$$n = \frac{k_L}{k_T} = \frac{c_T}{c_L} = \sqrt{\frac{1-2\mu}{2-2\mu}} \tag{3.138c}$$

is the index of refraction. From the range for Poisson's ratio, it follows that $0.5 \geq n^2 \geq 0$.

3.6.1.2 Reflection of L-Waves

When a plane L-wave is incident on the free surface, it is partially reflected with the reflection factor r_{LL} and partially converted into a T-wave, the relative amplitude of which is r_{LT}. Hence, the velocity field is given by Eq. (3.136) whereby

$$\begin{aligned} &k_x = \tilde{k}_x = \overline{=}{k}_x = k_L \sin\vartheta_L, \quad k_{yL} = \tilde{k}_{yL} = k_L \cos\vartheta_L, \\ &k_{yT} = \overline{=}{k}_{yT} = k_T \cos\vartheta_T, \quad \sin\vartheta_T = n\sin\vartheta_L \end{aligned} \tag{3.139}$$

from the discussion in the preceding section. Since the refraction index squared, $n^2 \leq 0.5$, a real-valued angle ϑ_T always exists.

With the expressions for the velocities in (3.136) introduced in (3.137), the stresses at the free surface are obtained as

$$\frac{\partial\sigma_y}{\partial t} = 2jGv_{1L}\left[(1+\gamma)\left(\frac{k_{yL}^2}{k_x} - r_{LL}\frac{k_{yL}^2}{k_x} + r_{LT}k_x\right) + \gamma\left(-k_x - r_{LL}k_x - r_{LT}k_x\right)\right]e^{-jk_x x},$$

$$\frac{\partial\tau_{xy}}{\partial t} = 2jGv_{1L}\left[-k_{yL} + r_{LL}k_{yL} - r_{LT}\frac{k_x^2}{k_{yT}} - k_{yL} + r_{LL}k_{yL} + r_{LT}k_{yT}\right]e^{-jk_x x},$$

whereby $\gamma = \mu\,(1 - 2\mu)$. From (3.138c),

$$\left(1 + \frac{\mu}{1-2\mu}\right) = \frac{1-\mu}{1-2\mu} = \frac{1}{2n^2}$$

and making use of (3.138a) and (3.139)

$$\begin{aligned} r_{LL}\left(k_T^2-2k_x^2\right)-2r_{LT}k_x^2 &= -\left(k_T^2-2k_x^2\right), \\ 2r_{LL}k_{yL}k_{yT}+r_{LT}\left(k_T^2-2k_x^2\right) &= 2k_{yL}k_{yT}, \end{aligned} \tag{3.140}$$

when the stresses at the free surfaces vanish. By solving for the reflection factors it is found that

$$\begin{aligned} r_{LL} &= \frac{-\left(k_T^2-2k_x^2\right)^2+4k_x^2k_{yT}k_{yL}}{\mathrm{Det}(k)} = \frac{n^2\sin 2\vartheta_L \sin 2\vartheta_T-\cos^2 2\vartheta_T}{\mathrm{Det}(\vartheta)}, \\ r_{LT} &= \frac{4k_{yT}k_{yL}\left(k_T^2-2k_x^2\right)}{\mathrm{Det}(k)} = \frac{4n\cos\vartheta_L\cos\vartheta_T\cos 2\vartheta_T}{\mathrm{Det}(\vartheta)}. \end{aligned} \tag{3.141a,b}$$

Herein,

$$\begin{aligned} \mathrm{Det}(k) &= 4k_x^2k_{yT}k_{yL}+\left(k_T^2-2k_x^2\right)^2, \\ \mathrm{Det}(\vartheta) &= n^2\sin 2\vartheta_L\sin 2\vartheta_T+\cos^2\vartheta_T. \end{aligned} \tag{3.141c}$$

The second version of (3.141a, b) is developed from a substitution of (3.139) into (3.140).

The reflection factors r_{LL} and r_{LT} express the amplitudes of the reflected waves relative that of the incident. In practice, also the reflection efficiency is an important quantity representing the energy ratio. The intensity in the direction of the wave propagation is given by Eq. (3.16) i.e.,

$$\begin{aligned} J_L &= e_{tot}\cdot c_L = \frac{1}{2}\rho c_L\left|\hat{v}_L\right|^2, \\ J_T &= e_{tot}\cdot c_T = \frac{1}{2}\rho c_T\left|\hat{v}_T\right|^2, \end{aligned}$$

in which $\left|\hat{v}_L\right|^2$ and $\left|\hat{v}_T\right|^2$ are the velocity magnitudes squared (peak value). The factor ½ follows from the temporal averaging. For the energy flow also the width of the strips of the L- and T-waves must be taken into account since these are different, cf. Fig. 3.18. If the power of the incident L-wave is denoted W_{iL}, the reflected L-wave W_{rL} and the emerging T-wave W_{rT}, the efficiencies

$$\begin{aligned} \rho_{LL} &= \frac{W_{rL}}{W_{iL}} = \frac{J_{rL}\cos\vartheta_L}{J_{iL}\cos\vartheta_L} = \left|r_{LL}\right|^2 \\ \rho_{LT} &= \frac{W_{rT}}{W_{iL}} = \frac{J_{rT}\cos\vartheta_T}{J_{iL}\cos\vartheta_L} = \frac{\rho c_L\left|r_{LT}\right|^2\left(1+k_x^2/k_{yT}^2\right)\left|\hat{v}_{1L}\right|^2\cos\vartheta_T}{\rho c_L\left(1+k_{yL}^2/k_x^2\right)\left|\hat{v}_{1L}\right|^2\cos\vartheta_L} \\ &= \frac{\left|r_{LT}\right|^2}{n}\frac{k_x^2\cos\vartheta_T}{k_{yT}^2\cos\vartheta_L} = \left|r_{LT}\right|^2 n\frac{\sin^2\vartheta_L}{\cos\vartheta_T\cos\vartheta_L} \end{aligned} \tag{3.142}$$

It should be observed that ρ without index refers to the density and with index to the reflection efficiency. Upon substituting (3.141a) and (3.141b) into (3.142), it follows that

$$\rho_{LL} = \frac{\left(n^2 \sin 2\vartheta_L \sin 2\vartheta_T - \cos^2 2\vartheta_T\right)^2}{\left|\mathrm{Det}\left(\vartheta\right)\right|^2}, \qquad \rho_{LT} = \frac{4n^2 \sin 2\vartheta_L \sin 2\vartheta_T \cos^2 2\vartheta_T}{\left|\mathrm{Det}\left(\vartheta\right)\right|^2}, \tag{3.142a}$$

respectively. By means of a few manipulations, it is readily corroborated that the energy conservation is preserved i.e., $\rho_{LL} + \rho_{LT} = 1$.

3.6.1.3 Reflection of T-Waves

If instead the incident wave is a T-wave, the analog to Eq. (3.136) reads

$$\begin{aligned} v_1 &= \hat{v}_{1T}\left[e^{-jk_{yT}y} + r_{TT}e^{jk_{yT}y} + r_{TL}e^{jk_{yL}y}\right]e^{-jk_x x}, \\ v_2 &= \hat{v}_{1T}\left[-\frac{k_x}{k_{yT}}e^{-jk_{yT}y} + \frac{k_x}{k_{yT}}r_{TT}e^{jk_{yT}y} - \frac{k_{yL}}{k_x}r_{TL}e^{jk_{yL}y}\right]e^{-jk_x x}, \\ v_3 &= \hat{v}_{3T}\left[e^{-jk_{yT}y} + r_3 e^{jk_{yT}y}\right]e^{-jk_x x}. \end{aligned} \tag{3.143}$$

The two first terms relate to the incident and reflected T-waves respectively whereas the third describes the emerging wave at the free surface, which is converted into an L-wave. For the determination of the *y*-component of the velocity field v_2, again Eq. (3.132) is employed. The amplitude v_{3T} is given by the incident wave as is the case for v_{1T} and for this component of the field no L-wave will arise.

The wavenumbers and the associated angle relations are given by equality of trace speeds, as discussed in Sect. 3.6.1.1;

$$k_x = k_T \sin\vartheta_T; \quad k_{yT} = \sqrt{k_T^2 - k_x^2} = k_T \cos\vartheta_T; \quad k_{yL} = \sqrt{k_L^2 - k_x^2}\,. \tag{3.143a}$$

In view of the law of refraction,

$$\sin\vartheta_L = \frac{1}{n}\sin\vartheta_T = \frac{k_T}{k_L}\sin\vartheta_T \tag{3.143b}$$

such that $k_{yL} = k_L \cos\vartheta_L$ which must be augmented by a restriction. Since $n^2 \le 0.5$, Eq. (3.143b) furnishes real-valued angles ϑ_L only in the range $0 < \vartheta_T < \arcsin n$. For the limiting angle

$$\vartheta_{Tg} = \arcsin n, \tag{3.143c}$$

ϑ_L equals $\pi/2$. This means that the secondary L-wave runs parallel with the free surface. The angular range is not wide for the secondary L-wave. Typically the limiting angle is about 35° for a Poisson's ratio of $\mu = 0.25$. With a larger angle of incidence, the angle relations cannot be applied. The expressions for the wavenumbers, however, are still applicable and show that for $\vartheta_T > \vartheta_{Tg}$, k_x is larger than k_L and hence k_{yL} becomes imaginary, corresponding to a nearfield. In the following section this issue is considered in some more detail.

If, again, Eq. (3.143) is introduced in (3.137), one obtains

$$\begin{aligned} &2r_{TT}k_x^2 - r_{TL}\left(k_T^2 - 2k_x^2\right) = -2k_x^2, \\ &r_{TT}\left(k_T^2 - 2k_x^2\right) + 2r_{TL}k_{yL}k_{yT} = \left(k_T^2 - 2k_x^2\right), \\ &r_3 = 1, \end{aligned} \tag{3.144}$$

at the free surface in a similar way as that leading to (3.140). From this can be developed,

$$\begin{aligned} r_{TT} &= \frac{-4k_x^2 k_{yL}k_{yT} + \left(k_T^2 - 2k_x^2\right)^2}{\mathrm{Det}\left(k\right)} = -r_{LL}, \\ r_{TL} &= \frac{4k_x^2\left(k_T^2 - k_x^2\right)}{\mathrm{Det}\left(k\right)} = 4n^2\frac{\sin^2\vartheta_L\cos 2\vartheta_T}{\mathrm{Det}\left(\vartheta\right)}, \\ r_3 &= 1. \end{aligned} \tag{3.145}$$

Since the z-component of the incident T-wave is totally reflected ($r_3 = 1$) its influence is fairly straightforwardly encompassed. Hence, to keep the mathematical description brief, the reflection efficiencies in the energy relations will be developed only for the case in which $v_3 = 0$. After some small manipulations is obtained

$$\begin{aligned} \rho_{TT} &= \frac{W_{rT}}{W_{iT}} = \left|r_{TT}\right|^2, \\ \rho_{TL} &= \frac{W_{rL}}{W_{iT}} = \frac{c_L}{c_T}\frac{\cos\vartheta_L\cos\vartheta_T}{\sin^2\vartheta_L}\left|r_{LT}\right|^2, \end{aligned}$$

such that, again, energy is conserved and $\rho_{TT} + \rho_{TL} = 1$.

3.6.1.4 Reflection Factors and Efficiencies

Figure 3.19 shows the calculated reflection efficiencies for a Poisson's ratio of $\mu = 0.25$. With the graphical layout used, it is readily seen that energy is conserved in accordance with $\rho_{LL} + \rho_{LT} = 1$ and $\rho_{TT} + \rho_{TL} = 1$ respectively. Also, can be noted that $\rho_{TL} = \rho_{LT}$ which is a consequence of the principle of reciprocity as well as the fact that the energy relations remain unaltered by a time reversal (the film is played backwards). For practice, it is facilitating that the reflection factors and efficiencies are independent of frequency at the free surface and hence apply to arbitrary signals. The reflection of a z-component of an incident T-wave is complete with the reflection factor $r_3 = 1$. This part is therefore not considered in the power considerations and discussions of the reflection efficiencies.

The question remains, however, what happens to an incident T-wave at a larger angle than the limiting of Eq. (3.143c). In this case,

$$k_{yL} = \sqrt{k_L^2 - k_x^2} = -j\sqrt{k_x^2 - k_L^2} = -jk_T\sqrt{\sin^2 \vartheta_T - n^2}\ . \tag{3.146a}$$

The last root is in the interesting range, $\vartheta_T > \vartheta_{Tg}$, purely real. Its sign is given by the physical requirement that the amplitude must decline for growing negative y. Accordingly, the y dependence of the longitudinal wave motion take the form

$$r_{TL} e^{jk_T y} = r_{TL} e^{\sqrt{k_x^2 - k_L^2}\, y}; \quad y < 0\ . \tag{3.146b}$$

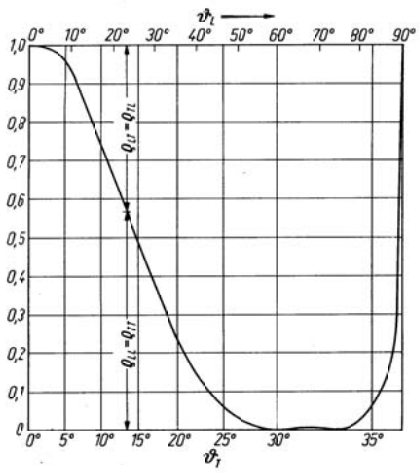

Fig. 3.19. Reflection efficiency at a free surface as function of angle of incidence; $\mu = 0.25$. Top: Longitudinal wave. Bottom: Transversal wave

This means an exponentially decaying nearfield, which already at a distance of $1/(k_x^2 - k_L^2)^{1/2}$ has decayed an e^{th} of the original. This type of wave motion is also called "surface wave" owing to some resemblance with the gravitational waves seen on the sea surface. The waves propagating obliquely from the surface towards the interior in contrast are called "body" or "bulk" waves.

The conditions for the occurrence of a nearfield – i.e., $k_L^2 < k_x^2$ – is identical to $\lambda_L > \lambda_T/\sin \vartheta_T = \lambda_x$. The fact that an exponentially decaying nearfield arises whenever the trace wavelength of the excitation is smaller than the "natural" or free wavelength of the medium will be encountered in numerous air- and structure-borne sound problem.

Upon substituting the imaginary value of k_{yL}, an expression is found for ρ_{TT} in the form $|(jA + B)/(-jA + B)|^2$, which with A and B real gives $\rho_{TT} = 1$. For an angle $\vartheta_T > \vartheta_{Tg}$, a total reflection takes place of the incident T-wave. In parallel there exists the exponentially decaying nearfield having the character of a longitudinal wave motion but propagating no energy in the y-direction. For wave trains of finite width, however, the surface wave must first be developed. Therefore, the reflection at the left boundary cannot be instantaneously complete as is also the case at the right where it cannot be abruptly disengaged since the surface wave must be distorted by radiation. This situation is not only qualitatively but also quantitatively analogous to that of a mass-spring system by pulse excitation. The SDOF system must first – in that case temporally – reach the resonance amplitude and, subsequent to the disengagement of the excitation, have a gradual decay.

Yet another feature of the surface wave should be pointed out. The components in the x and y directions exhibit a phase difference of $\pi/2$. From (3.132d)

$$\frac{\hat{v}_{2L}}{\hat{v}_{1L}} = \frac{k_y}{k_x}, \tag{3.147}$$

which, for surface waves, is purely imaginary since k_y is imaginary. This means that v_1 and v_2 do not combine to a resulting velocity with an unambiguous direction but instead the particles exhibit elliptical orbits.

3.6.2 Excitation of an Elastic Half-Space

The reflection of L- and T-waves treated in the previous sections are of significant importance but of at least equal importance is the behaviour of an externally excited elastic half-space. Considered is an isotropic elastic

continuum, occupying the semi-infinite space $y < 0$, which is excited by an external force distribution, see Fig. 3.20. For simplicity, it is assumed that the force distribution takes the form of a plane wave of angular frequency ω and wavenumbers k_x and k_z with the associated trace wavelengths λ_x and λ_z respectively.

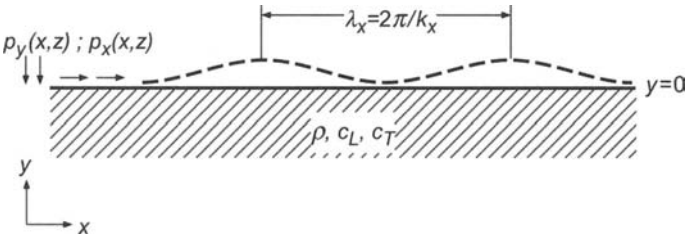

Fig. 3.20. Excitation of an elastic half-space by an external force distribution in terms of a plane wave

At the surface $y = 0$ hence, the exciting normal stress is $p_y = \hat{p}_N e^{-jk_x x} e^{-jk_z z}$, shear stress in x-direction $p_x = \hat{p}_{Tx} e^{-jk_x x} e^{-jk_z z}$ and shear stress in z-direction $p_z = \hat{p}_{Tz} e^{-jk_x x} e^{-jk_z z}$. Owing to the equality of trace wavelengths and trace speeds, the velocity field must have the same x and z dependence and this not only at the surface but for all planes $y \le 0$. Furthermore, since both L- and T-waves are possible, the following velocity fields are to be assumed

$$
\begin{aligned}
v_1(x,y,z) &= \left[\hat{v}_{1L} e^{jk_{yL}y} + \hat{v}_{1T} e^{jk_{yT}y}\right] e^{-jk_x x} e^{-jk_z z},\\
v_2(x,y,z) &= \left[\hat{v}_{1L} \frac{-k_{yL}}{k_x} e^{jk_{yL}y} + \left(\hat{v}_{1T} \frac{k_x}{k_{yT}} + \hat{v}_{3T} \frac{k_z}{k_{yT}}\right) e^{jk_{yT}y}\right] e^{-jk_x x} e^{-jk_z z},\\
v_3(x,y,z) &= \left[\hat{v}_{1L} \frac{k_z}{k_x} e^{jk_{yL}y} + \hat{v}_{3T} e^{jk_{yT}y}\right] e^{-jk_x x} e^{-jk_z z},
\end{aligned}
\qquad (3.147a)
$$

whereby the relations in Eqs. (3.132c,d) have been used taking the signs associated with the direction of propagation into account. The wavenumbers in the y-direction are given by

$$
k_{yL} = \begin{cases} \sqrt{k_L^2 - k_x^2 - k_z^2} \\ j\sqrt{k_x^2 + k_z^2 - k_L^2} \end{cases}, \quad k_{yT} = \begin{cases} \sqrt{k_T^2 - k_x^2 - k_z^2} \\ j\sqrt{k_x^2 + k_z^2 - k_T^2} \end{cases}, \qquad (3.147b)
$$

of which the second form is valid when $k_x^2 + k_z^2$ is larger than k_L^2 and k_T^2 respectively. Since there are no restrictions on the excitation wavenumbers

k_x and k_z, both forms of the radicals are possible. Also, those waves having opposite signs of the wavenumbers k_{yL} and k_{yT} would be solutions to the wave Eq. (3.122a) but since they represent waves propagating from infinity towards the surface, they are omitted in this case.

The three unknowns in Eq. (3.147a) can be determined from the conditions at the surface where the elastic stresses of the half-space must equal those externally applied, implying that

$$\begin{aligned} \sigma_y(x,0,z) &= p_y(x,z), \\ \tau_{xy}(x,0,z) &= p_x(x,z), \\ \tau_{yz}(x,0,z) &= p_z(x,z). \end{aligned} \tag{3.147c}$$

It is hence necessary to express the elastic stresses in the velocities via the constitutive relations (3.137). After some manipulations, observing that differentiations with respect to time corresponds to multiplication by $j\omega$ in the phasor notation, one finds that

$$\begin{aligned} &\hat{v}_{1L}(-k_T^2+2k_x^2+2k_z^2)+\hat{v}_{1T}2k_x^2+\hat{v}_{3T}2k_xk_z=\frac{\omega k_x}{G}\hat{p}_N, \\ &\hat{v}_{1L}2k_{yL}k_{yT}-\hat{v}_{1T}(-k_T^2+2k_x^2+k_z^2)-\hat{v}_{3T}k_xk_z=\frac{\omega k_{yT}}{G}\hat{p}_{Tx}, \\ &\hat{v}_{1L}2k_{yL}k_{yT}\frac{k_z}{k_x}-\hat{v}_{1T}k_xk_z-\hat{v}_{3T}(-k_T^2+k_x^2+2k_z^2)=\frac{\omega k_{yT}}{G}\hat{p}_{Tz}. \end{aligned} \tag{3.148a}$$

The determinant of this set of linear equations is

$$\text{Det}=-2k_{yT}^2\left[(k_T^2-2k_x^2-2k_z^2)^2+4k_{yL}k_{yT}(k_x^2+k_z^2)\right]. \tag{3.148b}$$

From Eqs. (3.148) the unknown amplitudes can be determined and thence the velocities in (3.147a). As an example, the velocity component perpendicular to the surface is obtained as

$$\begin{aligned} v_2(x,y,z)=&-\frac{\omega\hat{p}_N}{G\,\text{Det}}k_{yL}k_T^2 \\ &\times\left[(k_T^2-2k_x^2-2k_z^2)e^{jk_{yL}y}+2(k_x^2+k_z^2)e^{jk_{yT}y}\right]e^{-jk_xx}e^{-jk_zz}, \end{aligned} \tag{3.148c}$$

in a case where the tangential excitation components are identically zero i.e., $p_x = p_z = 0$. From this expression, the ratio of normal stress to normal velocity component that is, the wave impedance, can be found to be given by

$$\hat{Z}=\frac{p(x,z)}{v_2(x,0,z)}=\frac{G}{\omega}\frac{(k_T^2-2k_x^2-2k_z^2)^2+4k_{yL}k_{yT}(k_x^2+k_z^2)}{k_{yL}k_T^2}, \tag{3.148d}$$

for the excitation considered. With the procedure employed here, the structure-borne sound field in a half-space, excited by plane waves, can be treated for arbitrary combinations of the excitation components $\hat{p}_N$, $\hat{p}_{Tx}$ and $\hat{p}_{Tz}$. Also other kinds of problems can be handled, in which partly the stress and partly the velocities at the surface are prescribed. If, for instance, it is requested that $\hat{p}_N$ takes on a specific value and simultaneously the shear deformation at the surface should vanish, then the resulting set of linear equations to be solved consists of the first row of Eq. (3.148a) together with

$$v_1(x,0,z) = (\hat{v}_{1L} + \hat{v}_{1T})e^{-jk_x x}e^{-jk_z z} = 0 \Leftrightarrow \hat{v}_{1L} + \hat{v}_{1T} = 0,$$
$$v_3(x,0,z) = (\frac{k_z}{k_x}\hat{v}_{1L} + \hat{v}_{3T})e^{-jk_x x}e^{-jk_z z} = 0 \Leftrightarrow k_z\hat{v}_{1L} + k_x\hat{v}_{1T} = 0.$$

The above procedure is also applicable when the boundary conditions are given in terms of an impedance. The prerequisite is always, however, that plane waves are present such that the same exponentials for x and z are common for all expressions.

3.6.3. Surface Waves

From an examination of the impedance $\hat{Z}$ can be gained an impression of the amplitudes resulting in the excited half-space. It is shown in Fig. 3.21 for a two-dimensional case i.e., where k_z is set to zero. From this Figure and the formulae in (3.148c, d), the following observations can be made:

- For $k_x^2 << k_L^2$ or $\lambda_x >> \lambda_L$, the *L*- and *T*-waves propagates with the direction cosines $\cos\vartheta_L = k_{yL}/k_L$ and $\cos\vartheta_T = k_{yT}/k_T$ respectively. As a rough approximation $\hat{Z} \approx \rho c_L$.
- For $k_x^2 = k_L^2$ or $\lambda_x = \lambda_L$, $\hat{Z} = \infty$ irrespective of Poisson's ratio and the surface appears rigid.
- For $k_L^2 < k_x^2 < k_T^2$ i.e., $\lambda_L > \lambda_x > \lambda_T$, the *T*-waves propagates whereas only evanescent *L*-waves exist (near-fields). The wave impedance is complex.
- For $k_x^2 = k_T^2$ or $\lambda_x = \lambda_T$, the *T*-waves are grazing ($\vartheta_T = 90°$) and the *L*-waves are evanescent.

For $k_x^2 > k_T^2$ or $\lambda_x < \lambda_T$, only evanescent waves occur and $\hat{Z}$ is purely imaginary. In the vicinity of $k_x = k_T$, however, another feature arises owing to the vanishing impedance and this is briefly discussed in the following since it is of great practical importance in conjunction with seismic and ground-borne waves as well as in ultrasonic applications.

As for any set of linear equations, it has to be considered if the determinant to Eq. (3.148a) will become zero for real-valued k_x and k_z. From Eq.

(3.148b), it is seen that in the range of propagating waves i.e., where k_{yL} or k_{yT} or both are real, the determinant is non-zero since either both terms within brackets are positive or one is real and the other imaginary. When both k_{yL} and k_{yT} are imaginary, however, the situation is different and a zero-crossing is found for

$$\left(k_T^2 - 2k_R^2\right)^2 = 4k_R^2\sqrt{k_R^2 - k_T^2}\sqrt{k_R^2 - k_L^2}\,,$$

where $k_R^2 = k_x^2 + k_z^2$. Upon squaring both sides of the expression, it is seen that the condition for a vanishing of the determinant is given by the equation

$$16k_R^6\left(k_T^2 - k_L^2\right) + 8k_R^4\left(2k_L^2k_T^2 - 3k_T^4\right) + 8k_R^2k_T^6 - k_T^8 = 0\,. \tag{3.149}$$

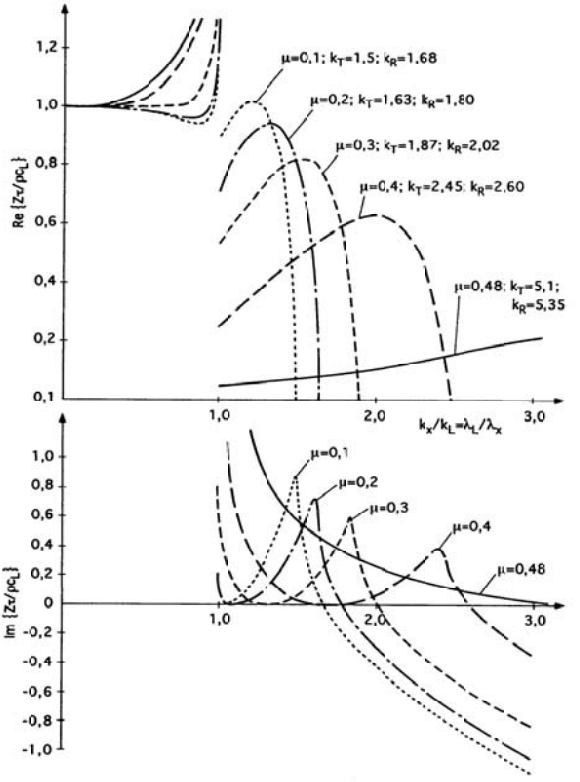

Fig. 3.21. Wave impedance of an elastic half-space at the stress-free surface

This third order equation in k_R^2 has a positive real root which is close to k_T^2. It thus exists a realizable excitation for which the determinant vanishes and which leads to arbitrarily large amplitudes of a surface wave, namely $k_x^2 + k_z^2 = k_R^2$. After its discoverer, this wave is named the Rayleigh wave [3.2]. Its wavenumber k_R and its wave speed c_R is found by solving Eq. (3.149) and for some different values of Poisson's ratio the following relative wave speeds are obtained:

Table 3.3. Rayleigh wave speeds for some values of Poisson's ratio

μ	0	0.1	0.2	0.3	0.4	0.5
c_R/c_T	0.874	0.887	0.91	0.928	0.943	0.955

Approximately, the Rayleigh wave speed is given by

$$c_R \approx c_T \frac{(0.874 + 1.12\mu)}{1+\mu} \tag{3.149a}$$

and it can be noted that it is independent of frequency and only slightly smaller than that of the transversal wave. The penetration depth of the Rayleigh wave is given by the wavenumber components in the *y*-direction $2\pi\Big/\sqrt{k_R^2 - k_L^2}$ and $2\pi\Big/\sqrt{k_R^2 - k_T^2}$. In Fig. 3.22 is illustrated the deformation pattern for a Rayleigh wave and it can be seen that the displacements become smaller with increasing depth.

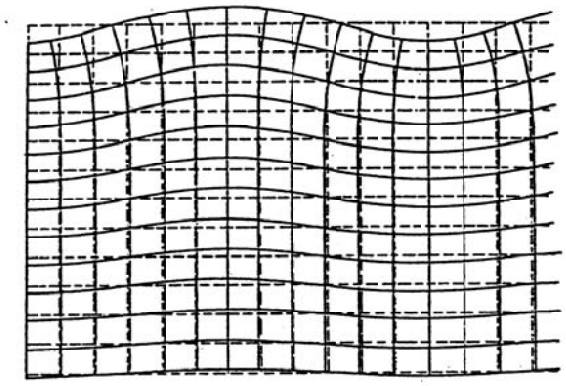

Fig. 3.22. Deformation pattern for a Rayleigh wave

3.7 Free Plate Waves

3.7.1 Boundary Conditions and Types of Solutions

In mechanics, one defines a "plate" as a homogeneous isotropic elastic continuum, bounded by two free parallel planes. The distance between these planes is designated by h and to facilitate the mathematical treatment, the origin of the co-ordinate system is set to coincide with the plane of symmetry between the two free planes. This means that the plate surfaces are situated at $y = \pm h/2$ respectively. For the treatment, moreover, it is assumed that only plane waves are present of angular frequency ω and that all processes are independent of the z co-ordinate. Therefore, the associated wave number component k_3 vanishes. This does not mean, however, that no motions can occur in the z-direction.
For shear waves it might be the prevailing situation. It is merely to understand that all quantities are equal in this direction and that the wave fronts are perpendicular to the cross-sectional plane at $z = 0$ for the plane waves considered here.

Since the plates of interest in this analysis can be arbitrarily big in x- and z-directions and are limited only in the y-direction, waves (and near-fields) can propagate in both positive and negative y-direction. This leads to the general assumption for the velocity components

$$\begin{aligned} v_1(x,y) &= \left(\hat{v}_{L-}e^{jk_{yL}y} + \hat{v}_{T-}e^{jk_{yT}y} + \hat{v}_{L+}e^{-jk_{yL}y}\hat{v}_{T+}e^{-jk_{yT}y}\right)e^{-jk_x x}, \\ v_2(x,y) &= \left(-\frac{k_{yL}}{k_x}\hat{v}_{L-}e^{jk_{yL}y} + \frac{k_x}{k_{yT}}\hat{v}_{T-}e^{jk_{yT}y} + \frac{k_{yL}}{k_x}\hat{v}_{L+}e^{-jk_{yL}y} - \frac{k_x}{k_{yT}}\hat{v}_{T+}e^{-jk_{yT}y}\right)e^{-jk_x x}, \\ v_3(x,y) &= \left(\hat{v}_{3-}e^{jk_{yT}y} + \hat{v}_{3+}e^{-jk_{yT}y}\right)e^{-jk_x x}. \end{aligned} \tag{3.150}$$

The six unknown amplitudes of the velocity components are to be obtained from the boundary conditions. If it is assumed that the stresses are prescribed at the free surfaces then the boundary conditions are

$$\begin{aligned} &\sigma(x,h/2,z) = \hat{p}_+ e^{-jk_x x}, \tau_{xy}(x,h/2,z) = \hat{p}_{xy+}e^{-jk_x x}, \\ &\tau_{yz}(x,h/2,z) = \hat{p}_{yz+}e^{-jk_x x}, \\ &\sigma(x,-h/2,z) = \hat{p}_- e^{-jk_x x}, \tau_{xy}(x,-h/2,z) = \hat{p}_{xy-}e^{-jk_x x}, \\ &\tau_{yz}(x,-h/2,z) = \hat{p}_{yz-}e^{-jk_x x}, \end{aligned} \tag{3.151}$$

see Fig. 3.23. The analysis is similar also when other variables are prescribed. Whenever the x-dependence is in the simple form used, it always consists of solving a set of linear equations.

In Eq. (3.151) the boundary conditions all have the same x-dependence as of the assumed solution in (3.150). For other x-dependencies, the prescribed conditions must first be Fourier transformed to be brought in the form of the assumed solution, cf. Sect. 4.4.3. Intricate it would be, however, to taken into account any sideways boundary conditions. In this case the boundaries are at infinity and hence not considered. With Eq. (3.150) substituted into the fundamental stress relations (3.119) and (3.120), observing the boundary conditions in (3.151), emerges

$$
\begin{aligned}
\frac{\omega\,\hat{p}_{+}k_x}{G} &= -A\hat{v}_{L-}e^{jL} + 2k_x^2\hat{v}_{T-}e^{jT} - A\hat{v}_{L+}e^{-jL} + 2k_x^2\hat{v}_{T+}e^{-jT},\\
\frac{\omega\,\hat{p}_{-}k_x}{G} &= -A\hat{v}_{L-}e^{-jL} + 2k_x^2\hat{v}_{T-}e^{-jT} - A\hat{v}_{L+}e^{jL} + 2k_x^2\hat{v}_{T+}e^{jT},\\
\frac{\omega\,\hat{p}_{xy+}k_{yT}}{G} &= 2k_{yL}k_{yT}\hat{v}_{L-}e^{jL} + A\hat{v}_{T-}e^{jT} - 2k_{yL}k_{yT}\hat{v}_{L+}e^{-jL} - A\hat{v}_{T+}e^{-jT},\\
\frac{\omega\,\hat{p}_{xy-}k_{yT}}{G} &= 2k_{yL}k_{yT}\hat{v}_{L-}e^{-jL} + A\hat{v}_{T-}e^{-jT} - 2k_{yL}k_{yT}\hat{v}_{L+}e^{jL} - A\hat{v}_{T+}e^{jT},\\
\frac{\omega\,\hat{p}_{yz+}}{G} &= -k_x\left(\hat{v}_{3-}e^{jT} + \hat{v}_{3+}e^{-jT}\right),\\
\frac{\omega\,\hat{p}_{yz-}}{G} &= -k_x\left(\hat{v}_{3-}e^{-jT} + \hat{v}_{3+}e^{jT}\right).
\end{aligned}
\tag{3.152}
$$

Herein are introduced the abbreviations

$$k_{yL}h/2 = L \quad , \quad k_{yT}h/2 = T \quad \text{and} \quad A = k_T^2 - 2k_x^2$$

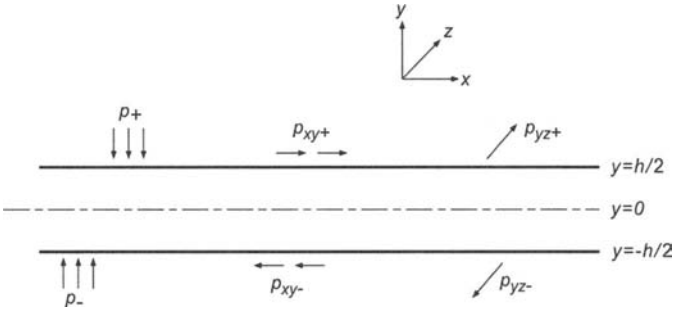

Fig. 3.23. Normal and tangential stresses at the plate surfaces

3.7.2 Waves with Displacements only Parallel to the Surface

As in Sect. 3.6, the conditions are particularly simple when the displacements are parallel to the surface i.e., there exists only the component v_3. Upon solving the two latter equations in (3.152) and substituting into the last of (3.150) is obtained

$$v_3(x,y) = \frac{-1}{\sin k_{yT} h}\left[\hat{p}_{xz+}\sin k_{yT}(y+h/2) - \hat{p}_{xz-}\sin k_{yT}(y-h/2)\right]\frac{\omega}{Gk_x}. \qquad (3.153a)$$

So-called free plate waves exist when a finite motion is possible also in the absence of excitation provided a loss-free medium. Evidently, the conditions are

$$\sin k_{yT} h = 0,$$

meaning that

$$k_{yT} h = \sqrt{k_T^2 - k_x^2}\, h = k_T h \cos\vartheta_T = m\pi\ , \qquad (3.153b)$$

where m = 0, 2, 4… establish a cross-sectionally symmetric field while m = 1, 3, 5… an anti-symmetric.

The case m = 0 implies a uniform velocity across the complete plate thickness and thus also uniform shear stress. This corresponds to a slice of thickness h from a plane transversal wave. Also in view of the given boundary conditions, such a slice is admissible since the shear stresses present, τ_{xz} and τ_{zx}, only arise on surfaces x = const. and z = const. but not on surfaces y = const..

With the exception of the case m = 0, these types of plate waves can be considered as superpositions of two crossing transverse waves impinging on the surfaces at an angle ϑ_T. This gives the trace velocity for both

$$c_x = \frac{c_T}{\sin\vartheta_T} = \frac{c_T}{\sqrt{1-(m\lambda_T/2h)^2}}, \qquad (3.153c)$$

a relation which also encompasses the m = 0 case.

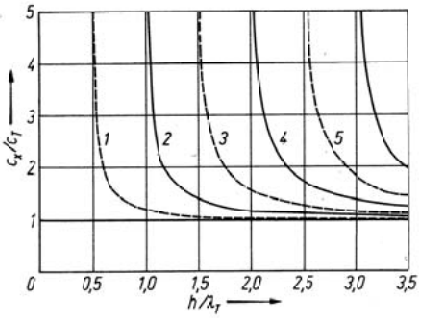

Fig. 3.24. Dispersion diagram for free transversal waves with displacements parallel to the surface (----) symmetric and (- - - -) anti-symmetric modes

Figure 3.24 shows the corresponding dispersion diagram. The fact that the trace velocity in the x-direction c_x can exceed the phase speed c_T is not a contradiction of physics. The energy of a plate wave associated with pure shear deformations propagates with the group velocity as was discussed at the end of Sect. 3.3. In this case it means that

$$c_{gx} = \frac{d\omega}{dk_x} = \left(\frac{dk_x}{d\omega}\right)^{-1} \tag{3.154a}$$

Following from (3.153c), $k_x = \left[k_T^2 - \left(m\pi / h\right)\right]^{1/2}$ whereby $k_T = \omega/c_T$ such that

$$c_{gx} = \frac{c_T k_x}{k_T} = c_T\sqrt{1-\left(m\lambda_T / 2h\right)^2} = c_T \sin\vartheta_T \le c_T. \tag{3.154b}$$

This enables a simple geometrical interpretation of the group speed in the x-direction, given by Schoch [3.3] as the speed of an energy package, which criss-crosses back and forth across the thickness of the plate thickness under the incidence angle ϑ_T like a billiard ball bouncing obliquely between the walls. Such an illustrative interpretation, however, should not mislead to thoughts that the rigorous wave theoretical treatise merely confirms observations made by elementary geometric ray tracing. Ray tracing is not limited to a particular angle whereas plate waves at a given frequency always propagate in discrete directions. Furthermore, the pair of crossing waves form specific sinusoidal or cosinusoidal distributions over the cross-section, which also must match those of an external excitation if a single specific plate wave should be excited. This cannot be obtained from ray tracing. On the contrary, ray tracing is only valid for the description of wave propagation when the wavelength is small in comparison with

all geometrical dimensions involved i.e., the ray width and plate thickness h in this case. For large h/λ_T, trains of plane transversal waves of finite width propagating at arbitrary angles, may be described by sets of superimposed plate waves, as discussed for infinite continua in Sect. 3.2.1.

3.7.3 Waves with Displacements Perpendicular to the Surface

Of much greater practical importance than the previously considered case is when displacement components occur which are perpendicular to the plate surfaces. This is so since such components can be excited by dynamic processes in the ambient medium as well as excite them also when that medium cannot support shear stresses.

The general treatise of plate waves which exhibit displacements in the xy-plane is complicated by the fact that two conditions at each boundary have to be satisfied by two wave types. As was discussed earlier, the two types, moreover, can appear as surface or volume waves [3.4]. For the dispersion diagram, which shall be developed, therefore, three ranges must be distinguished, giving the following table, cf. Sect. 3.6.3

Table 3.4. Three regions for plate waves

	Irrotational Part	Divergence-Free Part
$c_x > c_L$ $k_x^2 < k_L^2$	Longitudinal volume waves	Transverse volume waves
$c_L > c_x > c_T$ $k_L^2 < k_x^2 < k_T^2$	Surface waves	Transverse volume waves
$c_T > c_x$ $k_x^2 > k_T^2$	Surface waves	Surface waves

The dispersion problem consists of determining $\hat{v}_{L+}, \hat{v}_{L-}, \hat{v}_{T+}, \hat{v}_{T-}$ from the first four equations in (3.152). In this pursuit, it is convenient to replace the exponentials with the associated trigonometric functions. Then, the first equation is added to and subtracted from the second respectively, the third similarly added to and subtracted from the fourth. In this way is obtained

$$\begin{aligned}
&-A\left(\hat{v}_{L-}+\hat{v}_{L+}\right)\cos L+2k_x^2\left(\hat{v}_{T-}+\hat{v}_{T+}\right)\cos T=\frac{\omega k_x}{2G}\left(\hat{p}_{+}+\hat{p}_{-}\right),\\
&2k_{yT}k_{yL}\left(\hat{v}_{L-}+\hat{v}_{L+}\right)\sin L+A\left(\hat{v}_{T-}+\hat{v}_{T+}\right)\sin T=\frac{\omega k_{yT}}{2jG}\left(\hat{p}_{xy+}+\hat{p}_{xy-}\right),\\
&-A\left(\hat{v}_{L-}-\hat{v}_{L+}\right)\sin L+2k_x^2\left(\hat{v}_{T-}-\hat{v}_{T+}\right)\sin T=\frac{\omega k_x}{2jG}\left(\hat{p}_{+}-\hat{p}_{-}\right),\\
&2k_{yT}k_{yL}\left(\hat{v}_{L-}-\hat{v}_{L+}\right)\cos L+A\left(\hat{v}_{T-}-\hat{v}_{T+}\right)\cos T=\frac{\omega k_{yT}}{2jG}\left(\hat{p}_{xy+}-\hat{p}_{xy-}\right).
\end{aligned} \tag{3.155}$$

Hereby, the equations are brought into two independent pairs, which readily can be solved. In this context the study is confined to the free plate waves, which means that those wavenumbers are sought leading to non-trivial solutions. Mathematically, this is again found from the vanishing determinants to the two pairs of equation

$$\begin{aligned}\mathrm{Det}\, I &= \sin L \sin T \left[-\left(k_T^2 - 2k_x^2\right)^2 \cot L - 4k_x^2 k_{yL} k_{yT} \cot T \right], \\ \mathrm{Det}\, II &= \cos L \cos T \left[-\left(k_T^2 - 2k_x^2\right)^2 \tan L - 4k_x^2 k_{yL} k_{yT} \tan T \right].\end{aligned} \tag{3.156a, b}$$

In the expressions above, $A = k_T^2 - 2k_x^2$ is back substituted but the abbreviations $L = k_{yL}\, h/2$ and $T = k_{yT}\, h/2$ are retained.

Equating (3.156a, b) to zero furnishes the wavenumbers of the free plate waves and

$$\frac{\tan T}{\tan L} = -\frac{4k_x^2 k_{yL} k_{yT}}{\left(k_T^2 - 2k_x^2\right)^2}, \tag{3.156c}$$

$$\frac{\tan L}{\tan T} = -\frac{4k_x^2 k_{yL} k_{yT}}{\left(k_T^2 - 2k_x^2\right)^2}. \tag{3.156d}$$

The cosine and sine factors in Eqs. (3.156a, b) results in no additional roots of the determinant. Equations (3.156c, d) therefore establish all the roots and it is sufficient that one of the two equations vanishes for a free plate wave to exist and propagate. If, for example, Eq. (3.156c) vanishes, then the two first equations in (3.155) have non-trivial solutions for a vanishing right-hand-side. At the same time, trivial solutions can be chosen for the latter two such that $\hat{v}_{L-} = \hat{v}_{L+}$ and $\hat{v}_{T-} = \hat{v}_{T+}$ result. This means that for those free plate waves governed by Eq. (3.156c), the motion is given in the form

$$\begin{aligned}v_1(x,y) &= 2\left[\hat{v}_L \cos k_{yL} y + \hat{v}_T \cos k_{yT} y \right] e^{-jk_x x}, \\ v_2(x,y) &= 2j \left[\frac{k_{yL}}{k_x} \hat{v}_L \sin k_{yL} y + \frac{k_x}{k_{yT}} \hat{v}_T \sin k_{yT} y \right] e^{-jk_x x}.\end{aligned} \tag{3.157}$$

These waves represents the symmetric modes.

If, in contrast, (3.156d) vanishes, the same reasoning applies but with cosine and sine interchanged in (3.157). In such a case the anti-symmetric modes are promoted.

The dispersion equation, yielding the wavenumbers of the free plate waves could have been developed also employing the wave train closure

principle. For this, forwards propagating and reflected waves are assumed as in Sect. 3.4.1 and the wavenumber and angles respectively sought, for which the phase change due to reflection and propagation is multiples of 2π. This approach is here not chosen as it is interest also to encompass the case of forced vibration.

To further evaluate Eqs. (3.156c, d) usually numerical methods are employed. An example, taken from [3.5] is presented in Fig. 3.25.

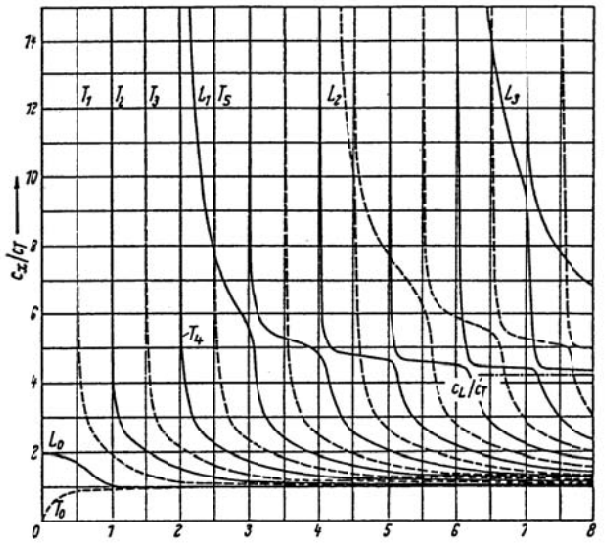

Fig. 3.25. Dispersion diagram for free plate waves comprising displacements perpendicular to the surface, after [3.5]. (——) symmetric and (- - - -) anti-symmetric modes

For specific values of the trace wavenumber in the x-direction $k_x = \omega/c_x$ it is easy to find the corresponding values of $k_T = \omega/c_T$. For $k_x = 0$, for example, are $k_{yT} = k_T$ and $k_{yL} = k_L$. Thereby vanishes the right-hand side of Eq. (3.156c) and hence, the governing equations for the free wavenumbers read $\tan T = 0$ and $\tan L = \infty$ for the symmetric modes whereas $\tan L = 0$ and $\tan T = \infty$ for the anti-symmetric. The frequencies corresponding to this trace wavenumber i.e., for a trace speed of $c_x = \infty$, are

$$\begin{aligned}
&\frac{k_T h}{2} = \pi\nu \Rightarrow \omega = \frac{2\pi c_T}{h}\nu, \\
&\frac{k_L h}{2} = \frac{\pi}{2}(2\nu+1) \Rightarrow \omega = \frac{\pi c_L}{h}(2\nu+1), \\
&\frac{k_L h}{2} = \pi\nu \Rightarrow \omega = \frac{2\pi c_L}{h}\nu, \\
&\frac{k_T h}{2} = \frac{\pi}{2}(2\nu+1) \Rightarrow \omega = \frac{\pi c_T}{h}(2\nu+1)
\end{aligned} \tag{3.158a}$$

A closed form approximation is also possible for thin plates and low frequencies. With the tangential functions series expanded to first order,

$$\frac{k_{yT} h}{k_{yL} h} = -\frac{4k_x^2 k_{yT} k_{yL}}{\left(k_T^2 - 2k_x^2\right)^2}$$

and

$$\left(k_T^2 - 2k_x^2\right)^2 = -4k_x^2\left(k_L^2 - k_x^2\right)$$

respectively. It follows that

$$k_x^2 = \frac{k_T^4}{4\left(k_T^2 - k_L^2\right)} \tag{3.158b}$$

leading to

$$\frac{c_x}{c_T} = \frac{k_T}{k_x} = 2\sqrt{1-h^2} = \sqrt{2/(1-\mu)}\,;\; k_T h << 1.$$

It is easy to convince oneself that this means that $c_L > c_x > c_T$ and that $c_x = c_{LI}$, see Eq. (3.34). For thin plates, the symmetric mode is hence identical to the tensional wave. It consists of a rotational free pair of surface wave because of $k_x > k_L$ or $c_x < c_L$ and of two crossing transversal waves since $k_x < k_T$ or $c_x > c_T$.

If also the cubic terms are taken into account in the series expansion of the tangential functions then

$$k_x^2 = \frac{k_T^4}{4\left(k_T^2 - k_L^2\right)}\left[1 + \frac{1}{3}\left(k_T \frac{h}{2}\right)^2 \frac{1-2n^2}{4\left(1-n^2\right)}\right]$$

or

$$c_x = c_{LI}\left[1-\frac{1}{6}\left(\frac{k_L h}{6}\right)^2\left(\frac{\mu}{1-\mu}\right)^2\right] \tag{3.158c}$$

respectively. With a typical Poisson's ratio of $\mu = 0.3$ it means that a phase speed deviation of around 3% of that of c_{LI} first then arises when $\lambda_{LI} < 3h$.

To find an approximative solution for the anti-symmetric mode (3.156d) at low frequencies, it is necessary to expand the tangential function to third order already for the simplest approximation i.e.,

$$\frac{\tan L}{\tan T} \approx \frac{k_{yL}h/2}{k_{yT}h/2}\frac{1+\frac{1}{3}\left(\frac{k_{yL}h}{2}\right)}{1+\frac{1}{3}\left(\frac{k_{yT}h}{2}\right)} = -\frac{4k_x^2 k_{yL}k_{yT}}{\left(k_T^2-2k_x^2\right)^2} \tag{3.159a}$$

In this case it follows that,

$$k_T^4 + \frac{h^2}{12}\left[k_L^2 k_T^4 + k_x^2\left(3k_T^4 - 4k_L^2 k_T^2\right) + 4k_x^4\left(k_L^2 - k_T^2\right)\right] = 0$$

For the approximation of interest where $k_x^2 >> k_T^2$, it sufficient to retain the highest order of k_x in the bracket, which yields

$$k_x^4 = 3\frac{k_T^4}{h^2}\frac{1}{k_T^2-k_L^2} = 3\frac{k_T^4}{k_T^2 h^2}\frac{1}{1-n^2}. \tag{3.159b}$$

By using the relations (3.34), (3.48), (3.75), (3.83) and (3.138c), this means that the trace speed approaches

$$c_x^2 = \frac{1}{6}\frac{\omega^2 h^2 G}{\rho(1-\mu)} = \frac{1}{12}\frac{\omega^2 h^2 E}{\rho\left(1-\mu^2\right)} = \frac{B'\omega^2}{m''} = c_{LI}\frac{\omega^2 h^2}{12};\ k_T h << 1 \tag{3.159c}$$

Herein, B' is the bending stiffness of the plate and m'' the mass per unit area.

From (3.159) is readily seen that for thin plates are $k_x > k_T > k_L$ such that $c_x > c_T > c_L$. Therefore, the *T*- and *L*-waves can only appear as near-fields. These combine in such a way that an anti-symmetric motion results having the form and propagation speed of the flexural wave. In this case also, the approximation is limited to the range in which $k_x^2 > k_T^2$ or $c_x < c_T$. An error analysis will be presented in Sect. 3.8.2.

The flexural wave and the symmetric longitudinal wave are clearly recognized in Fig. 3.25 where they are denoted by T_0 and L_0 respectively. Not equally clear is that the T_0 branch asymptotically tends to that of the Rayleigh wave and not to that of the slightly higher shear wave.

In this high frequency range, the dispersion diagram more and more resembles Fig. 3.24 and one is almost inclined to assume that the type *T*-waves approach $c_x = c_T$ whilst the type *L*-waves $c_x = c_L$. The latter is however not the case. Instead, is revealed by numerical calculations that all curves for the high orders step-wise approach $c_x = c_L$ whereby one curve succeeds the other. These steps not only approach the asymptote $c_x = c_L$ at $k_T h \to \infty$ but far earlier. The approach follows approximately the relation

$$c_x = \frac{c_L}{\sin \vartheta_L}, \tag{3.160}$$

which is analogous to that in Eq. (3.153c) and which is a necessary condition for the formation of obliquely propagating waves as discussed in that context.

The first dispersion curves of this kind i.e., T_1, L_1 and T_2, obtained by Götz [3.6] from measurements ($n = c_T/c_L = 0.53$) and point-wise graphically collated, did not clearly reveal such a tendency. It became evident, however, from the curves reaching T_7 and L_3, computed a couple of years later by Firestone [3.7] for steel ($n = 0.49$). Most clearly, though, the tendency is observed in the results of Naake and Tamm, here reproduced in Fig. 3.25. This is not only because the dispersion curves are presented up to T_{15} but also because they are calculated for the very small value of $n = 0.24$ i.e., $\mu = 0.47$.

In contrast to Fig. 3.24, the curves in Fig. 3.25 clearly show that the previously denoted *T*- and *L*-type waves, in general do not consist of pure transversal or longitudinal wave fields but are rather composed of both.

The fact that the flexural and Rayleigh waves do not reach the $c_x = c_T$ limit is not a contradiction. It simply becomes surface waves of the rotational free part of the volume waves.

Tamm and Weiss [3.8], moreover, have calculated the group speeds for the plate waves in Fig. 3.25, obtained from the dispersion diagram employing Eq. (3.154a). The results are presented in Fig. 3.26, for which the following remarks apply. No group speed exceeds the phase speed of the longitudinal wave c_L. This wave speed appears only as the common asymptote to the successive steps of the adjacent curves. The envelope to these steps approximately obeys

$$c_x = c_L \sin \vartheta_L . \tag{3.161}$$

At very high frequencies accordingly, obliquely propagating longitudinal rays may be constructed from plate waves. The same thing is true for the curves, which approach from below the genuine asymptote represented by the transverse wave speed c_T, even if it is temporarily exceeded. The

fact that the quasi-longitudinal and bending waves ends at the somewhat lower Rayleigh wave speed which exhibits no dispersion, is shadowed in the figure by the convergence of the many curve branches.

In practice, most structure-borne sound problems only concerns the limiting cases of quasi-longitudinal and bending waves when h/λ_T is small.

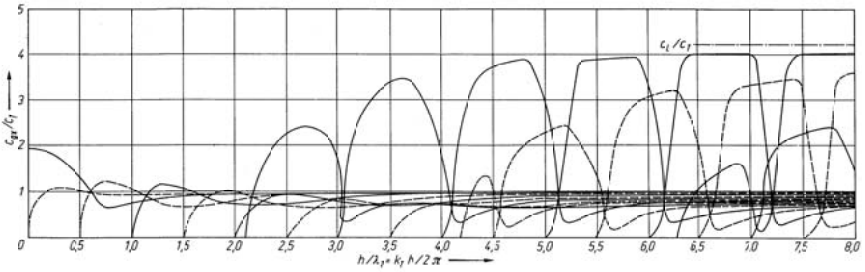

Fig. 3.26. Dispersion diagram for the group velocities corresponding to Fig. 3.25 [2.10]

3.7.4 Equations of Motion for Thin Plates from the General Field Equations

3.7.4.1 Quasi-Longitudinal and Shear Waves in Uniform, Isotropic Plates

In the preceding section were determined the dispersion curves for arbitrary thick strata of homogeneous, isotropic media from the field equation. In the following, these equations are employed for the derivation of the equations of motion of thin plates i.e., plates of thickness small in comparison with the wavelength cf., [3.9]. The required equations are the constitutive and the dynamic force equilibrium relations i.e., (3.119), (3.120) and (3.121) respectively. For a prescribed harmonic motion of angular frequency ω, the basic equations read

$$\begin{aligned}
\frac{\sigma_x}{2G} &= (\alpha+1)\frac{\partial \xi}{\partial x} + \alpha\eta' + \alpha\frac{\partial \zeta}{\partial z},\\
\frac{\sigma_y}{2G} &= \alpha\frac{\partial \xi}{\partial x} + (\alpha+1)\eta' + \alpha\frac{\partial \zeta}{\partial z},\\
\frac{\sigma_z}{2G} &= \alpha\frac{\partial \xi}{\partial x} + \alpha\eta' + (\alpha+1)\frac{\partial \zeta}{\partial z}\\
\frac{\tau_{xy}}{G} &= \xi' + \frac{\partial \eta}{\partial x}, \quad \frac{\tau_{yz}}{G} = \zeta' + \frac{\partial \eta}{\partial z}, \quad \frac{\tau_{xz}}{G} = \frac{\partial \xi}{\partial z} + \frac{\partial \zeta}{\partial x}
\end{aligned} \tag{3.162a}$$

and

$$
\begin{aligned}
-\omega^2 \rho \xi &= \frac{\partial \sigma_x}{\partial x} + \tau_{xy}{}' + \frac{\partial \tau_{xz}}{\partial z}, \\
-\omega^2 \rho \eta &= \frac{\partial \tau_{xy}}{\partial x} + \sigma_y{}' + \frac{\partial \tau_{yz}}{\partial z}, \\
-\omega^2 \rho \zeta &= \frac{\partial \tau_{xz}}{\partial x} + \tau_{xy}{}' + \frac{\partial \sigma_z}{\partial z}.
\end{aligned}
\tag{3.162b}
$$

Herein is introduced

$$
\frac{\mu}{1-2\mu} = \alpha \tag{3.162c}
$$

as an abbreviation. With the phasor notation, the time differentiation is replaced by a multiplication by $j\omega$. Differentiation with respect to y, moreover, is abbreviated by a 'prime' owing to its special role and frequency in the subsequent development.

Upon employing the above relations to the case of a flat plate of thickness h as depicted in Fig. 3.23, the stresses at the surfaces $y = \pm h/2$ can be expanded in Taylor series such that

$$
\begin{aligned}
\sigma_y(h/2) &= \sigma_y(0) + \frac{h}{2}\sigma_y{}'(0) + \frac{h^2}{8}\sigma_y{}''(0) + \frac{h^3}{48}\sigma_y{}'''(0) + ... = p_+, \\
\sigma_y(-h/2) &= \sigma_y(0) - \frac{h}{2}\sigma_y{}'(0) + \frac{h^2}{8}\sigma''(0) - \frac{h^3}{48}\sigma_y{}'''(0) + ... = p_-.
\end{aligned}
\tag{3.163a}
$$

Herein, p_+ and p_- denote the applied normal stress. By means of addition and subtraction of the two lines in (3.163a) one obtains

$$
\sigma_y(0) = -\frac{h^2}{8}\sigma_y{}''(0) + \frac{p_+ + p_-}{2}, \sigma_y{}'(0) = -\frac{h^2}{24}\sigma_y{}'''(0) + \frac{p_+ - p_-}{h} \tag{3.163b}
$$

In the same manner, the shear stresses acting at the surfaces $y = \pm h/2$ yield

$$
\begin{aligned}
\tau_{yx}(0) &= -\frac{h^2}{8}\tau_{xy}{}'' + \frac{p_{yx+} + p_{yx-}}{2}, \tau_{yx}{}'(0) = -\frac{h^2}{24}\tau_{yx}{}'''(0) + \frac{p_{yx+} - p_{yx-}}{h} \\
\tau_{yz}(0) &= -\frac{h^2}{8}\tau_{yz}{}'' + \frac{p_{yz+} + p_{yz-}}{2}, \tau_{yz}{}'(0) = -\frac{h^2}{24}\tau_{yz}{}'''(0) + \frac{p_{yz+} - p_{yz-}}{h}
\end{aligned}
\tag{3.163c}
$$

With the abbreviations for the various stresses in Fig. 3.23,

$$
\begin{aligned}
&p_+ + p_- = p_D, \quad p_+ - p_- = p_B, \quad p_{yx+} + p_{yx-} = p_1, \\
&p_{yx+} - p_{yx-} = p_2, \quad p_{yz+} + p_{yz-} = p_3, \quad p_{yz+} + p_{yz-} = p_4,
\end{aligned}
\tag{3.164}
$$

introduced in (3.163a) to (3.163c) and the Eq. (3.162b) substituted, is obtained

$$\begin{aligned}
-\omega^2\rho\xi &= \frac{\partial\sigma_x}{\partial x}+\frac{\partial\tau_{xz}}{\partial z}-\frac{h^2}{24}\tau_{xy}'''+\frac{p_2}{h},\\
-\omega^2\rho\eta &= -\frac{h^2}{8}\frac{\partial\tau_{xy}''}{\partial x}-\frac{h^2}{24}\sigma_y'''-\frac{h^2}{8}\frac{\partial\tau_{yz}}{\partial z}+\frac{1}{2}\frac{\partial p_1}{\partial x}+\frac{p_B}{h}+\frac{1}{2}\frac{\partial p_3}{\partial z},\\
-\omega^2\rho\zeta &= \frac{\partial\tau_{xz}}{\partial x}+\frac{\partial\sigma_z}{\partial z}-\frac{h^2}{24}\tau_{yz}'''+\frac{p_4}{h}.
\end{aligned} \tag{3.165}$$

In order to establish a set of equations of motion from (3.165), it is suitable to rewrite the normal and shear stresses such that all differentials with respect to y are eliminated at the final stage. Hereby, it should be observed that in the plane $y = 0$, there can only occur displacements and stresses as well as their x and z derivatives. For the sake of convenience, the argument (0) appearing in Eqs. (3.163b, c) is omitted in the following.

With the relation (3.163b) introduced in the second equation of (3.162a) it follows that

$$-\frac{h^2}{16G}\sigma_y''+\frac{p_D}{4G}=\alpha\frac{\partial\xi}{\partial x}+(\alpha+1)\eta'+\alpha\frac{\partial\zeta}{\partial z},$$

which means that as h approaches zero

$$\begin{aligned}
\eta' &= \frac{-\alpha}{\alpha+1}\left(\frac{\partial\xi}{\partial x}+\frac{\partial\zeta}{\partial z}\right)+\frac{p_D}{4G(\alpha+1)}\\
&= \frac{-\mu}{1-\mu}\left(\frac{\partial\xi}{\partial x}+\frac{\partial\zeta}{\partial z}\right)+\frac{1}{8G}\frac{1-2\mu}{1+\mu}p_D.
\end{aligned} \tag{3.166}$$

Thereby, η' can be eliminated from the rest of the equations in (3.162a) and after some manipulation it is found that

$$\begin{aligned}
\frac{\sigma_x}{G} &= \frac{2}{1-\mu}\left(\frac{\partial\xi}{\partial x}+\mu\frac{\partial\zeta}{\partial z}\right)+\frac{\mu}{1-\mu}\frac{p_D}{2G},\\
\frac{\sigma_z}{G} &= \frac{2}{1-\mu}\left(\mu\frac{\partial\xi}{\partial x}+\frac{\partial\zeta}{\partial z}\right)+\frac{\mu}{1-\mu}\frac{p_D}{2G},\\
\frac{\tau_{xz}}{G} &= \left(\frac{\partial\xi}{\partial z}+\frac{\partial\zeta}{\partial x}\right).
\end{aligned} \tag{3.167}$$

Upon combining Eqs. (3.165) and (3.167), the simplest form of equation of motion for a flat plate emerges when all terms of order h^2 or higher are omitted. This means that

$$\begin{aligned}\frac{-\omega^2\rho}{G}\xi &= \frac{2}{1-\mu}\frac{\partial^2\xi}{\partial x^2}+\frac{\partial^2\xi}{\partial z^2}+\frac{1+\mu}{1-\mu}\frac{\partial^2\zeta}{\partial x\partial z}+\frac{\mu}{1-\mu}\frac{1}{2G}\frac{\partial p_D}{\partial x}+\frac{p_2}{Gh},\\ \frac{-\omega^2\rho}{G}\zeta &= \frac{1+\mu}{1-\mu}\frac{\partial^2\xi}{\partial x\partial z}+\frac{2}{1-\mu}\frac{\partial^2\zeta}{\partial z^2}+\frac{\partial^2\zeta}{\partial x^2}+\frac{\mu}{1-\mu}\frac{1}{2G}\frac{\partial p_D}{\partial z}+\frac{p_4}{Gh}.\end{aligned} \tag{3.168a}$$

A rearrangement of these expressions yields

$$\begin{aligned}\left(\frac{2}{1-\mu}\frac{\partial^2}{\partial x^2}+\frac{\partial^2}{\partial z^2}+k_T^2\right)\xi+\frac{1+\mu}{1-\mu}\frac{\partial^2\zeta}{\partial x\partial z} &= -\frac{1}{G}\left[\frac{\mu}{2(1-\mu)}\frac{\partial p_D}{\partial x}+\frac{p_2}{h}\right],\\ \frac{1+\mu}{1-\mu}\frac{\partial^2\xi}{\partial x\partial z}+\left(\frac{2}{1-\mu}\frac{\partial^2}{\partial z^2}+\frac{\partial^2}{\partial x^2}+k_T^2\right)\zeta &= -\frac{1}{G}\left[\frac{\mu}{2(1-\mu)}\frac{\partial p_D}{\partial z}+\frac{p_4}{h}\right].\end{aligned} \tag{3.168b}$$

Herein, k_T is the shear or transversal wavenumber cf., Sect. 3.2.1. The fact that shear and extensional waves combine can be seen by, for example, letting $\partial/\partial z = 0$, which means that all quantities are constant in the z-direction. This leads to

$$\begin{aligned}\left(\frac{2}{1-\mu}\frac{\partial^2}{\partial x^2}+k_T^2\right)\xi &= -\frac{1}{G}\left[\frac{\mu}{2(1-\mu)}\frac{\partial p_D}{\partial x}+\frac{p_2}{h}\right],\\ \left(\frac{\partial^2}{\partial x^2}+k_T^2\right)\zeta &= -\frac{p_4}{Gh}.\end{aligned} \tag{3.169}$$

The second equation is seen to be the shear wave equation with the excitation p_4/Gh. Owing to

$$k_T^2\frac{1-\mu}{2}=\omega^2\rho\frac{1-\mu}{2G}=\omega^2\rho\frac{1-\mu^2}{2G(1+\mu)}=\frac{\omega^2\rho}{E}(1-\mu^2)=\frac{\omega^2}{c_{LI}^2}=k_{LI}^2, \tag{3.170a}$$

see Eqs. (3.48) and (3.34), the first equation in (3.169) turns into

$$\left(\frac{\partial^2}{\partial x^2}+k_{LI}^2\right)\xi=-\frac{\mu(1+\mu)}{2E}\frac{\partial p_D}{\partial x}-\frac{1-\mu^2}{E}\frac{p_2}{Gh}, \tag{3.170b}$$

whereby k_{LI} is the wavenumber of the quasi longitudinal or extensional wave in a thin plate. Thus, the one-dimensional extensional wave equation is obtained. The first part of the excitation depends on the normal stress and comes into play through cross-sectional contraction whilst the second is associated with forces parallel with the plane of the plate cf., Eqs. (3.39) and (3.40) as well as Fig. 3.23. That also the two wave types combine in the two-dimensional case is readily demonstrated by seeking those solutions which represent free plane waves i.e., the excitation is removed. By introducing

$$\xi = \hat{\xi}_0 e^{-jk_x x} e^{-jk_z z}, \zeta = \hat{\zeta}_0 e^{-jk_x x} e^{-jk_z z}, \tag{3.171}$$

in Eq. (3.168b), it is found that

$$\begin{aligned} &\left(\frac{2}{1-\mu}k_x^2 + k_z^2 - k_T^2\right)\hat{\xi}_0 + \frac{1+\mu}{1-\mu}k_x k_z \hat{\zeta}_0 = 0, \\ &\frac{1+\mu}{1-\mu}k_x k_z \hat{\xi}_0 + \left(\frac{2}{1-\mu}k_z^2 + k_x^2 - k_T^2\right)\hat{\zeta}_0 = 0. \end{aligned} \tag{3.172}$$

These two equations have non-trivial solutions only when the determinant of the coefficients vanishes. Rewriting $2/(1 - \mu)$ as $1 + (1 + \mu)/(1 - \mu)$, the characteristic equation in k_x and k_z becomes

$$\left(k_x^2 + k_z^2 - k_T^2 + \frac{1+\mu}{1-\mu}k_x^2\right)\left(k_x^2 + k_z^2 - k_T^2 + \frac{1+\mu}{1-\mu}k_z^2\right) - \left(\frac{1+\mu}{1-\mu}k_x k_z\right) = 0. \tag{3.173}$$

This expression is of the form $(a + b)(a + c) - bc = a(a + b + c) = 0$. Hence, the pair of equations in (3.172) has non-trivial solutions if either $a = 0$ or $(a + b + c) = 0$ i.e.,

$$\begin{aligned} &k_x^2 + k_z^2 = k_T^2, \\ &k_x^2 + k_z^2 + \frac{1+\mu}{1-\mu}\left(k_x^2 + k_z^2\right) = \frac{2}{1-\mu}\left(k_x^2 + k_z^2\right) = k_T^2 \Rightarrow k_x^2 + k_z^2 = k_{LI}^2, \end{aligned} \tag{3.174a}$$

respectively. The first of these solutions represents shear waves whilst the second extensional waves. From the outcome of the analysis so far, it can be concluded that the motions of the neutral layer of a thin plate are described by Eq. (3.168b). Also is clarified that the (3.167) establishes the relation between the forces $F_x = -\sigma_x h$ in the x-direction see Eq. (3.35) and $F_z = -\sigma_z h$ in the z-direction. This relation turns into (3.38) as expected.

The so called plate waves consist of shear and extensional waves having free wavenumber and the phase speeds given by (3.174a, b). When also the motion at the plate surfaces in the y-direction, resulting from the cross-sectional contraction, is of interest, Eq. (3.166) gives

$$\eta\left(\pm h/2\right) = -\frac{\pm\mu h}{2\left(1-\mu\right)}\left(\frac{\partial \xi}{\partial x} + \frac{\partial \zeta}{\partial z}\right) + \frac{h}{8G}\frac{1-2\mu}{1+\mu}p_D. \tag{3.175}$$

3.7.4.2 Bending Waves in Flat Isotropic Plates

To analyse the bending motion of a plate, it is necessary to determine the displacement η of its neutral layer. As indicated by the middle expression

in Eq. (3.165), the derivatives of the normal and tangential stresses are required

$$-\omega^2 \rho h = -\frac{h^2}{8}\left[\frac{\partial \tau''_{xy}}{\partial x} + \frac{1}{3}\sigma'''_3 + \frac{\partial \tau''_{yz}}{\partial z}\right] + \frac{p_B}{h}. \tag{3.176}$$

For reasons of brevity it is here assumed that the normal stresses at the upper and lower surfaces are equal in magnitude and that all shearing stresses p_1, p_2, p_3 and p_4 vanishes.

Fortunately, no principal difficulties arise in the determination of τ_{yx}'' etc. since these quantities are multiplied by the factor h^2 and accordingly the stresses need be determined only up to the order h^0. In the following development, one may furthermore set the plate thickness h equal to zero to retain the precision desired i.e., Eq. (3.166) to (3.168) can be used to determine τ_{yx}''. In principle, it is then possible to use the results recurrently to obtain approximations up to order h^4. The drawback, however, is that the expressions become rather lengthy and intractable.

The first derivative with respect to the y-direction of the stresses sought immediately follows from (3.162b)

$$\begin{aligned}
\tau_{xy}' &= -\frac{\partial \sigma_x}{\partial x} - \frac{\partial \tau_{xz}}{\partial z} - \omega^2 \rho \xi, \\
\sigma_y' &= -\frac{\partial \tau_{xy}}{\partial x} - \frac{\partial \tau_{yz}}{\partial z} - \omega^2 \rho \eta, \\
\tau_{yz}' &= -\frac{\partial \tau_{xz}}{\partial x} - \frac{\partial \sigma_z}{\partial z} - \omega^2 \rho \zeta.
\end{aligned} \tag{3.177}$$

In order to carry out the next differentiation, first the $\xi', \eta', \zeta', \sigma_x' \sigma_z'$ and τ_{xz}' must be determined. This is not difficult since $\tau_{yx} = \tau_{yz} = 0$ to the required precision, which means that

$$\xi' = -\frac{\partial \eta}{\partial x}, \quad \zeta' = -\frac{\partial \eta}{\partial z} \tag{3.178a}$$

follows from the last equation in (3.162a). Moreover, with $p_+ = -p_-$ i.e., $p_D = 0$ follows from Eq. (3.166) that

$$\eta' = \frac{-\mu}{1-\mu}\left(\frac{\partial \xi}{\partial x} + \frac{\partial \zeta}{\partial z}\right). \tag{3.178b}$$

The condition $p_D = 0$ in (3.167) furthermore implies that

$$\frac{\sigma_x'}{G} = \frac{-2}{1-\mu}\left(\frac{\partial^2\eta}{\partial x^2} + \mu\frac{\partial^2\eta}{\partial z^2}\right), \frac{\sigma_z'}{G} = \frac{-2}{1-\mu}\left(\mu\frac{\partial^2\eta}{\partial x^2} + \frac{\partial^2\eta}{\partial z^2}\right),$$
$$\frac{\tau_{xy}'}{G} = -2\frac{\partial^2\eta}{\partial x\partial z}, \tag{3.179}$$

using Eq. (3.175). Upon introducing this in (3.177) together with (3.178) one obtains

$$\tau_{xy}'' = \frac{2G}{1-\mu}\frac{\partial\nabla^2\eta}{\partial x} + \omega^2\rho h\frac{\partial\eta}{\partial x},$$
$$\tau_{zy}'' = \frac{2G}{1-\mu}\frac{\partial\nabla^2\eta}{\partial z} + \omega\rho h\frac{\partial\eta}{\partial z}. \tag{3.180}$$

Herein,

$$\nabla^2 = \frac{\partial^2}{\partial x^2} + \frac{\partial^2}{\partial z^2}$$

is the two-dimensional Laplace operator.

With a further substitution of (3.180) into the mid equation of (3.177), taking into account that

$$\eta'' = \frac{-\mu}{1-\mu}\left(\frac{\partial\xi'}{\partial x} + \frac{\partial\zeta'}{\partial z}\right) = \frac{\mu}{1-\mu}\nabla^2\eta, \tag{3.181}$$

it follows from (3.178a, b) that the third derivative of the normal stress in the *y*-direction is

$$\sigma_y''' = \frac{-2G}{1-\mu}\nabla^4\eta - \frac{\mu}{1-\mu}\omega^2\rho\nabla^2\eta. \tag{3.182}$$

Finally, is obtained the equation for bending motion of a plate by substituting (3.182) and (3.180) in (3.176),

$$\frac{h^3}{16}\frac{2G}{1-\mu}\frac{2}{3}\nabla^4\eta + \frac{h^3}{48}\frac{3-4\mu}{1-\mu}\omega^2\rho\nabla^2\eta - \omega^2\rho\frac{h}{2}\eta = \frac{p_B}{2}, \tag{3.183a}$$

or,

$$\frac{E}{1-\mu^2}\frac{h^3}{12}\nabla^4\eta + \frac{h^3}{24}\frac{3-4\mu}{1-\mu}\omega^2\rho\nabla^2\eta - \omega^2\rho h\eta = p_B. \tag{3.183b}$$

In this equation, $B' = Eh^3/[12\,(1-\mu^2)]$ is the bending stiffness and $m'' = \rho h$ the mass per unit area. $p_B = p_+ - p_-$ describes the external forces exerted onto the plate. This means that Eq. (3.183b) can be rewritten in the form

$$\frac{B'}{m''}\nabla^4\eta - \omega^2\eta = \frac{p_+ - p_-}{m''} - correction \approx \frac{p_B}{m''}. \tag{3.184a}$$

As is seen from a comparison with Eq. (3.81), the first two terms correspond to the ordinary flexural wave equation. The correction term on the right hand side represents a portion of the effects of shear stresses cf., Sect. 3.8.2. These effects becomes significant when the bending wavelength is smaller than six times the plate thickness and can therefore often be neglected.

In order to enable the employment of Eq. (3.183) also for the solution of boundary value problems where forces and moments are prescribed, it remains to establish expressions also for these quantities. The cross-sectional rotation is given by

$$-\beta_x = \xi' = -\frac{\partial\eta}{\partial x}, -\beta_z = \zeta' = -\frac{\partial\eta}{\partial z} \tag{3.184b}$$

for the small amplitudes of interest. In view of (3.74), the moments are analogously given by the product of local stress and distance from the neutral layer

$$\begin{aligned}
M_{xz} &= \int_{-h/2}^{h/2} \sigma_x y dy = \frac{-2G}{1-\mu}\left(\frac{\partial^2\eta}{\partial x^2} + \mu\frac{\partial^2\eta}{\partial z^2}\right)\int_{-h/2}^{h/2} y^2 dy = -B'\left(\frac{\partial^2\eta}{\partial x^2} + \mu\frac{\partial^2\eta}{\partial z^2}\right),\\
M_{zx} &= \int_{-h/2}^{h/2} \sigma_z y dy = \frac{-2G}{1-\mu}\left(\mu\frac{\partial^2\eta}{\partial x^2} + \frac{\partial^2\eta}{\partial z^2}\right)\int_{-h/2}^{h/2} y^2 dy = -B'\left(\mu\frac{\partial^2\eta}{\partial x^2} + \frac{\partial^2\eta}{\partial z^2}\right),\\
M_{xx} &= -M_{zz} = \int_{-h/2}^{h/2} \tau_{xz} y dy = 2G\frac{\partial^2\eta}{\partial x\partial z}\int_{-h/2}^{h/2} y^2 dy = -B'(1-\mu)\frac{\partial^2\eta}{\partial x\partial z}.
\end{aligned} \tag{3.184c}$$

In the above expressions σ_x', σ_z' and τ_{xz}' are introduced from (3.179) considering that $\sigma_x = \sigma_x' y, \sigma_z = \sigma_z' y, \tau_{xz} = \tau_{xz}' y$ apply in the approximation used here. Furthermore, is used the flexural stiffness of a plate

$$B' = \frac{E}{1-\mu^2}\frac{h^3}{12} = \frac{2G}{1-\mu}\frac{h^3}{12}. \tag{3.184d}$$

From the moments, the cross-sectional forces are obtained as

$$\begin{aligned}
Q_x &= -\frac{\partial M_{xz}}{\partial x} - \frac{\partial M_{zz}}{\partial z} = B'\frac{\partial\nabla\eta}{\partial x},\\
Q_z &= -\frac{\partial M_{zx}}{\partial z} - \frac{\partial M_{zz}}{\partial x} = B'\frac{\partial\nabla\eta}{\partial z}
\end{aligned} \tag{3.184e}$$

cf., Fig. 3.27.

In summary, it can be stated that the motion of a thin plate is well described by (3.168b) and (3.184a-e) whereby (3.168b) yields the in-plane motions whilst (3.184a) those out-of-plane. The accuracy is satisfactory for most engineering application provided the plate thickness is smaller than a sixth of the wavelength.

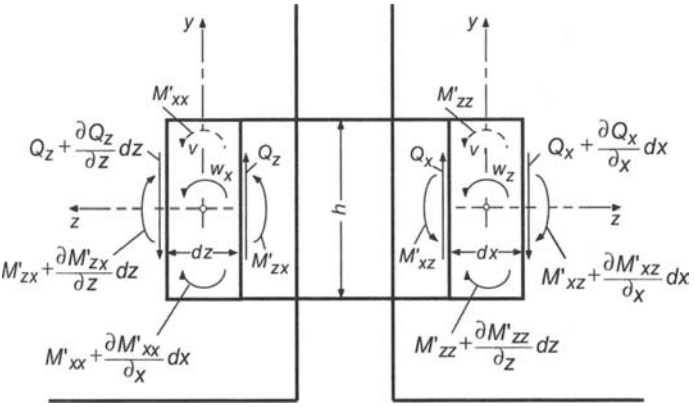

Fig. 3.27. Velocities, moments and forces for a plate in bending

3.7.4.3 Flexural Waves in Flat, Orthotropic Plates

Plates are termed orthotropic when the bending stiffness differs in two orthogonal directions. Typical examples are corrugated plates and plates with stiffeners in one direction as in the decks of a ship, cf. Fig. 2.28. The analysis in this section concerns configurations, for which the corrugation or stiffener distance is substantially smaller that the wavelength. If this condition is not met, the structure is rather to be considered as a periodic system, at least in the case of stiffened plates, see Sect. 6.5. The equation of motion for orthotropic plates can be derived in precisely the same manner as that of an isotropic plate; only the stress-strain relations have to be slightly modified

$$\begin{aligned}
\sigma_x &= \sigma_x' \cdot y = \left(-\frac{E_x}{1-\mu^2}\frac{\partial^2\eta}{\partial x^2} - E_\mu \frac{\partial^2\eta}{\partial z^2} \right) y, \\
\sigma_z &= \sigma_z' \cdot y = \left(-E_\mu \frac{\partial^2\eta}{\partial x^2} - \frac{E_z}{1-\mu^2}\frac{\partial^2\eta}{\partial z^2} \right) y, \\
\tau_{xz} &= \tau_{xz}' \cdot y = -2Gy\frac{\partial^2\eta}{\partial x \partial z}.
\end{aligned} \tag{3.185}$$

E_x and E_z are the Young's moduli for the x- and z-directions respectively, which can be measured using the conventional test on rod samples cut in the two directions respectively. The cross-contractional modulus E_μ and the shear modulus are more intricate. Commonly, they are approximated or assessed from the eigen-modes of an orthotropic plate i.e., from the eigen-functions of (3.186).

With Eq. (3.185) inserted in the relations (3.176), (3.177) and (3.180), which are valid also for orthotropic, thin plates, then with the exception for the $\omega^2\rho$-term, the flexural wave equation for an orthotropic plate is obtained as [3.10-3.13]

$$B_x' \frac{\partial^4 \eta}{\partial x^4} + 2\left(B_\mu' + 2B_G'\right)\frac{\partial^4 \eta}{\partial x^2 \partial z^2} + B_z' \frac{\partial^4 \eta}{\partial z^4} - \omega^2 m'' \eta = p(x,z,t). \qquad (3.186)$$

Herein, B_x' is the bending stiffness in one direction, B_z' that in the perpendicular direction, B_μ' denotes to the stiffness relating to E_μ whereas B_G' takes the shear stiffness into account. For a plate of thickness h and of orthotropic material with the moduli E_x, E_z, E_μ and shear modulus G, it follows from (3.185) that

$$B_x' = \frac{E_x}{1-\mu^2}\frac{h^3}{12},\ B_z' = \frac{E_z}{1-\mu^2}\frac{h^3}{12},\ B_\mu' = E_\mu \frac{h^3}{12},\ B_G' = G\frac{h^3}{12}. \qquad (3.186a)$$

As an example can be mentioned that for a three-layer plywood laminate the following approximate values apply

$$E_x \approx 130,\ E_z \approx 11,\ E_\mu \approx 3,\ G \approx 7.5 \text{ GPa}.$$

For corrugated or stiffened plates of homogeneous material with Young's modulus E, Poisson's ratio μ the formulae in Fig. 3.28 are found in the literature. With the exception of the term $\omega^2\rho\eta$, all other terms involving $\omega^2\rho$ in Eqs. (3.177), (3.180) and (3.182) are omitted in the developments since the thereby expressed shear stress corrections anyhow would be incorrect for corrugated and stiffened plates.

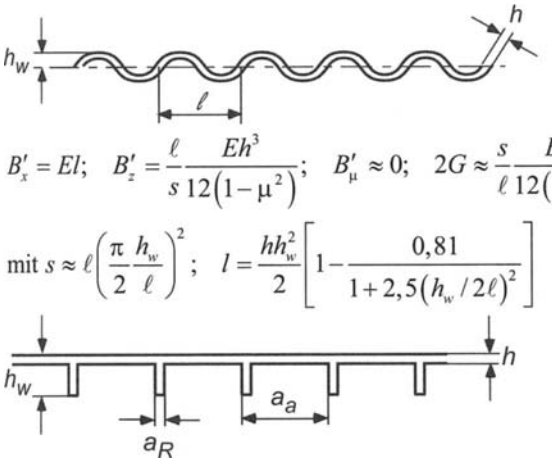

$$B'_x = El; \quad B'_z = \frac{\ell}{s}\frac{Eh^3}{12\left(1-\mu^2\right)}; \quad B'_\mu \approx 0; \quad 2G \approx \frac{s}{\ell}\frac{Eh^3}{12\left(1+\mu\right)}$$

$$\text{mit } s \approx \ell\left(\frac{\pi}{2}\frac{h_w}{\ell}\right)^2; \quad l = \frac{hh_w^2}{2}\left[1-\frac{0{,}81}{1+2{,}5\left(h_w/2\ell\right)^2}\right]$$

$$B'_x = El; \quad B'_z = \frac{Eh^3}{12}\frac{a_a}{a_a - a_R\left(1-h^3/h_w^3\right)}$$

$$B'_\mu \approx 0; \quad G \approx \frac{E}{6\left(1+\mu\right)}\left(h^3 + h_w^3 a_R / a_a\right)$$

$$l = \frac{a_a}{3}\left(s_1^2 - s_2^2\right) + \frac{a_R}{3}\left(s_2^2 + s_3^2\right)$$

$$s_1 = \frac{1}{2}\frac{a_a h_w^2 + \left(a_a - a_R\right)h^2}{a_a h_w + \left(a_a - a_R\right)h}; \quad s_2 = s_1 - h; \quad s_3 = h_w - s_1$$

Fig. 3.28. Bending stiffness of corrugated and stiffened plates (l and a_a must be substantially smaller than the flexural wavelength)

3.7.4.4 Thin Prestressed Plates on Winkler Bed

The methods of the previous sections can be employed to develop the equations of motion for a plate of bending stiffness B', prestressed with a (positive) tensile or a (negative) compressional stress and when this plate, possibly also rests upon a soft layer (Winkler bed) of stiffness s'' per unit area. Simpler still, Hamilton's principle [3.14] can be used as discussed in the next section. The result, given here without proof, reads

$$B\nabla^4\eta - T'\nabla^2\eta + s''\eta + m''\frac{\partial^2\eta}{\partial t^2} = p\left(x,z,t\right) \tag{3.187}$$

for the motion out of the plane of the plate. The units of the quantities used are: B' [Nm], T' [N/m], s'' [N/m^3], m'' [kg/m^2], η [m] and p [N/m^2]. p (x, z, t) is the externally applied pressure.

It is clear that Eq. (3.187) combines the plate Eq. in (3.184a) and a membrane equation. Included is also an additional reaction force $s''\eta$. By introducing the conventional exponential solution, the dispersion equation is found for $p(x, z, t) = 0$ to be

$$B'\left(k_x^2 + k_z^2\right)^2 + T'\left(k_x^2 + k_z^2\right) - \left(\omega^2 m'' - s''\right) = 0\,, \tag{3.187a}$$

revealing the possible free wavenumbers. A closer scrutiny of this expression leads to the following findings:

- Propagating waves are only possible when

$$\omega^2 > \frac{s'' - T^2/4B'}{m''},$$

  which, for vanishing prestress, means that the frequency must be higher than $\sqrt{s''/m''}$. For lower frequencies only evanescent waves exist.
- A consequence of the limiting frequency just defined is that, in contrast to the plate without a Winkler bed, the wave speed does not decrease below a certain limiting value, also for very low frequencies. For plates without prestress ($T' = 0$), the limiting phase speed is $c_{B\min} = (2\,s''B'/m'')^{1/4}$ which is reached at $\omega_{\min}^2 = 2\,s''/m''$. For railway rails the minimum phase speed is typically some 100 m/s and the cut-on occurs in the range 50 to 100 Hz.
- When the plate is compressed ($T' < 0$), it appears somewhat more flexible. Theoretically, a vanishing wavenumber is possible but has to be ruled out on physical grounds since the plate will buckle.
- Upon combining a membrane equation comprising the prestresses T_x' and T_z' with the equation of motion for orthotropic plates in (3.186) the applicability of Eq. (3.187) can be further extended.

3.8 Hamilton's Principle for the Derivation of the Equations of Motion

3.8.1 Fundamentals

As was already stated in Sect. 2.5.1, Hamilton's principle realizes one of the most important relations of physics. It is therefore to be anticipated that it is applicable also in structure-borne sound. As far as discretizations of a structure are concerned, the use of Hamilton's principle has experienced a renaissance in recent years since the application of the finite element method (FEM) can be seen as an employment of the principle. Despite this, FEM will not be a topic in this book because a large number of publi-

cations is devoted to the method. Instead, the wave equations will be developed from Hamilton's principle in Chapters 3 and 4 whereby the plate and the shell serve as examples, cf. Sect. 4.6.3. In Sect. 6.6, moreover, a further use will be demonstrated.

Naturally, also the wave equations employed in previous sections could have been derived from Hamilton's principle but besides the physics of structure-borne sound, also different methods should be presented.

In mechanics the Hamilton's principle reads, cf. Sect. 2.5.1

$$\delta \int_{t_1}^{t_2} \left(E_{kin} - E_{pot} \right) dt + \int_{t_1}^{t_2} \delta W dt = 0 \,. \tag{3.188}$$

Herein, E_{kin} and E_{pot} are the total kinetic and potential energies of the system respectively. W is the externally supplied work. The symbol δ means that a variation is undertaken. Equation (3.188) thus states that a mechanical system adjusts itself such that the variation vanishes of ($E_{kin} - E_{pot}$) and W respectively. In particular, ($E_{kin} - E_{pot}$) is a minimum when no energy is imparted on the system externally. The task consists of expressing E_{kin}, E_{pot} and W in terms of the field variables e.g., ξ, η and ζ and to perform the variation – a kind of differentiation.

3.8.2 Flat Plate with Shear Stiffness (The Corrected Bending Wave)

In conjunction with the bending wave equation in Sect. 3.3, it was pointed out that the simple bending theory loses its validity at high frequencies because the phase speed according to (3.85) would exceed all limits. This deficiency can partly be remedied by introducing a finite shear stiffness in the y-direction and, in addition, taking the rotational inertia into account. The co-ordinate system used in this case is shown in Fig. 3.29. Assumed is only that the motion η is constant over the thickness of the plate and that the displacements in the plane of the plate are composed of a displacement in the mid-plane ξ_M and rotational motions with angles φ_x and φ_z. For the displacements ξ, η and ζ of a volume element with co-ordinates x, y, z one has

$$\xi = \xi_M + \varphi_x y, \quad \eta = \eta, \quad \zeta = \zeta_M + \varphi_z y \,. \tag{3.189}$$

The kinetic energy thereby becomes

$$E_{kin} = \frac{\rho}{2}\int\left(v_x^2 + v_y^2 + v_z^2\right)dxdydz$$
$$= \frac{\rho}{2}\int\left[\dot{\xi}_M + y\,\dot{\varphi}_x\right]^2 + \dot{\eta}^2 + \left[\dot{\zeta}_M + y\dot{\varphi}_z\right]^2 dxdydz \qquad (3.190a)$$
$$= \frac{\rho}{2}\int\dot{\xi}_M^2 + \dot{\eta}^2 + \dot{\zeta}_M^2 + \frac{h}{12}\left(\dot{\varphi}_x^2 + \dot{\varphi}_z^2\right)dxdz.$$

In the last version of (3.190a) the integration across the cross-section is undertaken from $-h/2$ to $+h/2$.

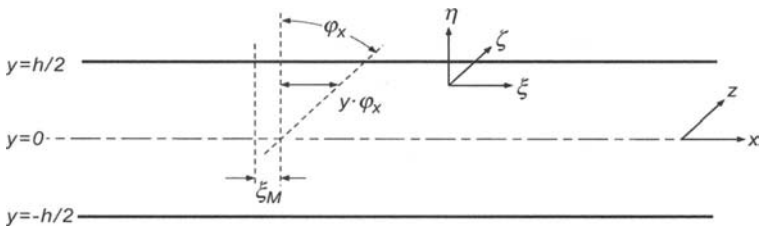

Fig. 3.29. Co-ordinate system for the derivation of the 'corrected bending wave' equation

For the potential energy of a volume element, the different stresses with the accompanying strains ε and γ are to be multiplied and added, cf. (3.115) and (3.120). Generally,

$$E_{pot} = \frac{1}{2}\int\left[\sigma_x\varepsilon_x + \sigma_y\varepsilon_y + \sigma_z\varepsilon_z + \tau_{xy}\gamma_{xy} + \tau_{yz}\gamma_{yz} + \tau_{xz}\gamma_{xz}\right]dxdydz\,. \qquad (3.190b)$$

For thin plates with stress-free surfaces, σ_y can be set to zero for the complete cross-section. Thence, (3.178b) follows from (3.120) which resubstituted in (3.120) gives

$$\sigma_x = \frac{E}{1-\mu^2}\left(\frac{\partial\xi}{\partial x} + \mu\frac{\partial\zeta}{\partial z}\right), \sigma_z = \frac{E}{1-\mu^2}\left(\mu\frac{\partial\xi}{\partial x} + \frac{\partial\zeta}{\partial z}\right). \qquad (3.190c)$$

Regarding the shear stresses, the general expressions in Eq. (3.119) are used. The strains and shear angles read

$$\begin{aligned}
\varepsilon_x &= \frac{\partial \xi}{\partial x} = \frac{\partial \xi_M}{\partial x} + y\frac{\partial \varphi_x}{\partial x}, \quad \varepsilon_z = \frac{\partial \zeta}{\partial z} = \frac{\partial \zeta_M}{\partial z} + y\frac{\partial \varphi_z}{\partial z}, \\
\gamma_{xy} &= \frac{\partial \xi}{\partial y} + \frac{\partial \eta}{\partial x} = \varphi_x + \frac{\partial \eta}{\partial x}, \quad \gamma_{yz} = \frac{\partial \zeta}{\partial y} + \frac{\partial \eta}{\partial z} = \varphi_z + \frac{\partial \eta}{\partial z}, \\
\gamma_{xz} &= \frac{\partial \xi}{\partial z} + \frac{\partial \zeta}{\partial x} = \frac{\partial \xi_M}{\partial z} + y\frac{\partial \varphi_x}{\partial z} + \frac{\partial \zeta_M}{\partial x} + y\frac{\partial \varphi_z}{\partial x}.
\end{aligned} \tag{3.190d}$$

With these expression inserted in (3.190b), results after integration over the cross-section

$$\begin{aligned}
E_{pot} = {} & \frac{1}{2}\frac{Eh}{1-\mu^2}\int\left(\xi_{M,x}^2 + 2\mu\,\xi_{M,x}\zeta_{M,z} + \zeta_{M,z}^2\right)dxdz \\
& + \frac{Gh}{2}\int\left(\xi_{M,z} + \zeta_{M,x}\right)^2 dxdz \\
& + \frac{1}{2}\frac{Eh}{1-\mu^2}\frac{h^2}{12}\int\left[\varphi_{x,x}^2 + 2\mu\,\varphi_{x,x}\varphi_{z,z} + \varphi_{z,z}^2 + \frac{1-\mu}{2}\left(\varphi_{x,z} + \varphi_{z,x}\right)^2\right]dxdz \\
& + \frac{Gh}{2}\int\left[\left(\varphi_x + \eta_{,x}\right)^2 + \left(\varphi_z + \eta_{,z}\right)^2\right]dxdz.
\end{aligned} \tag{3.190e}$$

In this expression the notation "," is used in indices to denote differentiations with respect to the subsequent co-ordinate.

The first and second lines in (3.190e), relate to the potential energy of the in-plane waves. The third line describes the potential energy of the ordinary Kirchhoff's bending theory whereas the last line gives the Timoshenko-Mindlin correction [3.15], stemming from the finite shear stiffness.

Upon undertaking the variation after substitution in (3.188), a set of expressions results in the following form:

$$\begin{aligned}
\delta\int\left(\frac{\partial \xi_M}{\partial x}\right)^2 dxdzdt &= \int 2\left(\frac{\partial \xi_M}{\partial x}\right)\delta\left(\frac{\partial \xi_M}{\partial x}\right)dxdzdt \\
&= \int 2\left(\frac{\partial \xi_M}{\partial x}\right)\delta\xi_M\,dzdt\Big|_{x_1}^{x_2} - 2\int\left(\frac{\partial^2 \xi_M}{\partial x^2}\right)\delta\,\xi_M\,dxdzdt \\
&= -2\int\left(\frac{\partial^2 \xi_M}{\partial x^2}\right)\delta\xi_M\,dxdzdt.
\end{aligned}$$

Herein, first, the variation is performed according to the product rule (analogous to that in a differentiation). Then, an integration by parts is made and finally, it is assumed that the field quantities vanish at the limits of integration, equivalent to a vanishing variation.

By means of the corresponding procedure is obtained

$$\delta \int \frac{\partial \xi_M}{\partial x} \frac{\partial \zeta_M}{\partial z} dxdxdt = -\int \frac{\partial^2 \xi_M}{\partial x \partial z} \delta\zeta_M dxdzdt - \int \frac{\partial^2 \zeta_M}{\partial x \partial z} \delta\xi_M dxdzdt,$$
$$\delta \int \varphi_x \frac{\partial \eta}{\partial x} dxdzdt = -\int \frac{\partial \varphi_x}{\partial x} \delta\eta dxdzdt - \int \frac{\partial \eta}{\partial x} \delta\varphi_x dxdzdt, \tag{3.190f}$$

and a set of similar expressions.

Regarding the external work W, it is assumed that it is solely due to distributed forces i.e., pressure. Since work is the product of force and displacement,

$$W = \int \left(p_B \eta + p_2 \xi_M + p_4 \zeta_M \right) dxdz \tag{3.191}$$

As in Fig. 3.23 and in Eq. (3.164), p_B is the external pressure in the y-direction and p_2 and p_4 are the pressures in the x- and z- directions respectively. Upon undertaking the same manipulation as in Eq. (3.190f), it is found that

$$\int_{t_1}^{t_2} \delta W dt = \int \left(p_B \delta\eta + p_2 \delta\xi_M + p_4 \delta\zeta_M \right) dxdzdt. \tag{3.192}$$

where the pressure need not be varied since it is prescribed.

By combining all equations, beginning with (3.188), is obtained an expression in the form

$$\int \left[A_1 \delta\xi_M + A_2 \delta\eta + A_3 \delta\zeta_M + A_4 \delta\varphi_x + A_5 \delta\varphi_z + p_B \delta\eta + p_2 \delta\xi_M + p_4 \delta\zeta_M \right] dxdzdt = 0$$

This formula reveals why all variations in (3.190f) are transposed to the quantities ξ_M, η, ζ_M, φ_x, φ_z. Pivotal is namely that Hamilton's principle must be valid for any variation. For instance, also for the variation $\delta\xi_M \neq 0$ but $\delta\eta = \delta\zeta_M = \delta\varphi_x = \delta\varphi_z = 0$. It follows that $A_1 + p_2$ must vanish since $\delta\xi_M$ is arbitrary. This argument, applied on $\delta\eta$ etc., shows that the factors in front of the variations $\delta\xi_M$, $\delta\eta$ and the other must vanish independently. With the expressions for A_1 to A_5 introduced, from Eq. (3.188) to (3.190), result

$$
\begin{aligned}
&\delta\xi_M : \rho\ddot{\xi}_M - \left[\frac{E}{1-\mu^2}\frac{\partial^2}{\partial x^2} + G\frac{\partial^2}{\partial z^2}\right]\xi_M - \frac{1+\mu}{1-\mu}G\frac{\partial^2\zeta_M}{\partial x\partial z} = \frac{p_2}{h}\\
&\delta\zeta_M : -\frac{1+\mu}{1-\mu}G\frac{\partial^2\xi_M}{\partial x\partial z} + \rho\ddot{\zeta}_M - \left[\frac{E}{1-\mu^2}\frac{\partial^2}{\partial z^2} + G\frac{\partial^2}{\partial x^2}\right]\zeta_M = \frac{p_4}{h}\\
&\delta\eta : \rho h\ddot{\eta} - Gh\nabla^2\eta - Gh\frac{\partial\varphi_x}{\partial x} - Gh\frac{\partial\varphi_z}{\partial z} = p_B\\
&\delta\varphi_x : Gh\frac{\partial\eta}{\partial x} + \rho I\ddot{\varphi}_x + \left[G\left(h - I\frac{\partial^2}{\partial z^2}\right) - B'\frac{\partial^2}{\partial x^2}\right]\varphi_x - \frac{1+\mu}{2}B'\frac{\partial^2\varphi_z}{\partial x\partial z} = 0\\
&\delta\varphi_z : Gh\frac{\partial\eta}{\partial z} - \frac{1+\mu}{2}B'\frac{\partial^2\varphi_x}{\partial x\partial z} + \rho I\ddot{\varphi}_z + \left[G\left(h - I\frac{\partial^2}{\partial x^2}\right) - B'\frac{\partial^2}{\partial z^2}\right]\varphi_z = 0
\end{aligned}
\tag{3.193}
$$

where $B' = EI/(1 - \mu^2)$ is the bending stiffness of the plate and $I = h^3/12$ the second area moment. As can be observed, the two first equations are fully decoupled from the rest. Owing to the fact that these are identical to the equations of motion for the in-plane waves, cf. Eq. (3.186b), they will not be discussed further in this context.

The three remaining equations form relations between the displacement η and the two rotations φ_x and φ_z. They hence describe the bending motion. It would be possible to retain them in the present form as a system of differential equations. This would indeed give the advantage that the relationship is seen between the cross-sectional force, established from the variation $\delta\eta$, and the moments from the variations of the rotations. It is customary, however, to bring them together in one differential equation of higher order. Therefore, the expressions are rewritten as

$$
\begin{aligned}
&Gh\left(\nabla^2\eta + \frac{\partial\varphi_x}{\partial x} + \frac{\partial\varphi_z}{\partial z}\right) = \rho h\ddot{\eta} - p_B\\
&\frac{B'}{2}\left[(1-\mu)\nabla^2\varphi_x + (1+\mu)\left(\frac{\partial^2\varphi_z}{\partial x\partial z} + \frac{\partial^2\varphi_x}{\partial x^2}\right)\right] - Gh\left(\varphi_x + \frac{\partial\eta}{\partial x}\right) = \rho I\ddot{\varphi}_x\\
&\frac{B'}{2}\left[(1-\mu)\nabla^2\varphi_z + (1+\mu)\left(\frac{\partial^2\varphi_x}{\partial x\partial z} + \frac{\partial^2\varphi_z}{\partial z^2}\right)\right] - Gh\left(\varphi_z + \frac{\partial\eta}{\partial z}\right) = \rho I\ddot{\varphi}_z
\end{aligned}
\tag{3.194a}
$$

where use is made of the relation $GI = B'(1 - \mu)/2$. By differentiating the penultimate equation with respect to x and the last with respect to z, a subsequent addition yields

$$
\begin{aligned}
&Gh\left(\nabla^2\eta + \psi\right) = \rho h\ddot{\eta} - p_B,\\
&B'\nabla^2\psi - Gh\left(\nabla^2\eta + \psi\right) = \rho I\ddot{\psi},
\end{aligned}
\tag{3.194b}
$$

where the abbreviation,

$$\psi = \frac{\partial \varphi_x}{\partial x} + \frac{\partial \varphi_z}{\partial z}, \tag{3.194c}$$

is introduced for clarity. From an elimination of ψ it is found that

$$B'\nabla^4\eta - \left(\frac{B'\rho}{G} + \rho I\right)\nabla^2\ddot{\eta} + \rho h\ddot{\eta} + \rho I\frac{\rho}{G}\ddot{\eta} = p_B + \frac{B'}{Gh}\nabla^2 p_B - \frac{\rho I}{Gh}\ddot{p}_B \tag{3.195}$$

This formula, which in the one-dimensional case dates back to Timoshenko [3.12] and to Mindlin [3.15] in the two-dimensional, furnishes an improvement of the simple bending wave Eqs. (3.81) and (3.184a) respectively. It takes the shear stiffness into account via terms involving I. Of the two, the latter, already derived by Rayleigh, is the least important.

Often, the modified shear stiffness G^* cf., Sect. 3.2.2, is introduced in Eq. (3.195) instead of the ordinary shear modulus G. In this way, the flexural wave speed approaches the Rayleigh wave speed at high frequencies.

To assess how much (3.195) deviates from (3.81) and (3.184a) respectively, a one-dimensional case without external excitation can be considered, Upon letting $\eta \sim e^{j\omega t}e^{-jk_x x}$, the dispersion equation results as

$$k_C^4 - \omega^2 k_C^2\left[\frac{1}{c_T^2} + \frac{1}{c_{LII}^2}\right] - k_B^4 + \frac{\omega^4}{c_{LII}^2 c_T^2} = 0 \tag{3.196a}$$

Herein, k_B is the non-corrected flexural wave number according to (3.83) and k_C the free wave number of flexural waves in thick plates. This means that the wave speed of the corrected flexural wave is approximated by

$$c_C \approx c_B\left[1 - \frac{1}{2}c_B^2\left(\frac{1}{c_T^2} + \frac{1}{c_{LII}^2}\right)\right] \approx c_B\left[1 - 4\left(h/\lambda_B\right)^2\right] \tag{3.196b}$$

A 10% deviation is accordingly first then approached when the wavelength λ_B becomes smaller than six times the plate thickness; $\lambda_B < 6h$. Further aspects of plates with finite shear stiffness are given in Sect. 4.4.3.1.

3.8.3 Cylindrical Shells

3.8.3.1 Fundamental Equations

In Figs. 3.30 and 3.31 are depicted, the polar co-ordinates and the displacement variables – ξ tangential, η radial and ζ axial – appropriate for cylindrical shells. The conversion to Cartesian co-ordinates for very large radii is given by $r\vartheta \to x$, $r \to y$, $\zeta \to z$.

To be able to employ Hamilton's principle, the potential energy is required, given by the stresses and strains. This means that the general stress-strain relations have to be developed in polar co-ordinates. As can be seen from Fig. 3.30, the strain in radial direction is

$$\varepsilon_r = \frac{1}{\Delta r}\left[\left(\eta + \frac{\partial \eta}{\partial r}\Delta r\right) - \eta\right] = \frac{\partial \eta}{\partial r} \tag{3.197a}$$

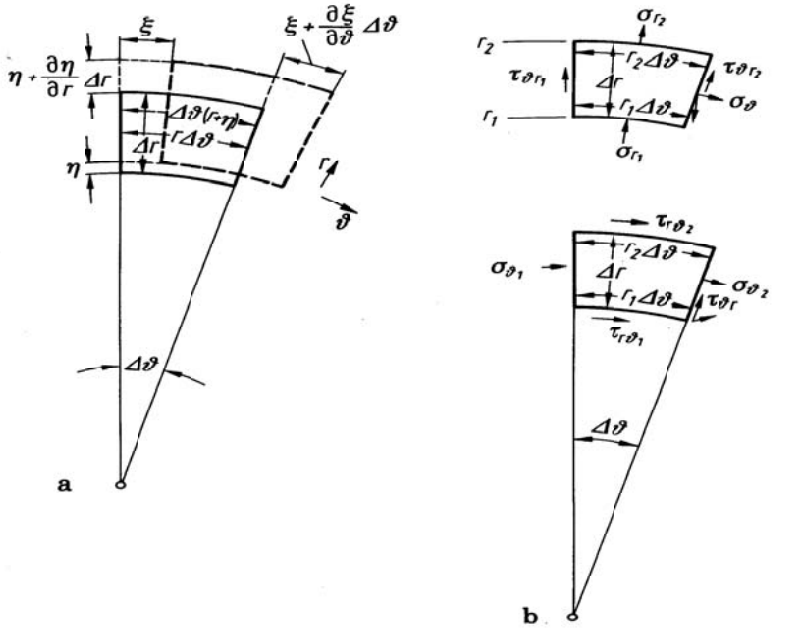

Fig. 3.30. Deformation (a) of a volume element in polar co-ordinates and normal and shear stresses (b)

The tangential strain consists of two parts. The first occurs for pure radial motion because the element is elongated,

$$\varepsilon_{\vartheta 1} = \frac{1}{r\nabla^2\vartheta}\left[\nabla^2\vartheta\,(r+\eta) - r\nabla^2\vartheta\right] = \frac{\eta}{r}.$$

The second comes about due to motion in tangential direction whereby

$$\varepsilon_{\vartheta 2} = \frac{1}{r\nabla^2\vartheta}\left[\left(\xi + \frac{\partial \xi}{\partial \vartheta}\nabla^2\vartheta\right) - \xi\right] = \frac{1}{r}\frac{\partial \xi}{\partial \vartheta}.$$

Accordingly, the tangential strain becomes

$$\varepsilon_\vartheta = \varepsilon_{\vartheta 1} + \varepsilon_{\vartheta 2} = \frac{\eta}{r} + \frac{1}{r}\frac{\partial \xi}{\partial \vartheta} \tag{3.197b}$$

By a similar consideration for the shear deformation, it is found in analogy with (3.162a) that the stress-strain relations in polar co-ordinates are given by [3.9, 3.16-18]

$$\begin{aligned}
\frac{\sigma_\vartheta}{2G} &= (\alpha+1)\varepsilon_\vartheta + \alpha\varepsilon_r + \alpha\varepsilon_z = (\alpha+1)\left(\frac{\eta}{r} + \frac{1}{r}\frac{\partial \xi}{\partial \vartheta}\right) + \alpha\frac{\partial \eta}{\partial r} + \alpha\frac{\partial \zeta}{\partial z},\\
\frac{\sigma_r}{2G} &= \alpha\varepsilon_\vartheta + (\alpha+1)\varepsilon_r + \alpha\varepsilon_z = \alpha\left(\frac{\eta}{r} + \frac{1}{r}\frac{\partial \xi}{\partial \vartheta}\right) + (\alpha+1)\frac{\partial \eta}{\partial r} + \alpha\frac{\partial \zeta}{\partial z},\\
\frac{\sigma_z}{2G} &= \alpha\varepsilon_\vartheta + \alpha\varepsilon_r + (\alpha+1)\varepsilon_z = \alpha\left(\frac{\eta}{r} + \frac{1}{r}\frac{\partial \xi}{\partial \vartheta}\right) + \alpha\frac{\partial \eta}{\partial r} + (\alpha+1)\frac{\partial \zeta}{\partial z},\\
\frac{\tau_{\vartheta r}}{G} &= \gamma_{\vartheta r} = r\frac{\partial}{\partial r}\left(\frac{\xi}{r}\right) + \frac{1}{r}\frac{\partial \eta}{\partial \vartheta} = \frac{\partial \xi}{\partial r} - \frac{\xi}{r} + \frac{1}{r}\frac{\partial \eta}{\partial \vartheta},\\
\frac{\tau_{rz}}{G} &= \gamma_{rz} = \frac{\partial \zeta}{\partial r} + \frac{\partial \eta}{\partial z},\\
\frac{\tau_{\vartheta z}}{G} &= \gamma_{\vartheta z} = \frac{\partial \xi}{\partial z} + \frac{1}{r}\frac{\partial \zeta}{\partial \vartheta},
\end{aligned} \tag{3.198a}$$

where $\alpha = \mu/(1 - 2\mu)$. Henceforth, it is assumed that the thickness of the shell h is substantially smaller than the radius of curvature and the wavelength, see Fig. 3.31. For such a case, σ_r can be set to zero when the shell is free of external stresses i.e., a state of plane stress. In analogy with (3.190c) it follows that

$$\begin{aligned}
\sigma_\vartheta &= \frac{E}{1-\mu^2}(\varepsilon_\vartheta + \mu\varepsilon_z) = \frac{E}{1-\mu^2}\left(\frac{\eta}{r} + \frac{1}{r}\frac{\partial \xi}{\partial \vartheta} + \mu\frac{\partial \zeta}{\partial z}\right),\\
\sigma_z &= \frac{E}{1-\mu^2}(\mu\varepsilon_\vartheta + \varepsilon_z) = \frac{E}{1-\mu^2}\left(\mu\frac{\eta}{r} + \mu\frac{1}{r}\frac{\partial \xi}{\partial \vartheta} + \frac{\partial \zeta}{\partial z}\right),
\end{aligned} \tag{3.199}$$

whilst the shear stresses remain unaltered.

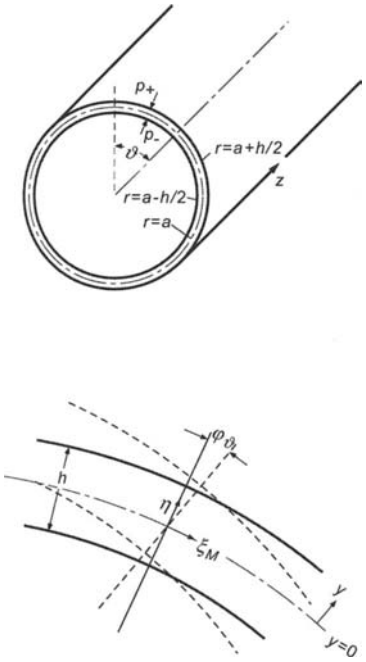

Fig. 3.31. Displacement co-ordinates for a thin-walled shell

The proceeding analysis follows that of the preceding section. Thus, the radial component η is constant over the cross-section whereas the tangential and axial motion will consist of an "in-plane" part and bending part, which depends linearly on the radius cf., (3.189),

$$\begin{aligned} \xi &= \frac{r}{a}\xi_M + (r-a)\varphi_\vartheta, \\ \zeta &= \zeta_M + (r-a)\varphi_z. \end{aligned} \tag{3.200a}$$

Accordingly, there are again five independent variables i.e., the motion of the mid-plane of the shell ξ_M, η and ζ_M and rotations φ_ϑ and φ_z. The shell radius is a assumed constant in this analysis, Fig. 3.31. With (3.200a) substituted into the equations for the strain (3.197) and approximating

$$(r-a) = y, \quad \frac{1}{r} \approx \frac{1}{a}\left(1-\frac{y}{a}\right), \quad \frac{a}{r} \approx 1-\frac{y}{a}, \quad \frac{r-a}{r} \approx \frac{y}{a}, \tag{3.200b}$$

the strains and shear angles become

$$\varepsilon_\vartheta = \frac{1}{a}\left(1-\frac{y}{a}\right)\eta + \frac{1}{a}\frac{\partial \xi_M}{\partial \vartheta} + \frac{y}{a}\frac{\partial \varphi_\vartheta}{\partial \vartheta}, \quad \varepsilon_z = \frac{\partial \zeta_M}{\partial z} + y\frac{\partial \varphi_z}{\partial z},$$
$$\gamma_{r\vartheta} = \left(1-\frac{y}{a}\right)\varphi_\vartheta + \frac{1}{a}\left(1-\frac{y}{a}\right)\frac{\partial \eta}{\partial \vartheta}, \quad \gamma_{rz} = \varphi_z + \frac{\partial \eta}{\partial z}, \tag{3.201}$$
$$\gamma_{z\vartheta} = \left(1+\frac{y}{a}\right)\frac{\partial \xi_M}{\partial z} + y\frac{\partial \varphi_\vartheta}{\partial z} + \frac{1}{a}\left(1-\frac{y}{a}\right)\frac{\partial \zeta_M}{\partial \vartheta} + \frac{y}{a}\frac{\partial \varphi_z}{\partial \vartheta}.$$

Thereby are terms involving y^2 omitted. Furthermore, since ξ_M and ζ_M are constant across the cross-section, their derivatives vanish in the radial direction. It should also be noted that $\partial\xi/\partial r = 1$.

The next step to use Hamilton's principle for the derivation is to express the energies. The kinetic energy is obtained as

$$E_{kin} = \frac{\rho}{2}\int_0^{2\pi}\int_{-h/2}^{h/2}\int_{-L}^{L}\left(\dot{\xi}^2 + \dot{\eta}^2 + \dot{\zeta}^2\right) a\,d\vartheta\,dy\,dz = \frac{\rho h}{2}\int_0^{2\pi}\int_{-L}^{L}\left[\dot{\xi}_M^2 + \dot{\eta}^2 + \dot{\zeta}_M^2 + I'\left(\dot{\varphi}_\vartheta^2 + \dot{\varphi}_z^2 + \frac{2}{a}\dot{\xi}_M\dot{\varphi}_\vartheta\right)\right] a\,d\vartheta\,dz, \tag{3.202a}$$

and the potential energy

$$E_{pot} = \frac{1}{2}\int_0^{2\pi}\int_{-h/2}^{h/2}\int_{-L}^{L}\left(\sigma_\vartheta\varepsilon_\vartheta + \sigma_z\varepsilon_z + \tau_{r\vartheta}\gamma_{r\vartheta} + \tau_{rz}\gamma_{rz} + \tau_{z\vartheta}\gamma_{z\vartheta}\right) a\,d\vartheta\,dy\,dz = \frac{1}{2}\int_0^{2\pi}\int_{-h/2}^{h/2}\int_{-L}^{L}\left[\frac{E}{1-\mu^2}\left(\varepsilon_\vartheta^2 + \varepsilon_z^2 + 2\mu\varepsilon_\vartheta\varepsilon_z\right) + G\left(\gamma_{r\vartheta}^2 + \gamma_{rz}^2 + \gamma_{z\vartheta}^2\right)\right] a\,d\vartheta\,dy\,dz \tag{3.202b}$$

In Eq. (3.202a) is $I' = h^2/12$ introduced.

By substituting Eq. (3.201) in (3.202b) and integrating with respect to y, a lengthy expression results, which contains the displacements ξ_M, η etc. as well as their spatial derivatives. The subsequent treatment is as for (3.190) to (3.192) i.e., the variation is undertaken and an integration by parts such that the variation refers to the field variables. Use is also made of the fact that the values of the integrand at the limits 0 and 2π are equal due to the periodicity and that $+L$ and $-L$ are so remote that all field variables have decayed and the variations vanish. As in Eq. (3.193), a system of linear differential equations results in the independent variables ξ_M, η, ζ_M, φ_ϑ and φ_z. Abbreviated, this reads

$$\begin{bmatrix} A_{11} & A_{12} & A_{13} & A_{14} & A_{15} \\ A_{21} & A_{22} & & & \vdots \\ \vdots & & \ddots & & \vdots \\ \vdots & & & \ddots & \vdots \\ A_{51} & & & & A_{55} \end{bmatrix} \begin{bmatrix} \xi_M \\ \zeta_M \\ \eta \\ \varphi_\vartheta \\ \varphi_z \end{bmatrix} = \begin{bmatrix} 0 \\ 0 \\ -p_B\left(1-\mu^2\right)/Eh \\ 0 \\ 0 \end{bmatrix} \tag{3.203}$$

Herein, the coefficients are

$$A_{11} = -\frac{\partial^2}{\partial s^2} - \alpha_-\left(1+\beta^2\right)\frac{\partial^2}{\partial z^2} + \frac{1+\beta^2}{c_{LI}^2}\frac{\partial^2}{\partial t^2},$$

$$A_{12} = \left(-\alpha_+ - \beta^2\alpha_-\right)\frac{\partial^2}{\partial s \partial z} = A_{21},$$

$$A_{13} = -\frac{1}{a}\frac{\partial}{\partial s} = A_{31}, \quad A_{14} = \beta^2 a\left(-\alpha_-\frac{\partial^2}{\partial z^2} + \frac{1}{c_{LI}^2}\frac{\partial^2}{\partial t^2}\right) = A_{41},$$

$$A_{15} = -\beta^2 a\alpha_-\frac{\partial^2}{\partial s \partial z} = A_{51}, \quad A_{22} = -\frac{\partial^2}{\partial z^2} - \alpha_-\left(1+\beta^2\right)\frac{\partial^2}{\partial s^2} + \frac{1}{c_{LI}^2}\frac{\partial^2}{\partial t^2},$$

$$A_{23} = -\frac{\mu}{a}\frac{\partial}{\partial z} = A_{32}, \quad A_{24} = \beta^2 a\alpha_-\frac{\partial^2}{\partial s \partial z} = A_{42},$$

$$A_{25} = \beta^2 a\alpha_-\frac{\partial^2}{\partial s^2} = A_{52}, \quad A_{33} = -\left\{\frac{1+\beta^2}{a^2} - \alpha_-\left[\left(1+\beta^2\right)\frac{\partial^2}{\partial s^2} + \frac{\partial^2}{\partial z^2}\right] + \frac{1}{c_{LI}^2}\frac{\partial^2}{\partial t^2}\right\},$$

$$A_{34} = \left[\alpha_- + \beta^2\left(1+\alpha_-\right)\right]\frac{\partial}{\partial s} = A_{43}, \quad A_{35} = \left(\alpha_- + \mu\beta^2\right)\frac{\partial}{\partial z} = A_{53},$$

$$A_{44} = \alpha_-\left(1+\beta^2\right) - I'\frac{\partial^2}{\partial s^2} - \alpha_- I'\frac{\partial^2}{\partial z^2} + \frac{I'}{c_{LI}^2}\frac{\partial^2}{\partial t^2},$$

$$A_{45} = -\alpha_+ I'\frac{\partial^2}{\partial s \partial z} = A_{54}, \quad A_{55} = \alpha_- - I'\frac{\partial^2}{\partial z^2} - \alpha_- I'\frac{\partial^2}{\partial s^2} + \frac{I'}{c_{LI}^2}\frac{\partial^2}{\partial t^2},$$

$$\alpha_- = \frac{1-\mu}{2}, \quad \alpha_+ = \frac{1+\mu}{2}, \quad \beta^2 = \frac{h^2}{12a^2}, \quad I' = \frac{h^2}{12} = \beta^2 a^2,$$

$$\frac{\partial}{\partial s} = \frac{1}{a}\frac{\partial}{\partial \vartheta}, \quad s = a\vartheta$$

3.8.3.2 Special Cases

The rather extensive system of Eq. (3.203) permits the following conclusions:

a) The system is symmetric as usual for wave equations derived by means of Hamilton's principle for stationary or uniformly moving media.

b) As the wall thickness tends to zero $h \to 0$, $\beta = 0$ and $I' = 0$ and $\varphi_\vartheta = -\partial\eta / \partial s$ as well as $\varphi_z = -\partial\eta/\partial z$. Thence, Eq. (3.203) turns into the membrane equation [3.18].

$$\left[-\frac{\partial^2}{\partial s^2} - \frac{1-\mu}{2}\frac{\partial^2}{\partial z^2} + \frac{1}{c_{LI}^2}\frac{\partial^2}{\partial t^2}\right]\xi_M - \frac{1+\mu}{2}\frac{\partial^2 \zeta_M}{\partial s \partial z} - \frac{1}{a}\frac{\partial \eta}{\partial s} = 0,$$

$$-\frac{1+\mu}{2}\frac{\partial^2 \xi_M}{\partial s \partial z} + \left[-\frac{\partial^2}{\partial z^2} - \frac{1-\mu}{2}\frac{\partial^2}{\partial s^2} + \frac{1}{c_{LI}^2}\frac{\partial^2}{\partial t^2}\right]\zeta_M - \frac{\mu}{a}\frac{\partial \eta}{\partial z} = 0, \qquad (3.204a)$$

$$\frac{1}{a}\frac{\partial \xi_M}{\partial s} + \frac{\mu}{a}\frac{\partial \zeta_M}{\partial z} + \left[\frac{1}{a^2} + \frac{1}{c_{LI}^2}\frac{\partial^2}{\partial t^2}\right]\eta = \frac{p_B\left(1-\mu^2\right)}{Eh},$$

which is fully valid for numerous applications.

c) When the radius grows large i.e., $a \to \infty$, all terms involving $1/a$ and β disappears. The remaining expressions are identical to those for in-plane waves (3.168b) and the Mindlin-Timoshenko bending wave description (3.195).

d) Upon approximating $h/a \approx 0$ in Eq. (3.203) for non-vanishing h, all terms involving β and I'/a vanish while those with I' remains. If, in addition, the terms representing the rotational inertia i.e., $(I'/c_{LI}^2)\,\partial^2/\partial t^2$ as is the case for the simple bending theory, one obtains the "Donell-Mushtari equation" [3.19, 3.20]. It differs from Eq. (3.204a) merely in that the η term in the last relation takes the form

$$\left[\frac{1}{a^2} + I'\left(\frac{\partial^2}{\partial s^2} + \frac{\partial^2}{\partial z^2}\right) + \frac{1}{c_{LI}^2}\frac{\partial^2}{\partial t^2}\right]\eta. \qquad (3.204b)$$

Thereby, is taken into account the bending of the cylinder wall.

e) For a transition to a ring, $\partial/\partial z = 0$ is employed and c_{LI} as well as $E/\left(1-\eta^2\right)$ are replaced by c_{LII} and E respectively owing to the cross-sectional contraction in axial direction cf., Eq. (3.32) to (3.34). Thereby, two independent expressions result: Shear in axial direction

$$\frac{\partial^2 \zeta_M}{\partial s^2} - \frac{2}{\left(1-\mu\right)c_{LI}^2}\frac{\partial^2 \zeta_M}{\partial t^2} = \frac{\partial^2 \zeta_M}{\partial s^2} - \frac{1}{c_T^2}\frac{\partial^2 \zeta_M}{\partial t^2} = 0 \qquad (3.204c)$$

and motion in tangential and radial directions

$$\left[\frac{\partial^2}{\partial s^2} - \frac{1+\beta^2}{c_{LII}^2}\frac{\partial^2}{\partial t^2}\right]\xi_M - \left[\frac{1}{a}\frac{\partial}{\partial s} + \frac{I'}{a c_{LII}^2}\frac{\partial^3}{\partial s \partial t^2}\right]\eta = 0,$$

$$\left[\frac{1}{a}\frac{\partial}{\partial s} + \frac{I'}{a c_{LII}^2}\frac{\partial^3}{\partial s \partial t^2}\right]\xi_M + \left[\frac{1}{a^2} + \beta^2\left(\frac{1}{a} + a\frac{\partial^2}{\partial s^2}\right)^2 + \frac{1}{c_{LII}^2}\frac{\partial^2}{\partial t^2} - \frac{I'}{c_{LII}^2}\frac{\partial^4}{\partial s^2 \partial t^2}\right]\eta = \frac{P_B}{Eh}. \qquad (3.204d)$$

To arrive at these expressions, the last three equations in (3.203) are added to account for the rotational energy. Moreover, the approximation $\varphi_\vartheta = -\partial\eta/\partial s$ is introduced as employed in simple bending theory.

f) Besides the shell Eq. (3.203) presented and the simplified versions in Eqs. (3.204), the literature comprises a suite of other formulae, which differ in the terms involving β^2 [3.21]. As long as the wavelengths and the radius of curvature are larger than six times the shell thickness, however, no significant differences arise.

3.8.3.3 Phase Speeds

To better understand the shell equations it is suitable to consider their features for the special case of plane waves spiralling along a cylinder. It is thus assumed that the field variables ξ, η, ζ, p_B, φ_2 and φ_ϑ take the form

$$\left(\hat{\xi},\hat{\eta},\hat{\zeta},\hat{p}_B,\hat{\varphi}_z,\hat{\varphi}_\vartheta\right)e^{-jk_z z}e^{jns/a}e^{j\omega t}. \tag{3.205}$$

Herein, index M is omitted for brevity. For an infinitely long cylinder, the associated waves propagate with the speed $c_z = \omega/kz$ in the axial direction and exhibit $2n$ nodes over the perimeter, see Fig. 3.32a. They can be imagined as screw-formed propagating disturbances of "threading" $\lambda_z = 2\pi/kz$. In the literature appears often $\cos ns/a$ or $\sin ns/a$ instead of $e^{jns/a}$ but also $\cos n\vartheta$ or $\sin n\vartheta$ for symmetric and antisymmetric problems. For the general case, however, the notation $e^{jns/a}$ is most suitable and for the dispersion diagrams and wave impedances this does not lead to any differences.

Upon inserting (3.205) in Eq. (3.203) and simultaneously letting $\varphi_\vartheta = -\partial\eta/\partial s$ and $\varphi_z = -\partial\eta/\partial z$ as is customary in conjunction with simple bending theory, is obtained

$$\begin{pmatrix} a_{11} & -a_{12} & -j\,a_{13} \\ -a_{12} & a_{22} & -j\,a_{23} \\ ja_{13} & ja_{23} & a_{33} \end{pmatrix}\begin{pmatrix}\hat{\xi}\\ \hat{\zeta}\\ \hat{\eta}\end{pmatrix} = \begin{pmatrix} 0 \\ 0 \\ \hat{p}_B\nu/\omega^2\rho h \end{pmatrix}. \tag{3.206a}$$

The manipulations required to arrive at this system of equations consists in differentiating the fourth equation with respect to s, the fifth with respect to z and adding the last three of the resulting expressions. In Eq. (3.206a),

$$
\begin{aligned}
a_{11} &= n^2 + \alpha_- k_z^2 a^2 - \nu^2 + \beta^2 \left(\alpha_- k_z^2 a^2 - \nu^2 \right), \\
a_{12} &= \alpha_+ n k_z a + \beta^2 \alpha_- n k_z a, \\
a_{13} &= n + \beta^2 n \left(2\alpha_- k_z^2 a^2 - \nu^2 \right), \\
a_{22} &= k_z^2 a^2 + \alpha_- n^2 - \nu^2 + \beta^2 \alpha_- n^2, \\
a_{23} &= -\mu k_z a + 2\beta^2 \alpha_- n^2 k_z a,
\end{aligned}
\tag{3.206b}
$$

and

$$
a_{33} = 1 - \nu^2 + \beta^2 \left[1 - 2n^2 - 2\mu k_z^2 a^2 + \left(k_z^2 a^2 + n^2 - \nu^2 \right) \left(k_z^2 a^2 + n^2 \right) \right].
$$

In addition, $\nu = \omega a / c_{LI} = \omega / \omega_{\text{ring}}$, is a non-dimensional frequency based on the ring frequency $\omega_{\text{ring}} = c_{LI}/a = 2\pi f_{\text{ring}}$.

The determinant of (3.206a) is given by

$$
\text{Det} = a_{33} \left(a_{11} a_{22} - a_{12}^2 \right) - 2 a_{12} a_{13} a_{23} - a_{11} a_{23}^2 - a_{22} a_{13}^2 \tag{3.206c}
$$

and its vanishing furnishes the wave numbers of the free waves, which can exist in loss-free media also in the absence of excitation. With (3.206b) in (3.206c), a fourth-order polynomial in $(k_z a)^2$ is obtained. Accordingly, four free waves can exist at most at every frequency. At least one thereof, does not propagate implying an exponentially decaying nearfield. For the remaining three propagating waves, the dispersion diagram in Fig. 3.32 is obtained by equating (3.206c) to zero. Shown is the phase speed for the axial direction instead of the associated wavenumber for a Poisson's ratio of $\mu = 0.3$ and normalized with respect to c_{LI}. The following conclusions can be drawn from the curves.

a) The branches denoted by *T* which come down from infinity at $\nu^2 = n^2 (1\text{-}\mu)/2$ approach asymptotically $c_z = c_{LI} \sqrt{(1-\mu)/2}$. They correspond to pure transversal waves (no compression of the material, see Sect. 3.2.1).
b) The branches denoted by *L* which come down from infinity at $\nu^2 = 1 + n^2$ approach asymptotically $c_z = c_{LI}$. They correspond to quasi-longitudinal waves (see Sect. 3.1.2).
c) For low frequencies is obtained the relation

$$
c_z = \sqrt[4]{\omega^2 a^2 / 2 c_{LI}^2}
$$

for $n = 1$. Since $a^2/2$ is the square of the radius of gyration of a thin-walled cylinder, this relation constitutes the flexural wave speed of a cylindrical shell vibrating as a beam.
d) A fundamental role plays the non-dimensional frequency $\nu = 1$ i.e., the ring frequency $f_{\text{ring}} = c_{LI}/2\pi a$ where the cylinder perimeter equals one wavelength of the longitudinal wave.

e) For $n = 0$ there exist at low frequencies longitudinal waves of speed $c_z = c_{LI}\sqrt{1-\mu^2} = \sqrt{E/\rho}$ and torsional waves of speed $c_z = c_{LI}\sqrt{1-\mu/2} = \sqrt{G/\rho}$. In the first case, a volume element of the cylinder wall moves in radial direction – breathing mode – neglecting the comparatively much smaller cross-contraction. In the second, the motion is torsional.

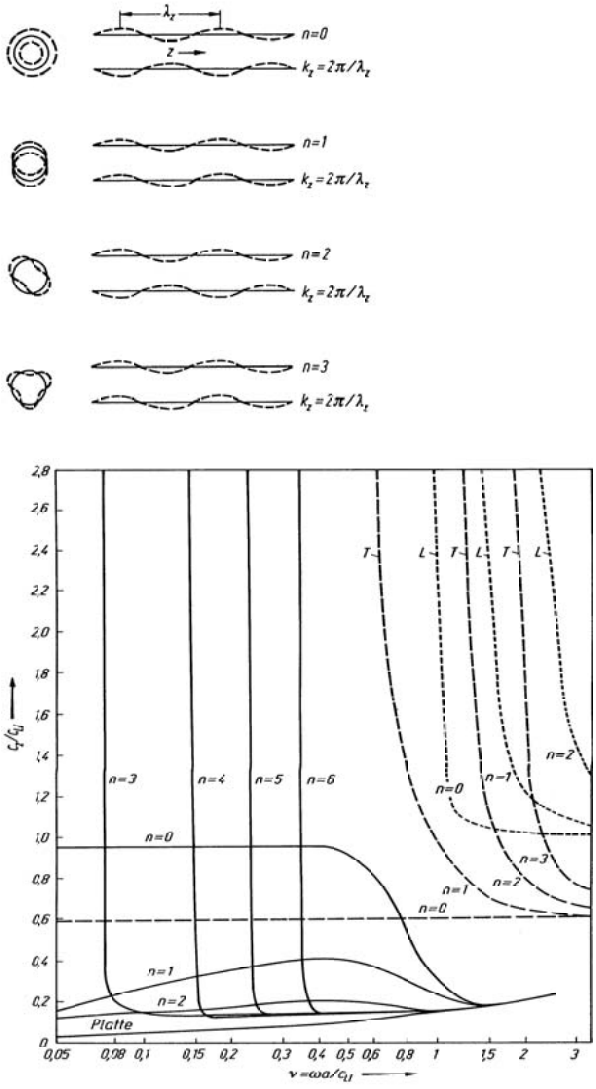

Fig. 3.32. Spatial displacements of modes $n = 0, 1, 2, 3$ and dispersion diagram according to (3.206c) for $a = 15$ and $\mu = 0.3$

f) For $n \geq 2$, the characteristic Eq. (3.206) yields three groups of dispersion curves. The first two – long and short dashed curves in Fig. 3.32 – were discussed in a) and b). The third group – solid curves – is only possible above the associated ring-resonance frequencies, see Eq. (3.210c). All the solid curves approach that of the bending wave speed of a plate of thickness h – also drawn solid – at high frequencies.

g) At frequencies above $\nu > 2$, the dispersion curves are practically identical to those of a flat plate of thickness h and width πa exhibiting bending and in-plane waves. The boundary condition for the strip are those shown in Fig. 3.15 top left or bottom right. In this frequency range, therefore, the cylinder wall can be treated as a flat plate. The dispersion curves obtained from the characteristic Eq. (3.206) are corroborated by experimental results.

3.8.3.4 Wave Impedances

In addition to the phase speeds, Eq. (3.206a) also furnishes the so-called wave impedance, cf. Sect. 5.4. It is defined by

$$Z_{\sim} = \frac{\hat{p}_B}{\hat{v}_r} = \frac{\hat{p}_B}{j\omega\hat{\eta}} \tag{3.207}$$

i.e., the ratio of the exciting pressure amplitude $\hat{p}_B$ to the resulting radial velocity amplitude $\hat{v}_r$ for an infinitely extended cylinder. For discrete n, Eq. (3.206a) gives

$$Z_{\sim n} = \frac{\rho h}{j\nu^2}\left[a_{33} - \frac{2a_{12}a_{13}a_{23} + a_{11}a_{23}^2 + a_{22}a_{13}^2}{a_{11}a_{22} - a_{12}^2}\right], \tag{3.208}$$

from which a good approximation is found to be [3.21]

$$Z_{\sim n} \approx \frac{\omega\rho h}{j\nu^2}\left\{-\nu^2 + \beta^2\left[\left(n^2 + k_z^2a^2\right)^2 - \frac{n^2(4-\mu) - 2 - \mu}{2(1-\mu)}\right] + \left[\frac{\left(1-\mu^2\right)\left[\frac{1-\mu}{2}k_z^2a^2 - \nu^2\right]k_z^2a^2 - \left[\frac{1-\mu}{2}\left(k_z^2a^2 + n^2\right) - \nu^2\right]\nu^2}{\left[\frac{1-\mu}{2}\left(k_z^2a^2 + n^2\right) - \nu^2\right]\left[k_z^2a^2 + n^2 - \nu^2\right]}\right]\right\}. \tag{3.209}$$

The wave impedance indicates whether a cylinder will be strongly or weakly excited by a pressure of the form (3.205); small and large $Z_{\sim n}$ respectively. From $Z_{\sim n} = 0$, the wavenumbers of the free waves can be de-

termined and, in turn, the dispersion curves can be generated by using $c_x / c_{LI} = \nu / k_z a$ for given values of n.

3.8.3.5 Resonance Frequencies

The resonance frequencies of a circular ring can be obtained from Eqs. (3.204c, d) by setting $p_B = 0$ and employing the solution given by (3.205). From Eq. (3.204c) it is found that

$$-\frac{n^2}{a^2} + \frac{\omega^2}{c_T^2} = 0\,,$$

giving the possible resonance frequencies for the particle motion in axial direction

$$\omega_{n,III}^2 = n^2 c_T^2 / a^2\,. \tag{3.210a}$$

For the other, important motion components, the dispersion equation is obtained in a similar manner as (3.206). It is sufficient to put $k_z = 0$ since no z dependence exists. Some further manipulations yield the characteristic equation

$$\nu^4\left[1+\beta^2\left(1+n^2\right)\right]-\nu^2\left[n^2+1-2\beta\left(n^2-1\right)^2\right]+n^2\beta^2\left(1-n^2\right)^2=0\,.$$

By focussing on thin-walled cylinders ($\beta^2 << 1$), the approximations

$$\begin{aligned}\nu_{nI}^2 &= \frac{\omega_{nI}^2}{c_{LI}^2}a^2 \approx n^2+1,\\ \nu_{nII}^2 &= \frac{\omega_{nII}^2}{c_{LI}^2}a^2 \approx \beta^2\frac{n^2\left(n^2-1\right)^2}{n^2+1}\end{aligned} \tag{3.210b, c}$$

result for the quasi-longitudinal and flexural motion respectively. Thus, the resonances are determined.

It should be pointed out, however, that the ring resonances are not accurately predicted by means of the approximation for the wave impedance in (3.209) for $k_z = 0$. The error amounts to 14 % for $n = 2$, 4 % for $n = 3$, 2 % $n = 4$ and is smaller than 1.5 % when $n \geq 5$.

As for slender beams, the calculation of the eigen-frequencies of a cylindrical tube of length l_z can be readily made only for two ideal boundary conditions. This means that the eigen-functions

$$\xi(\vartheta, z) = \xi_{m,n} \sin\frac{m\pi z}{l_z} \sin n\vartheta,$$
$$\eta(\vartheta, z) = \eta_{m,n} \sin\frac{m\pi z}{l_z} \cos n\vartheta, \tag{3.211}$$
$$\zeta(\vartheta, z) = \zeta_{m,n} \cos\frac{m\pi z}{l_z} \cos n\vartheta,$$

apply or the corresponding ones in which the terms $\cos(m\pi z/l_z)$ and $\sin(m\pi z/l_z)$ are interchanged.

The eigen-functions in (3.211) imply that the tube wall at $x = 0$ and $x = l_z$ are simply supported and, simultaneously the axial motion is unconstrained, see Fig. 3.15, top-left. With the sine and cosine functions interchanged the eigen-functions satisfy guided tube ends and blocked with respect to axial motion $\zeta(\varphi, 0) = \zeta(\varphi, l_z) = 0$, see Fig. 3.15, bottom-right.

A similar analysis as that of the preceding section can be used also in this case to determine the resonance frequencies. The only modification necessary is that $k_z a$ is replaced by $m\pi a/l_z$. The resonance frequencies then correspond to those values of ν for which the wave impedance in Eq. (3.208) vanishes. This means that the resonance frequencies correspond to the intersections of the dispersion curves c_z/c_{LI} in Fig. 3.32 with curves $\nu\, l_z/m\pi a$ since

$$\frac{c_z}{c_{LI}} = \frac{\omega a}{c_{LI}} \frac{l_z}{m\pi a} \Leftrightarrow m\pi = \frac{\omega}{c_z} l_z = k_z l_z \Leftrightarrow m\lambda_z = 2l_z$$

at these points. For the flexural motion of primary interest, the resonance frequencies are closely approximated by [3.22]

$$\nu_{n,m}^2 = \frac{\omega_{n,m}^2 a^2}{c_{LI}} \approx \frac{\left(m\pi a/l_z\right)^4}{\left[\left(m\pi a/l_z\right)^2 + n^2\right]^2} + \beta^2 \left\{\left[\left(m\pi a/l_z\right)^2 + n^2\right]^2 - \frac{n^2(4-\mu) - 2 - \mu}{2(1-\mu)}\right\}, \tag{3.212a}$$

whereas for the other types of motion,

$$\nu_{n,m}^2 \approx \frac{1-\mu}{2}\left[\left(m\pi a/l_z\right)^2 + n^2\right],$$
$$\nu_{n,m}^2 \approx 1 + \left[\left(m\pi a/l_z\right)^2 + n^2\right]. \tag{3.212b}$$

The formulae in (3.212) encompass for $n = 0$ the very important ring frequency $\nu = 1$ as $m\pi a/l_z$ tends to zero. Other expressions for resonance fre-

quencies as well as comparison of different shell equations can be found in [3.21].

From the results of a few calculated examples, it is clear that the resonances for long tubes ($l_z > 10\ a$) tend to occur just above the corresponding ring frequencies of Eq. (3.210b). Additionally, it is realized that $\omega_{n1,\,m} > \omega_{n2,\,m}$ even if $n_1 < n_2$. Thus, it is possible that two modes of the same number m of nodes in axial direction but of differing nodes in circumferential exhibit the highest resonance for the smaller n.

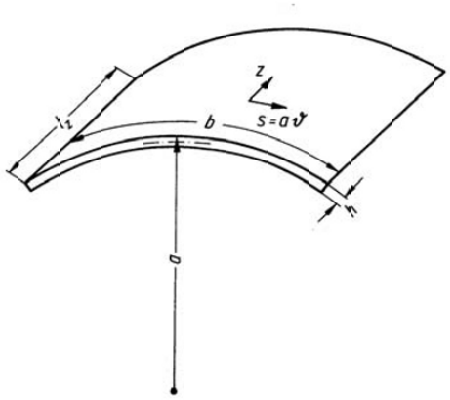

Fig. 3.33. Notations for a cylinder segment

Equations (3.212a, b) also apply for segments of cylindrical shells owing to the fact that the basic differential equations are the same. For a cylindrical segment of arc and edge lengths b and l_z as sketched in Fig. 3.33, the eigen-functions

$$\begin{aligned}
\xi &= \xi_{m1,m2} \sin\frac{m_1 \pi z}{l_z} \sin\frac{m_2 \pi s}{b}, \\
\eta &= \eta_{m1,m2} \sin\frac{m_1 \pi z}{l_z} \cos\frac{m_2 \pi s}{b}, \\
\zeta &= \zeta_{m1,m2} \cos\frac{m_1 \pi z}{l_z} \sin\frac{m_2 \pi s}{b},
\end{aligned} \tag{3.213}$$

apply for $m_{1,\,2} = 1, 2, 3 \ldots$ provided that the boundary conditions fulfil

$$\xi = \eta = 0, \quad \frac{\partial^2 \xi}{\partial z^2} = \frac{\partial^2 \eta}{\partial z^2} = 0, \quad \frac{\partial \zeta}{\partial z} = 0; \quad z = 0, l_z,$$

$$\xi = \eta = 0, \quad \frac{\partial^2 \xi}{\partial s^2} = \frac{\partial^2 \eta}{\partial s^2} = 0, \quad \frac{\partial \zeta}{\partial s} = 0; \quad s = 0, b.$$

This means that the supports present no moments with respect to radial and axial motions and no forces to the tangential. It is readily verified that the eigen-functions in (3.213) satisfy the spatial dependencies of the cylindrical shell equations and lead to a characteristic equation of the same form as that for a complete cylinder, the only alteration being that n is replaced by $m_2\pi a/\mathrm{b}$ and m by m_1.

It is easy to demonstrate that as the radius of curvature tends to infinity, $a \to \infty$, the expressions for flexural as well as shear and extensional resonances given above collapse into those of a flat plate.

Unfortunately, no simple expressions are available for other boundary conditions but it can be mentioned that the resonance frequencies rise considerably as the tangential motion at edges $x = 0$ and $x = b$ are restrained [3.23]. In this context, it is of interest to consider also doubly curved shells. Without derivation [3.24], are given the resonance frequencies for bending waves for a rectangular patch with radii of curvature a_1 and a_2 having simple supports along all edges,

$$\omega_{m_1,m_2}^2 \approx c_{LI}^2 \left\{ \frac{\left[\frac{1}{a_1} \left(\frac{m_1 \pi}{l_z} \right)^2 + \frac{1}{a_2} \left(\frac{m_2 \pi}{b} \right)^2 \right]^2}{\left[\left(\frac{m_1 \pi}{l_z} \right)^2 + \left(\frac{m_2 \pi}{b} \right)^2 \right]^2} + \frac{h^2}{12} \left[\left(\frac{m_1 \pi}{l_z} \right)^2 + \left(\frac{m_2 \pi}{b} \right)^2 \right]^2 \right\}. \quad (3.214)$$

3.9 Structure-Borne Sound Intensity

3.9.1 Fundamental Equations

The well-thumbed definition of the intensity vector for air-borne sound can readily be extended to the structure-borne sound case [3.25-3.27],

$$\overline{\mathbf{J}_{air}} = \overline{p \cdot \mathbf{v}} = \left(\overline{pv_x}, \overline{pv_y}, \overline{pv_z} \right). \quad (3.215)$$

In the structure-borne case, however, it is necessary to take into account that the dynamic quantities are not represented by the pressure but the

stress tensor. In Cartesian co-ordinates, therefore, the general definition of the three components of the intensity vector reads

$$\begin{aligned} J_x &= -\left[\overline{\sigma_x v_x} + \overline{\tau_{xy} v_y} + \overline{\tau_{xz} v_z}\right] \\ J_y &= -\left[\overline{\tau_{xy} v_x} + \overline{\sigma_y v_y} + \overline{\tau_{yz} v_z}\right] \\ J_z &= -\left[\overline{\tau_{xz} v_x} + \overline{\tau_{yz} v_y} + \overline{\sigma_z v_z}\right]. \end{aligned} \tag{3.216}$$

In this text only the temporal average of the stress and velocity product will be considered and referred to as the intensity. Instantaneous intensity as well as the imaginary intensity will not be treated [3.28, 3.29].

As can be observed, the intensity is formed by the scalar product of the force acting on a surface element and the velocity at that surface. The overbar denotes that each term is temporally averaged. The negative sign in front stems from the fact that σ and τ are defined positive as extensional stresses and hence act like elemental forces opposite a positive velocity cf., Eqs. (3.27), (3.28) and (3.35).

A special case of Eq. (3.216) was treated previously in Sect. 3.1.1 whereby the intensity was given in a pure longitudinal wave, for which $\boldsymbol{v}_y = v_z = 0$ and $J_x = -\sigma_x v_x$. Also shown in this context was that the intensity equals the power transmitted through a surface element. This statement also holds in the three-dimensional case for the separate directions. It should be noted, however, that the vector resulting from the components J_x, J_y, J_z, not necessarily is perpendicular to the wave front, in contrast to the analogous airborne intensity cf., [3.29].

3.9.2 Intensity in this Plates

Due to the severe difficulties to measure stresses and velocities interior to a structure without detrimentally disturbing the field, the following treatise is confined to thin plates and thin-walled shells for which the measurements can be undertaken comparatively easy at the surfaces. The analysis, moreover, is confined to the x-component of the intensity since the y-component vanishes and the z-component readily is obtained from a replacement of x by z for homogeneous media. The notation is the same as in Sect. 3.8.2 and is found in Fig. 3.29 as well as in Eqs. (3.189-3.190d).

Upon substituting these expressions into Eq. (3.216) is obtained

$$-J_x = \frac{E}{1-\mu^2}\overline{\left(\frac{\partial \xi_M}{\partial x} + y\frac{\partial \varphi_x}{\partial x} + \mu\frac{\partial \zeta_M}{\partial z} + \mu y\frac{\partial \varphi_z}{\partial z}\right)\left(\dot{\xi}_M + y\dot{\varphi}_x\right)} + G\left[\overline{\left(\varphi_x + \frac{\partial \eta}{\partial x}\right)\dot{\eta}} + \overline{\left(\frac{\partial \xi_M}{\partial z} + y\frac{\partial \varphi_x}{\partial z} + \frac{\partial \zeta_M}{\partial x} + y\frac{\partial \varphi_z}{\partial x}\right)\left(\dot{\zeta}_M + y\dot{\varphi}_z\right)}\right]. \tag{3.217}$$

Herein, the differentiation with respect to time is denoted by a dot i.e., $v_x = \dot{\xi}_M + y\dot{\varphi}_x$, $v_y = \dot{\eta}$ and $v_z = \dot{\zeta}_M + y\dot{\varphi}_z$. Equation (3.217) furnishes the intensity in a plane y = const. Of greater practical interest, however, is the cross-sectionally integrated power per unit width,

$$W_x' = -\int_{h/2}^{h/2} J_x dy. \tag{3.218}$$

With Eq. (3.217) inserted in (3.218), the power per unit width becomes

$$\frac{W_x'}{h} = \frac{E}{1-\mu^2}\overline{\left(\frac{\partial \xi_M}{\partial x} + \mu\frac{\partial \zeta_M}{\partial z}\right)\dot{\xi}_M} + G\overline{\left(\frac{\partial \xi_M}{\partial z} + \frac{\partial \zeta_M}{\partial x}\right)\dot{\zeta}_M} + \frac{EI'}{1-\mu^2}\overline{\left(\frac{\partial \varphi_x}{\partial x} + \mu\frac{\partial \varphi_z}{\partial x}\right)\dot{\varphi}_x} + G\overline{\left(\varphi_x + \frac{\partial \eta}{\partial x}\right)\dot{\eta}} + GI'\overline{\left(\frac{\partial \varphi_x}{\partial z} + \frac{\partial \varphi_z}{\partial x}\right)\dot{\varphi}_z} \tag{3.219}$$

In this expression $I' = h^2/12$ is the radius of gyration squared and stems from the integration of y^2-terms whereas all y-terms vanish.
The terms of the first line in Eq. (3.219) both depend only on the motion of the neutral layer of the structure and thus represent the power carried by the in-plane waves cf., Sect. 3.7.4.1. In contrast, those of the second line are all associated with the flexural motion and can be rewritten such that only the translatory motion perpendicular to the surface η appears. Also, it is suitable to alter the factor G ($\varphi_x + \partial\eta/\partial x$) to improve on its present appearance as $\infty \cdot 0$.

Upon back-tracking this expression it is seen that

$$G\overline{\left(\varphi_x + \frac{\partial \eta}{\partial x}\right)\dot{\eta}} = \frac{1}{h}\overline{\int \tau_{xy}\dot{\eta}\, dy} = -\frac{\overline{\dot{\eta}\int \tau_{xy} dy}}{h} = -\frac{1}{h}\overline{\dot{\eta} Q_x} = -\frac{B'}{h}\frac{\partial}{\partial x}\overline{\left(\frac{\partial^2 \eta}{\partial x^2} + \frac{\partial^2 \eta}{\partial z^2}\right)\dot{\eta}}. \tag{3.220}$$

In this, the fact is used that the cross-sectionally integrated shear stress equals the total force at the cross-section Q_x given by Eq. (3.184e), see Fig. 3.27. Another possibility to arrive at this form would be to rewrite the first line in Eq.(3.193) as

$$Gh\left(\varphi_x + \frac{\partial \eta}{\partial x}\right) = \left(GI\frac{\partial^2}{\partial z^2} + B'\frac{\partial^2}{\partial x^2}\right)\varphi_x + \frac{1+\mu}{2}B'\frac{\partial^2 \varphi_z}{\partial x \partial z} - \rho I \ddot{\varphi}_z \tag{3.221}$$

With the approximations $\varphi_x = -\partial\eta/\partial x$ and $\varphi_z = -\partial\eta/\partial z$, applicable for thin plates, the right hand side of (3.221) turns into (3.220) with the negligible difference of the small term $\rho I \ddot{\varphi}_x$ associated with the approximation, and Eq. (3.219) finally becomes [3.26]

$$\begin{aligned}\frac{W_x'}{h} = {} & \frac{E}{1-\mu^2}\overline{\left(\frac{\partial \xi_M}{\partial x} + \mu\frac{\partial \zeta_M}{\partial z}\right)\dot{\xi}_M} + G\overline{\left(\frac{\partial \xi_M}{\partial z} + \frac{\partial \zeta_M}{\partial x}\right)\dot{\zeta}_M} \\ & + \frac{B'}{h}\left[\overline{\left(\frac{\partial^2 \eta}{\partial x^2} + \mu\frac{\partial^2 \eta}{\partial z^2}\right)\frac{\partial \dot{\eta}}{\partial x}} + (1-\mu)\overline{\frac{\partial^2 \eta}{\partial x \partial z}\frac{\partial \dot{\eta}}{\partial z}} - \overline{\frac{\partial}{\partial x}\left(\frac{\partial^2 \eta}{\partial x^2} + \frac{\partial^2 \eta}{\partial z^2}\right)\dot{\eta}}\right]\end{aligned} \tag{3.222a}$$

For the one-dimensional case and pure bending, it is readily found that

$$W_{xB} = B\overline{\left(\frac{\partial^2 \eta}{\partial x^2}\frac{\partial \dot{\eta}}{\partial x} - \frac{\partial^3 \eta}{\partial x^3}\dot{\eta}\right)}$$

is in agreement with the previous results in (3.91) or (3.91a).

Equation (3.222a) demonstrates that measurement of structure-borne sound power is not so simple even for thin plates. This is due to the averaging of lateral motions ξ, ζ and their derivatives measured at the plate surfaces $y = \pm h/2$, which yield the quantities ξ_M and ζ_M. Moreover is required the translation η to its third order spatial derivative with a high degree of accuracy cf., Figs. 8.42 and 8.43.

If bending wave nearfields are disregarded, then

$$\frac{\partial^2 \eta}{\partial x^2} = -k_B^2 \eta = -\omega\sqrt{\frac{m'}{B}}\eta \tag{3.223a}$$

applies in the one-dimensional case, for regions more than half a wavelength away from structural discontinuities and excitations. This means that (3.222b) becomes

$$W_{xB} = -\omega\sqrt{m'B}\overline{\left(\eta\frac{\partial \dot{\eta}}{\partial x} - \frac{\partial \eta}{\partial x}\dot{\eta}\right)}, \tag{3.223b}$$

which can be further simplified by making use of the chain rule

$$\frac{\partial}{\partial t}\left(\eta\frac{\partial \eta}{\partial x}\right) = \frac{\partial \eta}{\partial x}\frac{\partial}{\partial t} + \eta\frac{\partial^2}{\partial x \partial t} = \dot{\eta}\frac{\partial \eta}{\partial x} + \eta\frac{\partial \dot{\eta}}{\partial x} \tag{3.223c}$$

and observing that every arbitrary function of time $g(t)$, oscillating around zero will vanish when averaged,

$$\overline{\frac{\partial}{\partial t} g(t)} = \frac{1}{T}\int_{t_1}^{t_2} \frac{\partial}{\partial t} g(t)\, dt = \frac{1}{T}\left[g(t_2) - g(t_1) \right] \approx 0. \tag{3.223d}$$

Implicit is that the average is taken over a long time. With this relation, then

$$\overline{\frac{\partial}{\partial t}\left(\eta \frac{\partial \eta}{\partial x} \right)} = 0 = \overline{\dot{\eta} \frac{\partial \eta}{\partial x}} + \overline{\eta \frac{\partial \dot{\eta}}{\partial x}} \quad \Leftrightarrow \quad \overline{\dot{\eta} \frac{\partial \eta}{\partial x}} = -\overline{\eta \frac{\partial \dot{\eta}}{\partial x}} \tag{3.223e}$$

From Eq. (3.223b) [3.25] therefore

$$W_{xB} = 2\omega \sqrt{m'B}\, \overline{\frac{\partial \eta}{\partial x} \dot{\eta}} = -2\omega \sqrt{m'B}\, \overline{\frac{\partial \dot{\eta}}{\partial x} \eta} \tag{3.223f}$$

applies for the farfield in the one-dimensional case.

Upon employing two accelerometers with identical amplitude and phase characteristics, placed a small distance Δx apart, a good approximation for the power transmitted is given by

$$W_{xB} = -2\omega \sqrt{m'B}\, \overline{\frac{\eta_1 + \eta_2}{2} \frac{1}{\Delta x} \int_{-\infty}^{t} (a_2 - a_1)\, d\tau}, \tag{3.224}$$

provided that $\Delta x << \lambda_B/10$. Herein, η_1, η_2 are the measured displacements and a_1, a_2 the accelerations. Use is also made of the approximation

$$\frac{\partial \dot{\eta}}{\partial x} \approx \frac{\dot{\eta}_2 - \dot{\eta}_1}{\Delta x}, \quad \dot{\eta} = v = \int_0^t a\, d\tau.$$

For a narrow frequency band, $\eta \approx -a/\omega^2$, such that

$$W_{xB} \approx \frac{\sqrt{m'B}}{\omega} \frac{1}{\Delta x} \overline{(a_1 + a_2) \int_{-\infty}^{t} (a_2 - a_1)\, d\tau} \tag{3.224a}$$

With the exception of the factor in front, this is the same formula as is used in the airborne sound case, with the acceleration substituted instead of pressure. Outside regions with significant, nearfields, it is thus possible to assess the power carried by bending waves applying the same signal processing equipment as is used for airborne sound intensity. Also, as in the airborne sound intensity context [3.28], it is finally possible to put

$$\int_{-\infty}^{t} a_1 d\tau = g_1(t) \Rightarrow a_1 = \frac{\partial g}{\partial t},$$

which means that

$$\begin{aligned} W_{xB} &= \frac{\sqrt{m'B}}{\omega\Delta x}\left[\overline{\frac{\partial g_1}{\partial t}g_2}+\overline{\frac{\partial g_2}{\partial t}g_2}-\overline{\frac{\partial g_1}{\partial t}g_1}-\overline{\frac{\partial g_2}{\partial t}g_1}\right] \\ &= \frac{\sqrt{m'B}}{\omega\Delta x}\left[2\overline{\frac{\partial g_1}{\partial t}g_2}-\overline{\frac{\partial\left(g_1g_2\right)}{\partial t}}+\frac{1}{2}\overline{\frac{\partial g_2^2}{\partial t}}-\frac{1}{2}\overline{\frac{\partial g_1^2}{\partial t}}\right] \\ &= 2\frac{\sqrt{m'B}}{\omega\Delta x}a_1\int_{-\infty}^{t}a_2 d\tau . \end{aligned} \tag{3.224b}$$

As in Eq. (3.223d), the averaged time derivatives cancel.

From a transition to power-spectral densities, it is possible to show that the power spectrum W_{xB} (ω) is proportional to the imaginary part of the cross-power spectrum between the two accelerations. This is most readily demonstrated in that a single frequency is considered i.e.,

$$a_1 = \mathrm{Re}\left[\hat{a}_1 e^{j\omega t}\right] = \frac{1}{2}\left[\hat{a}_1 e^{j\omega t}+a_1^* e^{-j\omega t}\right],$$

$$a_2 = \mathrm{Re}\left[\hat{a}_2 e^{j\omega t}\right] = \frac{1}{2}\left[\hat{a}_2 e^{j\omega t}+a_2^* e^{-j\omega t}\right].$$

Substitution into Eq. (3.224a) yields

$$W_{xB}\left(\omega\right) = \frac{\sqrt{m'B}}{\omega\Delta x}\left|\hat{a}_1\right|\left|\hat{a}_2\right|\sin\left(\varphi_2-\varphi_1\right), \tag{3.224c}$$

in which (φ_2 - φ_1) is the usually small phase difference between the two accelerations.

3.9.3 Power Transmission in Thin-Walled Cylindrical Shells

In cylindrical co-ordinates, the general expressions for the components of the intensity vector read

$$\begin{aligned} J_\vartheta &= -\left[\overline{\sigma_\vartheta\dot{\xi}}+\overline{\tau_{r\vartheta}\dot{\eta}}+\overline{\tau_{\vartheta z}\dot{\zeta}}\right], \\ J_r &= -\left[\overline{\tau_{r\vartheta}\dot{\xi}}+\overline{\sigma_r\dot{\eta}}+\overline{\tau_{rz}\dot{\zeta}}\right], \\ J_z &= -\left[\overline{\tau_{\vartheta z}\dot{\xi}}+\overline{\tau_{rz}\dot{\eta}}+\overline{\sigma_z\dot{\zeta}}\right], \end{aligned} \tag{3.225}$$

and are analogous to those in Eq. (3.216). The following analysis is confined to thin-walled cylinders, free from excitations on the cylinder wall. For such cases, there is no power transmitted in the radial direction i.e.,

$J_r = 0$. The stress and strain relations in Eqs. (3.198) to (3.201), moreover, can also be employed in this context owing to the vanishing radial stress, $\sigma_r = 0$. With those expressions introduced in (3.225), some manipulations yield the principal power transmission in axial direction as

$$\begin{aligned}\frac{W_z'}{h} &= \frac{E}{1-\mu}\overline{\left(\frac{\partial\zeta_M}{\partial z}+\mu\frac{\partial\xi_M}{\partial s}\right)\dot{\zeta}_M}+G\overline{\left(\left(1+\beta^2\right)\frac{\partial\xi_M}{\partial z}+\left(1-\beta^2\right)\frac{\partial\zeta_M}{\partial s}\right)\dot{\xi}_M}\\ &+\frac{EI'}{1-\mu^2}\overline{\left(\frac{\partial\varphi_z}{\partial z}+\mu\frac{\partial\varphi_\vartheta}{\partial s}\right)\dot{\varphi}_z}+G\left(\varphi_z+\frac{\partial\eta}{\partial z}\right)\dot{\eta}+GI'\overline{\left(\frac{\partial\varphi_z}{\partial s}+\frac{\partial\varphi_\vartheta}{\partial z}\right)\dot{\varphi}_\vartheta}\\ &+\frac{EI'}{1-\mu^2}\frac{\mu}{a}\overline{\left(\eta\dot{\xi}_M-\frac{I'}{a}\eta\dot{\varphi}_z\right)}\\ &+\frac{GI'}{a}\left[\overline{\left(\frac{\partial\varphi_z}{\partial s}+\frac{\partial\varphi_\vartheta}{\partial z}\right)\dot{\xi}_M}-\overline{\left(\frac{\partial\zeta_M}{\partial s}-\frac{\partial\xi_M}{\partial z}\right)\dot{\varphi}_\vartheta}\right].\end{aligned} \tag{3.226}$$

The first line of this expression describes the in-plane intensity in the absence of radial motion of the cylinder. In the second, is contained that associated with bending motion. This is clearly seen from a comparison of Eqs. (3.226) and (3.219) whereby it is taken into account that the power in z-direction is considered in the latter. The last two lines, finally, represent mixed terms which vanish as the radius a tends to infinity, $a \to \infty$.

To proceed with the analysis, the cross-sectional force is in this case obtained from the equation of motion for the system i.e., from (3.203). By calculating $G\,(\varphi_z + \partial\eta/\partial z)$ from the last of the expressions and subsequently introducing the approximations $\varphi_z = -\partial\eta/\partial z$ and $\varphi_\vartheta = -\partial\eta/\partial s$, the power transmitted is obtained as

$$\begin{aligned}\frac{W_z'}{h} &= \frac{E}{1-\mu^2}\left[\overline{\frac{\partial\zeta_M}{\partial z}\dot{\zeta}_M}+\mu\overline{\frac{\partial\xi_M}{\partial s}\dot{\zeta}_M}\right]+G\left[\overline{\frac{\partial\xi_M}{\partial z}\dot{\xi}_M}+\overline{\frac{\partial\zeta_M}{\partial s}\dot{\xi}_M}\right]\\ &+\frac{EI'}{1-\mu^2}\left[\overline{\left(\frac{\partial^2\eta}{\partial z^2}+\mu\frac{\partial^2\eta}{\partial s^2}\right)\frac{\partial\dot{\eta}}{\partial z}}-\overline{\left(\frac{\partial\nabla^2\eta}{\partial z}-\frac{1}{c_{LI}^2}\frac{\partial^3\eta}{\partial z\partial t^2}\right)\dot{\eta}}+(1-\mu)\overline{\frac{\partial^2\eta}{\partial s\partial z}\frac{\partial\dot{\eta}}{\partial s}}\right]\\ &+\frac{E}{1-\mu^2}\frac{\mu}{a}\left[\overline{\eta\dot{\zeta}_M}+\frac{I'}{a}\overline{2\eta\frac{\partial\dot{\eta}}{\partial z}}\right]+\frac{GI'}{a}\left[\overline{\frac{\partial\zeta_M}{\partial s}\frac{\partial\dot{\eta}}{\partial s}}-\overline{\frac{\partial^2\zeta_M}{\partial s^2}\dot{\eta}}\right].\end{aligned} \tag{3.227}$$

Practical measurements according to this expression are highly complicated and time-consuming. Most often, therefore, the simplified one-dimensional formulae (3.224) to (3.224c) are employed to assess the order of magnitude and, above all, the direction of the intensity.

As in the case of airborne sound intensity, structure-borne intensity due to multiple tonal coherent sources must be treated cautiously. Any phase

shift between the sources may result in highly differing directivity of the intensity.

References

[3.1] Morse P.M., 1948. Vibration and sound, Ch. 4. McGraw-Hill, New York NY
[3.2] Rayleigh J.W.S., 1885. On waves propagated along the plane surface of an elastic solid. Proc. Mathematical Society London, 17, 4-11
[3.3] Schoch A., 1950. Periodische Wellen im schubspannungsfreien planparallelen Schichten. Ergebnisse der exakten Naturwissenschaften, 23, p. 172
[3.4] Achenbach J.D., 1975. Wave propagation in elastic solids. North-Holland, Amsterdam
[3.5] Naake H.J. and Tamm K., 1958. Sound propagation in plates and rods of rubber-elastic materials. Acustica, 8, p. 65
[3.6] Götz J.,1943. Über den Schalldurchgang durch Metallplatten in Flüssigkeiten bei schrägem Einfall einer Welle. Akustische Zeitschrift, 8, p. 145
[3.7] Firestone F.A., 1948. Tricks with the supersonic reflectoscope. Non-destructive testing, 7, p. 5
[3.8] Tamm K. and Weiss O., 1959. Untersuchungen über periodische Wellen, exponentielle und komplexe Nahfelder im begrenzten Festkörper. Acustica, 9, p. 275
[3.9] Epstein P.S., 1942. On the theory of elastic vibrations in plates and shells. Journal of Mathematics and Physics, 21, p. 198
[3.10] Huber M.T., 1914. Die Grundlagen einer rationellen Berechnung der kreuzweise bewehrten Eisenbetonplatte. Zeitschrift des Östereichischen Ingenieur- und Architekten-Vereins, 30, p. 557
[3.11] Hearmon R.F.S. and Adams E.H., 1952. The bending and twisting of an isotropic plates. British Journal of Applied Physics, 3, p. 155
[3.12] Timoshenko S.P. and Woinowsky-Krieger S., 1959. Theory of plates and shells (2nd ed.), Ch. 11. McGraw-Hill, Auckland
[3.13] Heckl M., 1960. Untersuchungen an orthotropen Platten. Acustica, 10, 109-115
[3.14] Heckl M., 1990. Einfache Anwendung des Hamiltonschen Prinzips bei Körperschallproblemen. Acustica, 72, 189-196
[3.15] Mindlin R.D., 1951. Influence of rotatory inertia and shear on flexural motions of isotropic, elastic plates. Journal of Applied Mechanics, 18, p. 155
[3.16] Junger M.L. and Feit D., 1972. Sound structures and their interaction, Ch. 9. MIT Press, Cambridge MA
[3.17] Love A.E.H., 1948. A treatise on the mathematical theory of elasticity, Ch. XXIII. Dover Publications, New York NY
[3.18] Rayleigh J.W.S., 1945. Theory of sound (2nd ed.), Vol. 1, §235e. Dover Publications, New York NY
[3.19] Cremer L., 1955. Theorie der Luftschalldämmung zylindrischer Schalen. Acustica, 5, p. 245

[3.20] Donell L.H., 1939. Discussion of thin shell theory. Proc. 5th International Congress on Applied Mechanics, p. 66
[3.21] Leissa A.W., 1973. Vibration of shells. NASA-SP 288
[3.22] Heckl M., 1962. Vibrations of point-driven cylindrical shells. Journal of the Acoustical Society of America, 34, 1553-1557
[3.23] Cremer L., 1984. Physics of the violin, §3.3. MIT Press, Cambridge MA
[3.24] Reissner E., 1955. On transverse vibration of thin, shallow elastic shells. Quarterly Applied Mathematics, 13, p. 169
[3.25] Noiseux D.U., 1970. Measurement of power flow in uniform beams and plates. Journal of the Acoustical Society of America, 47, p. 238
[3.26] Pavic G., 1976. Measurement of structure borne wave intensity, part I: Formulation of the methods. Journal of Sound and Vibration, 49, p. 221
[3.27] Pavic G.,1986. The influence of curvature on structure-borne acoustical power propagation in a cylindrical circular shell. Proc. 12th International Congress on Acoustics, Paper D6-6. Toronto
[3.28] Fahy F.J., 1995. Sound intensity (2nd ed.). E & FN Spon, London
[3.29] Maysenhölder W., 1994. Körperschallenergie. Grundlagen zur Berechnung von Energiedichten und Intensitäten. S. Hirzel Verlag, Stuttgart